Reprogramming murine Müller glia for the regeneration of retinal ganglion cells

Wesley Jenkins

A dissertation

submitted in partial fulfillment of the

requirements for the degree of

Doctor of Philosophy

University of Washington

2023

Reading Committee:

Thomas Reh, Chair

Timothy Cherry

Cecilia Moens

Program Authorized to Offer Degree:

Molecular and Cellular Biology

University of Washington

Abstract

Reprogramming murine Müller glia for the regeneration of retinal ganglion cells

Wesley Jenkins

Chair of the Supervisory Committee:
Thomas Reh
Department of Biological Structure

Degenerative diseases of the retina often result in the loss of specific types of neurons. Some vertebrates, such as frogs and fish, exhibit an intrinsic regenerative capacity that can replenish lost neurons and functionally restore vision. However, the mammalian retina cannot regenerate and any vision loss from degenerative disease is permanent. Recently, it has been shown that overexpression of the proneural bHLH transcription factor Ascl1 in Müller glia (MG) can stimulate the regeneration of neurons in adult mice. While promising, regeneration is limited to one cell type – bipolar cells. Common degenerative diseases of the retina often result in the loss of other retinal neurons, such as retinal ganglion cells (RGCs) in glaucoma and diabetic retinopathy. This highlights the need to develop strategies for redirecting the fate of regenerated neurons. In this dissertation, I describe a method for inducing RGC-like neurons through the combined overexpression of Ascl1 with Pou4f2 and Isl1. I also identified three other transcription factors, Atoh1, Neurod2, and Irx2 that can improve RGC regeneration by reducing glial gene expression, improving conversion efficiency, increasing activation of axon outgrowth genes, and enhancing both the size and complexity of neurites *in vitro*. Overall, these studies show it is possible to induce the regeneration of clinically important neurons in the mammalian retina and suggest new strategies to further refine the approach.

Acknowledgements

I would like to thank my advisor, Tom Reh, for his wisdom, guidance, and encouragement. Tom helped me navigate this PhD through a global viral pandemic and many experimental hurdles to a successful conclusion. His genuine curiosity and relentless optimism are inspiring and served to create an atmosphere in the lab conducive of exploration and perseverance. Many other members of both the Reh lab and Bermingham-McDonogh lab have aided this research either directly or indirectly with their insightful suggestions, technical expertise, and above all their friendship. I'm very grateful to have been surrounded by such supportive and wonderful people. I'd also like to thank my supervisory committee for their continual feedback and support over the years. Most of all, I'd like to thank my partner in adventure, Cristina Olivares, for her unwavering belief in me.

Dedication

For my grandfather, Oliver Wesley Wilcox (03/13/1924 – 07/14/2017)

Table of contents

List of figures and tables

Chapter 1:

Introduction

Overview

Retinal disease is a major cause of blindness worldwide[1]. Despite advances in available treatment options, any vision loss associated with retinal cell death is permanent. Unfortunately, human retinal tissue does not regrow new cells once lost. Many potential strategies for restoring retinal function are currently being investigated, which can be broadly classified into three categories: neuroprosthetics, cell or tissue transplants, and regenerative therapies. The latter approach seeks to restore retinal function by stimulating the tissue to replace lost cells, akin to what naturally occurs in more regenerative species, such as teleost fish, which are capable of regrowing retinal tissue lost to damage.

In my thesis work, I have expanded on recent efforts to stimulate retinal regeneration in mammals. Specifically, I have explored methods for directing mammalian retinal regeneration towards replacement of specific cell types. As different degenerative retinal diseases result in loss of specific cell types (largely photoreceptors and retinal ganglion cells), one imperative is to establish control over the differentiation of newly regenerated neurons. To this end I sought out to discover factors that may influence cell fate in a mammalian model of retinal regeneration. Specifically, I hoped to discover factors that can re-direct the fate of regenerated neurons towards the retinal ganglion cell lineage.

This chapter serves to orient the reader and provide context through a focused review of the retina and the molecular biology of its development, the cell types and processes involved with various degenerative diseases, regeneration in other vertebrates, and finally the prior work that

established a mouse model for mammalian retinal regeneration and the subsequent efforts to improve the efficiency and diversity of cell types regenerated in this model.

Retinal cell types, organization, and function

The retina is sensory tissue of the central nervous system (CNS) located at the back of the eye which enables sight in mammals and other vertebrates. The basic structure and function of the retina is well described and highly conserved from fish to humans.

Thus, the use of model organisms, such as the mouse, may directly inform research into therapeutics to fight blindness. Further, due to the relative accessibility of the retina compared with the rest of the CNS – it has been described as the "approachable part of the brain"[2] – experimental manipulation in live organisms can be much easier. Thus, the retina can serve as tractable model for more general questions of CNS biology.

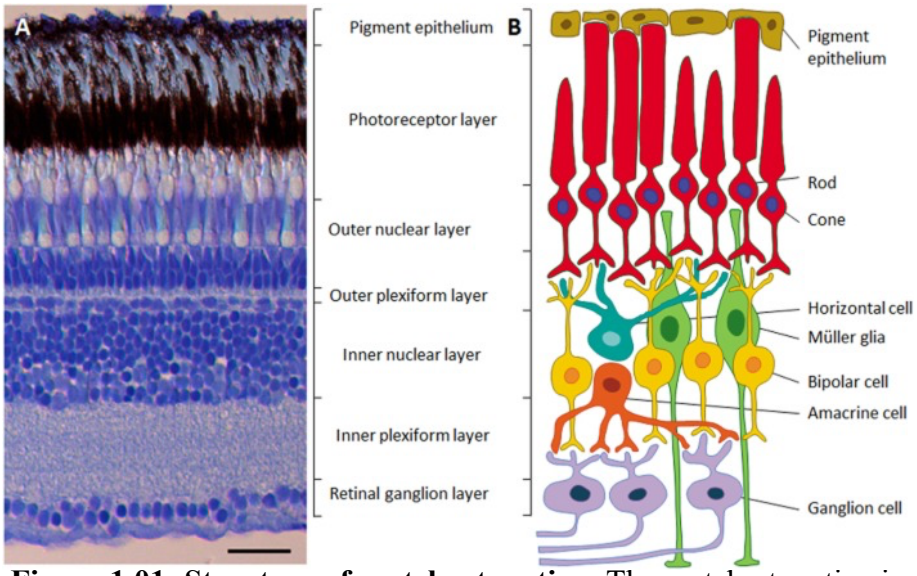

Figure 1.01: Structure of vertebrate retina. The vertebrate retina is composed of three basic layers: the outer nuclear layer (ONL), inner nuclear layer (INL), and ganglion cell layer (GCL). The rod and cone photoreceptors are found in the ONL; bipolar, amacrine, horizontal cells, and Müller glia are in the INL; the ganglion cells are in the GCL (image: Gramage et al., 2014).

The retina is a laminated tissue composed of three layers of neurons, of which there are five broad classes (Figure 1.01)[3]. The most posterior layer of the neurosensory retina contains the photoreceptors – rods and cones in mammals – with the soma residing in the outer nuclear layer (ONL). The photoreceptors synapse to interneurons at the outer plexiform layer (OPL). The soma of these interneurons (bipolar, amacrine, and horizontal cells), along with Müller glia, are found in the inner nuclear layer (INL). The synapses of neurons from the INL, along with ganglion cells, form in the inner plexiform layer (IPL). Finally, the most anterior layer, the ganglion cell layer (GCL), contains retinal ganglion cells (RGCs), displaced amacrine cells, and astrocytes, which are not derived from retinal progenitor cells but migrate into the retina. The axons of the RGCs project back through the retina at the optic nerve head, then collectively make up the optic nerve, a myelinated structure which transmits information from the retina to the thalamus for further processing[4]. Below are brief functional descriptions for each broadly classified cell type in the retina.

Photoreceptors

Light must pass through the retina to interact with the photoreceptors; this physical interaction is what ultimately enables the sense of sight. The chromophore, retinal, is present in all photoreceptors and undergoes a conformational change upon absorption of a photon, which initiates visual phototransduction[5]. Different types of photoreceptors produce different opsin proteins that interact with retinal to enable a diversity of sensitivity to different wavelengths of light. The human retina contains rod cells and three types of cone cells, S-, M-, and L-cones which each produce distinct opsins with a peak absorbance of light at different wavelengths. The rod cells are the most abundant and produce rhodopsin, the most sensitive opsin in the retina

capable of detecting a single photon; they are mostly responsible for vision in low-light conditions[6,7]. The three cones are found in highest density in the macula, the structure at the focal center of the retina, enabling red-blue-green daytime color vision. The exact composition of photoreceptors varies between species. The mouse retina, for instance, lacks a macula, contains mostly rod cells, and lacks the L-cone[8].

Bipolar cells

Bipolar cells have two processes, at 180 degrees from one another, which form synapses with photoreceptors in the OPL and with the other neurons of the retina in the IPL, collectively establishing a communication relay between the outer and inner layers of the retina. There are at least 15 distinct types of bipolar cells which can be broadly classified according to which photoreceptors they interact with (rod or cone) and whether they depolarize or hyperpolarize in response to light (ON or OFF, respectively)[9]. Different bipolar cells can thus provide different pre-processed signals to amacrine and ganglion cells by synapsing at distinct layers of the IPL.

Horizontal cells

Horizontal cells form wide horizontal projections, strictly in the OPL, that interact with photoreceptors and bipolars. There are 3 types of horizontal cells, collectively they largely serve to modulate the transfer of information from photoreceptors to bipolar cells. This is largely carried out through inhibitory signaling and serves to enhance color discrimination and contrast[10-12]. Through lateral inhibition carried out by horizontal cells, activity from one group of photoreceptors can reduce signaling from nearby photoreceptors, thereby aiding in two-point discrimination[13].

Amacrine cells

Like horizontal cells, amacrine cells modulate signaling in the retina. However, there is far more diversity of amacrine cells (roughly 60 types)[14]. They also form synapses in the IPL where they interact laterally with bipolar, ganglion, and other amacrine cells – largely through inhibitory signaling. As the vast diversity of subtypes implies, amacrine cells serve a variety of functions in the pre-processing of visual information of the retina including motion detection and light adaptation. They are also key integrators of information, serving as functional units for the ganglion cells with which they interact. Additionally, a unique amacrine cell, AII, forms synapses throughout the IPL to participate directly in the vertical flow of information from photoreceptor to RGC[15].

Retinal Ganglion Cells

The sole output cell of the retina, RGCs receive inputs from bipolar and amacrine cells in the IPL and project their axons to targets in the lateral geniculate nucleus, superior colliculus, hypothalamus, and midbrain to relay both image-forming and non-image-forming information. Unlike the other retinal neurons, which exhibit graded potentials, RGCs fire spontaneous action potentials, the rate of which are modulated by their inputs. While RGCs make up relatively few of the total neurons in the retina, they are quite diverse with over 45 subtypes identified[16]. A small set of RGCs, the intrinsically photosensitive RGCs (ipRGCs), produce melanopsin that can interact with light much like the opsins produced by photoreceptors. The ipRGCs have non-vision roles such as in aiding the control of pupil size and the entrainment of circadian rhythms.

Müller Glia

Aside from astrocytes residing in the GCL, which are not derived from retinal progenitor cells, the Müller glia (MG) is the only glial cell of the retina. While their soma resides in the INL, their processes span all layers of the retina and help give rise to the inner and outer limiting membranes. MG provide structural support for the retina and play a number of housekeeping roles in the retina including the maintenance of extracellular levels of neurotransmitters, ions, water, and recycling metabolic waste. Interestingly, they have also been shown to help focus light through the retina onto photoreceptor outer segments[17].

Development of the retina and molecular specification of cell types

The relative timing of the appearance of each major cell type in the retina is conserved across vertebrate species. Here, I will focus on the developmental timeline of the mouse retina, as it is the model system utilized in my thesis work. The neural retina forms from the inner neuroepithelium of the optic cup, a structure itself derived from sections of neural tube expressing eye field genes, such as Rax, Pax6, and Sox2. An expanding pool of multipotent retinal progenitor cells (RPCs) begins to give rise to neurons by embryonic day 12 (E12)[18]. Development continues until around postnatal day 12 (P12), with each major cell type appearing within distinct but overlapping temporal windows. The earliest cell types to appear are RGCs, cones, and horizontal cells followed by amacrine, rod, bipolar, and MG (Figure 1.02)[19-22]. How exactly competence is conferred for any given progenitor, and what causes this competence to change is not completely understood.

While it has been shown that extrinsic signaling factors play a role in fate acquisition (such Notch, Jak/Stat, BMP, and Shh signaling as well as various growth and neuronal factors), RPCs seem to exhibit the same temporally restricted competence and generate neurons of the same relative abundance as seen in the retina when they are cultured away from their native signaling evnironment[23-27]. This implies a model where both intercellular signaling and cell autonomous mechanisms regulate developmental timing and fate choice, which is ultimately achieved through the activation of different transcription factors which instruct different retinal cell types[19,22,28,29]. Some genes have been implicated in the switch from early-to-late progenitors, such as Ikaros, Nfi factors, and the miRNA processing gene Dicer, but no comprehensive model currently exists to describe the mechanism of this competence shift[30-33]. Moreover, it is not known precisely how any given post-mitotic precursor initially begins the upregulation of factors that fix the cell along one cell fate trajectory versus another and the degree to which this process is stochastic versus deterministic.

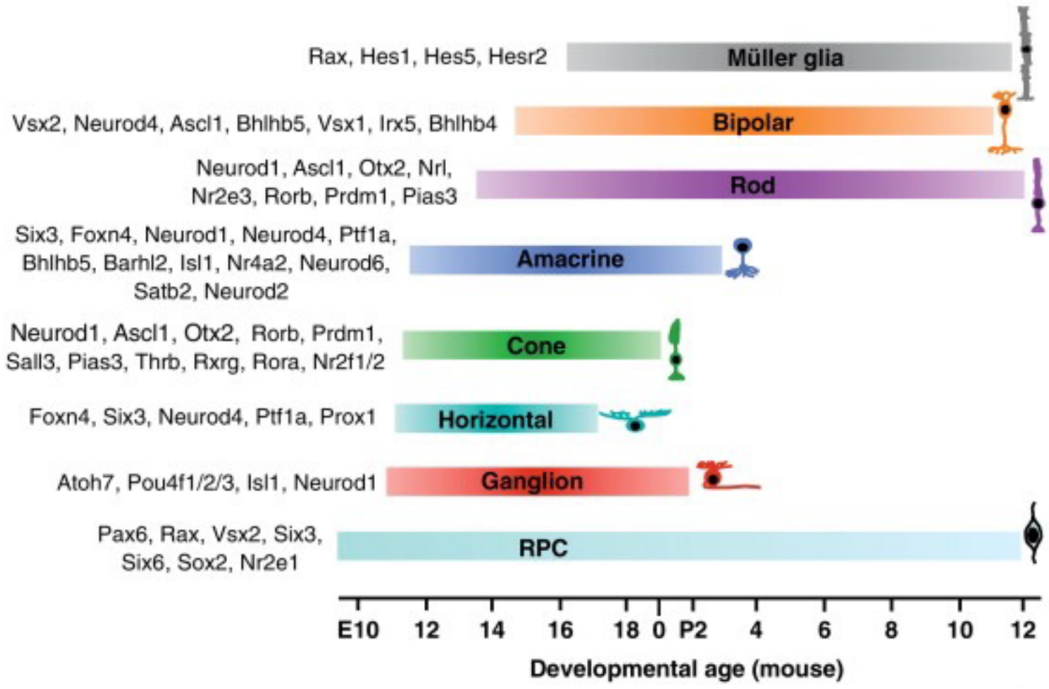

Fig 1.02 Developmental timeline of mouse retina (Basset and Wallace 2012).

However, much is known about how the molecular profile of the retina changes over developmental time and what genes are key regulators for each major cell type in the retina. In this section I will review murine retinal development, focusing on the various transcription factors involved with the specification and survival of the major cell types such to provide the reader with sufficient knowledge of how these cell types are identified molecularly and an understanding of the rationale for the different gene perturbations used in my thesis work.

Embryonic retina

The first neurons to appear in the retina are RGCs, followed shortly thereafter by photoreceptors, horizontal, and then amacrine cells. Many of these cell types continue to be born postnatally, for instance, peak production of rods occurs around P0. At the onset of neurogenesis, a pool of Sox2+, Vsx2+ dividing RPCs transiently express the basic helix-loop-helix (bHLH) proneural pioneering transcription factors Neurog2/Ngn2 and Atoh7 upon exiting the cell cycle, giving rise to postmitotic retinal precursor cells [34]. This population differs from one another transcriptomically as they become restricted along a distinct cell fate trajectory. Below, I will detail the transcription factors that play key roles in the regulatory networks that give rise to each cell type during this developmental window.

RGCs

RGC fate determination is a topic of utmost importance for my thesis work; it is also a topic with an interesting and somewhat contentious history of discovery. One key gene known to be critical for RGC development for some time, largely due to the work of Tom Glaser, Lin Gan, and

colleagues, is Atoh7 (aka Math5). Atoh7 is expressed post mitotically prior to differentiation of the retinal precursor[35-37]. Early lineage tracing experiments in mice have shown Atoh7 expressing cells give rise to every retinal cell type, but heavily biased towards RGCs, cones, amacrine cells, and horizontal cells – all early born cell types[38-40]. However, conditional Atoh7 KO experiments in mice have shown only RGCs are depleted, with a corresponding increase in cone cells[41-43]. While homologues of Atoh7, such as the xenopus Xath5 and drosophila Ato, have been shown to bias the production of RGCs when overexpressed in the developing retina, this has not been shown to be the case with Atoh7[36]. Further, misexpression of Atoh7 in either Crx+ or Ascl1+ progenitors does not lead to an overabundance of RGCs[44,45]. Finally, misexpression of either NeuroD or Ascl1 in place of Atoh7 in early progenitor cells does not bias against RGC production[45,46]. Thus, the activity of Atoh7 has historically been thought to serve a permissive, rather than instructive role in the RGC lineage.

One recent study suggests Atoh7 merely promotes RGC survival and some aspects of maturation, rather than directly driving fate. In this study, the concurrent knockout of Atoh7 with the pro-apoptotic factor Bax in early mouse RPCs resulted in a substantial but transient population of RGCs[47]. However, this finding has an alternative interpretation. Significant culling of RGCs via apoptosis occurs during normal retinal development[48]. Further, a fraction of RGCs has already been shown to be present in Atoh7-null retinas, suggesting not all subtypes require Atoh7[41-43,49,50]. Thus, perhaps this population is normally culled to small numbers during development but is found in greatly increased numbers in Bax-deficient mice. Further, Atoh7 directly binds to the regulatory regions of two other genes critical for the development of RGCs, Pou4f2 and Isl1, and has been shown to activate the Pou4f2 promoter in a reporter construct[51,52].

Finally, and most confoundingly, in some contexts misexpression of Atoh7 indeed does bias the RGC fate, suggesting Atoh7 may still have some instructive function in specifying RGCs[44,46,53,54].

While the exact role of Atoh7 in the RGC lineage remains unclear, two other genes have emerged as being both necessary and sufficient for the production of RGCs from early progenitor cells: Pou4f2 and Isl1. Pou4f2 is expressed selectively in RGC precursors and expression is maintained in a significant subset of RGCs[55,56]. Pou4f2 is involved with the activation of other RGC genes, such as Pou4f1[57,58]. Conditional Pou4f2 knockout results in a similar phenotype to the conditional Atoh7 knockout with ablation of most RGCs; the remaining RGCs express markers of amacrine and horizontal genes as well[56,59,60]. Isl1-null retinas still initially generate RGCs, however Pou4f2+ RGCs are lost with time, with only 5% remaining by P16[61]. Further, Pou4f2 and Isl1 form a complex to co-regulate RGC genes and co-expression of the two factors in RPCs has been shown to be sufficient to rescue RGC ablation in a conditional Atoh7 knockout in mice[61-64]. Mice that express Pou4f2 and Isl1, but not either alone, in lieu of Atoh7 will develop RGCs and optic nerves without an obvious decrease in other cell types[64]. The above, when taken together, suggest a central role for Pou4f2 in the specification of the RGC fate, with Isl1 being necessary for the survival and possibly differentiation of RGCs in the retina and establishes these genes as being sufficient for RGC genesis without a requirement for the upstream factor Atoh7.

Additional factors have also been shown to be important for RGC fate acquisition or survival, such as Dlx1 and Dlx2 and the SoxC family transcription factors. Dlx1/Dlx2-null mice show

substantial RGC reduction due to the apoptosis of late-born RGCs[65]. The SoxC factors, in particular Sox4 and Sox11, are redundantly required for RGCs in mice, with individual knockouts only modestly reducing RGC numbers[66].

Photoreceptors

The first photoreceptors to appear are cone cell at E12, followed by rod cells a day later, though most rod cells are formed later in development, including postnatally. Photoreceptor precursors upregulate Otx2, shown through conditional knockout experiments performed in mice to be necessary for both rod and cone development (in addition to bipolar and horizontal cells)[67,68]. Additionally, Otx2 is required for photoreceptor survival – knockout in adult mice causes degradation of the photoreceptor layer[69]. Otx2 has been shown to drive expression of the cone-rod homeobox gene (Crx), which co-regulates many photoreceptor genes alongside Otx2[70-73]. However, a distinct set of genes are activated in rod cells versus cones. Rorβ is an early fate-determination factor for rods; the knockout model in mice fails to develop rods, with an overabundance of S-cones observed[74,75]. Overexpression of Nrl rescues rods in this model, suggesting Nrl acts downstream of Rorβ to specify rod cells[75]. Nrl has separately been shown to be both necessary and sufficient to drive the rod lineage via conditional knockout and overexpression studies[76-78]. Nrl drives the expression of Nr2e3, which both represses cone lineage genes while also activating rod genes alongside Nrl and Crx[78-82].

Horizontal and amacrine cells

Through lineage tracing and conditional knockout experiments, it has been shown that retinal precursors expressing Foxn4 and Ptf1a give rise to both amacrine and horizontal cells[83-85].

Downstream of these, Prox1 plays a key role in fating the precursors to become horizontal cells. Overexpression of Prox1 biases horizontal cells, which express markers of terminal differentiation such as Lim1[86]. Prox1 knockout results in a complete loss of horizontal cells[86]. Interestingly, Prox1$^{-/-}$ mice do not develop an overabundance of amacrine cells, suggesting this population does not switch to the amacrine fate by default[86]. Despite this, precursors which express Ptf1a but not Prox1 will develop as amacrine cells. There are other genes involved in the specification of horizontal and amacrine cells (such as Onecut NeuroD factors), but these genes are not specific to these cell fates, rather they are expressed in differing combinations in multiple cell types[87,88].

Late embryonic and postnatal retina

The potency of RPCs is restricted across developmental time[23,89]. The early born cell types above are largely no longer produced in the postnatal retina. Further, peak production of bipolar cells and MG occurs postnatally. One exception to this is rod cells, which are produced nearly throughout the entirety of retinal development, with peak production happening around P0. How exactly a switch in competency from early to late progenitor cells is regulated is not well understood. However, some differences in the gene expression of early vs late neurogenic precursors have been observed, which coincide with the shift in cell type genesis[33]. Most notably, there is a shift in expression in the basic bHLH transcription factors Ngn2 and Atoh7 to Ascl1. While Ngn2 and Atoh7 lineage traces marks all cell types with a bias towards earlier retinal cell types, Ascl1 traces bias later born cell types, marking almost no RGCs[40,90]. The role of the various bHLH genes in retinal development will be explored in more detail below. In this

section, I will discuss the transcription factors that play instructive roles in the specification of the late born cell types, bipolar cells, and MG.

Bipolar cells

Bipolar cells are considered a sister cell to photoreceptors. Both are derived from the Otx2 lineage, and bipolar cells likely evolved from a common ancestral cell to the photoreceptors – one which synapsed directly onto RGCs in ancient retinas[6,91]. There are a few genes that play both cross-repressive and activating roles in the photoreceptor versus bipolar cell decision of $Otx2^{+}$ cells. Vsx2 plays a central role in specifying bipolar cells. Vsx2 is expressed in progenitor cells but is upregulated in bipolars[92,93]. Otx2 has been shown to upregulate Vsx2 by binding to a specific enhancer region that is only active in bipolar cells and not photoreceptors[94]. Conversely, another gene downstream of Otx2, Prdm1, has been shown to suppress the bipolar fate in developing photoreceptors and can bind and repress the Vsx2 enhancer[95,96]. Vsx2 can also bind and repress the Prdm1 enhancer, and overexpression of Vsx2 results in an overabundance of bipolar cells at the expense of rods[97,98]. This suggests a cross-repressive mechanism exists to bias Otx2+ cells to become either photoreceptors or bipolar cells depending on the activities of downstream targets Vsx2 and Prdm1.

Müller glia

MG are the final cell type made in the retina, their genesis ending shortly after no new neurons are made. MG are somewhat unique in that the factors known to be involved with specifying this cell fate are not solely expressed in the postmitotic precursors but rather are mostly genes that are also expressed in progenitor cells, including Lhx2, Sox9, and the Hes family bHLH

factors[99-104]. The Hes factors, Hes1 and Hes5, are particularly important. While both genes are expressed to some extent in progenitor cells, Hes1-null retinas will develop with all cell types except MG, while Hes5-null retinas produce roughly 50% fewer MG[104,105].

Hes1 has further been shown to repress expression of proneural bHLH factors[106,107]. In neural progenitor cells derived from brain, it has been shown that oscillatory activities of Ascl1 and Hes1 can act to maintain potency, while sustained expression of either will promote neurogenesis or gliogenesis, respectively[108-110]. Although this oscillatory relationship has not been demonstrated specifically in retinal progenitors, it is consistent with roles of Hes and Ascl1 factors in driving glial vs neuronal fates in the retina.

Finally, Hes1 and Hes5 are notch effector genes[111]. Notch signaling plays a complex role in MG fate acquisition. Active notch signaling in the developing retina is required to maintain the progenitor pool and Hes1 expression; inhibition of notch with the γ-secretase inhibitor DAPT halts retinal development by inducing neuronal differentiation[102,112]. However, while notch signaling is reduced in differentiating neurons, it is initially maintained in postmitotic MG[113]. Further, misexpression of the notch intracellular domain (NICD) in postmitotic retinal precursors induces them to acquire glial features, suggesting notch may directly promote the specification or maturation of MG[31,112].

Neuron loss from degenerative diseases and damage to the retina

Now that we have established the key molecular processes that give rise to the diversity of neurons of the retina and their respective functions, I will outline the processes that result in loss

of specific neurons in common retinal disorder. Nearly every major cell type of the retina can be lost from various degenerative diseases, however the most common diseases result in the loss of photoreceptors (macular degeneration and retinitis pigmentosa) and RGCs (glaucoma and diabetic retinopathy). Below, I will briefly review the most common degenerative diseases by the retinal layer affected, and what is known of the molecular process involved in each pathology.

Photoreceptor layer

Age-related macular degeneration (AMD): Accounting for 6-9% of blindness globally, AMD is the most common degenerative disease of the retina[1]. In AMD, the most pronounced changes occur in the macula which over time results in central vision loss. The exact cause is not known, but multiple factors have been found to contribute to risk: age-related changes, genetics, and environment and lifestyle (such as exposure to cigarette smoke). Drusen, a subretinal fatty deposit often present with age, builds up in excess with AMD. This may occur due to a dysfunction of the retinal pigment epithelium (RPE), possibly due to pathology of the local vasculature, decreasing oxygen and nutrient supply for the RPE and photoreceptors while also reducing clearance of lipoprotein deposits. In the healthy retina, these lipoproteins are secreted into the vasculature by the RPE, which is involved with photoreceptor outer segment turnover.

As the disease progresses the drusen continue to build, a local inflammatory response is seen, and a breakdown of basement membrane occurs. The RPE layer degrades and photoreceptor cell death follows – this is known as "dry AMD." Microvasculature may also form; rupture and leaking of fluid from this vasculature ("wet AMD") can quickly lead to blindness. Often, the rod

cells will die before the cone cells with AMD, leading first to loss of low-light vision[114]. Little can be done to prevent dry AMD from progressing; wet AMD can be treated by targeting Vascular Endothelial Growth Factor (VEGF) to slow down and potentially reverse some neovascularization[115].

Retinitis pigmentosa (RP): RD is the most common cause of vision loss in those under 60 years old. RP comprises a group of inherited disorders that cause the degenerative loss of photoreceptors, primarily rods, resulting in night blindness that progresses to concentric vision loss (tunnel vision) and finally central vision loss. Many different genes can be affected, which can be inherited in either an autosomal-dominant, autosomal-recessive, or X-linked fashion. In 20-30% of cases other systems are also affected which can result in hearing loss, cognitive defects, and other symptoms depending on the genes affected. Of the at roughly 45 mutations discovered so far that lead to RP, many are involved with rod cell structure or function such as phototransduction, vitamin A metabolism, and formation of the outer segment[116].

Because many different biochemical pathways can be affected, the exact cause of cell death can vary. For instance, rhodopsin mutations, which are quite prevalent in this disease, may result in the formation of the accumulation of a toxic misfolded protein. In the case of mutated cGMP-phosphodiesterase subunits, excessive cGMP concentrations lead to a toxic influx of Ca^{2+} ions. Any loss of cone cells, however, is thought to be indirect and due to the primary loss of rods[116].

Treatment options depend on the underlying cause of the disease. For most patients, only supportive treatment is available. For patients who are completely blind, there is an FDA-

approved retinal implant available that shows a modest restoration of sight over control that is stable for years, however, there are risks associated with serious adverse events[117]. Most excitingly, RP is the first retinal disease with an FDA approved gene therapy treatment. It is an AAV-based therapy that delivers a functional, wildtype gene to patients with biallelic loss-of-function RPE65 mutations. However, it is of limited availability to most due to cost and will not help patients with severe cell loss[118]. There are also numerous ongoing clinical trials of other gene and cell therapies, but no other FDA-approved treatments at this time[119].

Ganglion cell layer

Glaucoma: Glaucoma is the second leading cause of blindness worldwide and the leading cause of irreversible blindness. Glaucoma results in damage to the optic nerve and loss of RGCs. This results initially in loss of peripheral vision but can progress to blindness. The disease is characterized by an obstruction of aqueous humor outflow, either due to anatomical narrowing that restricts drainage from the anterior chamber (angle closure type) or restricted drainage despite an open anatomy (open-angle type). This often results in an increase in intraocular pressure (IOP). Malformations at the optic nerve head result in damage to the RGC axons, impeding axonal transport and eventually resulting in cell death.

The primary damage occurs at the lamina cibrosa, a perforated structure found at the base of the optic nerve head. RGC axons run through the pores of the lamina cibrosa which provides support to the nerve bundle. In glaucoma, this structure becomes deformed, especially so with high IOP. However, pressure is not the sole cause of the disorder as these malformations and subsequent optic nerve damage can occur with normal IOP.

Finally, many mutations have also been shown to be associated with glaucoma. It is not clear how most of these mutations influence the pathology, however it is suspected that mutations of some genes, such as Six6, result in dysregulation of pathways involved with RGC survival making them more susceptible to glaucoma-induced cell death[120]. As the molecular mechanisms outside of IOP that contribute to the disease are not well understood, the only therapeutics that exist aim to reduce the progression of the disease by lowering IOP.

Diabetic retinopathy (DR): The pathology of DR is complex and involves a number of deleterious changes in the retina. Hyperglycemia due to diabetes leads initially to two primary observations: neurodegeneration and changes in the microvasculature. Mitochondrial dysfunction from high glucose levels induces apoptosis of neurons, largely of RGCs but loss of amacrine cells and sometimes photoreceptors is also observed. Meanwhile, dilation of the blood vessels and apoptosis of pericytes, which provide structure support to the capillaries, leads to microaneurysms and capillary occlusion. Chronic inflammation also contributes to epithelial cell loss. All this in turn results in hypoxia of the retina and upregulation of VEGF, which drives abnormal neovascularization. These vascular changes can result in leakage of fluid into the retina which can cause a buildup of IOP and subsequent glaucoma, resulting in further loss of RGCs. Additionally, retinal detachment is also possible from the microvasculature changes[121]. There are various treatments currently available that target different aspects of the pathophysiology. The primary FDA-approved treatments consist of anti-VEGF therapies to target neovascularization[122]. However, other therapies targeting inflammatory pathways and

mitochondrial function are also used. Managing the underlying diabetes can also prevent future tissue damage.

Interneurons

While less common, there are also some diseases that lead to loss of cells in the INL, bipolar and amacrine cells. While not necessarily specific to cells in the INL, certain retinal ischemia can result in loss of bipolar cells. For instance, in retinopathy of prematurity (ROP), retinal vascularization is temporarily halted due to administration of supplemental oxygen to babies born prematurely. This is followed by a period of hypoxia in the retina with removal of supplemental oxygen, and then destructive neovascularization. In mouse models of ROP, developing mice (P7) are kept in a hyperoxic environment for 5 days and then transitioned to a normoxic environment at P12. While this results in loss of RGCs, the INL also thins, with a notable loss of bipolar cells, before neovascularization occurs while the retina is hypoxic[123].

Retinal damage

Finally, outside of degenerative disease, physical damage to the retina can also result in loss of specific neurons. The most common causes of retinal damage include retinal tears and detachment, and light damage. In all cases, photoreceptors are the main cell type lost in the neural retina. With retinal detachments and tears, the photoreceptors become separated from the RPE leading to cell death. With overexposure to light, photooxidative stress causes loss of rod cells and, indirectly, a subsequent loss of cones[124].

Regeneration of the retina in non-mammalian vertebrates

While loss of neurons in the mammalian retina from damage or disease is permanent, other vertebrate species are capable of varying degrees of retinal regeneration. The zebrafish, for instance, is capable of fully regenerating the retina after extensive cell loss[125]. Studies into the molecular processes that guide regeneration of the zebrafish retina have shed light on key genes involved that have directly inspired efforts to induce regeneration in the mammalian retina. Because of this, I will focus this review on insights gleaned from zebrafish studies, with some discussion on relevant findings from studies in the avian retina.

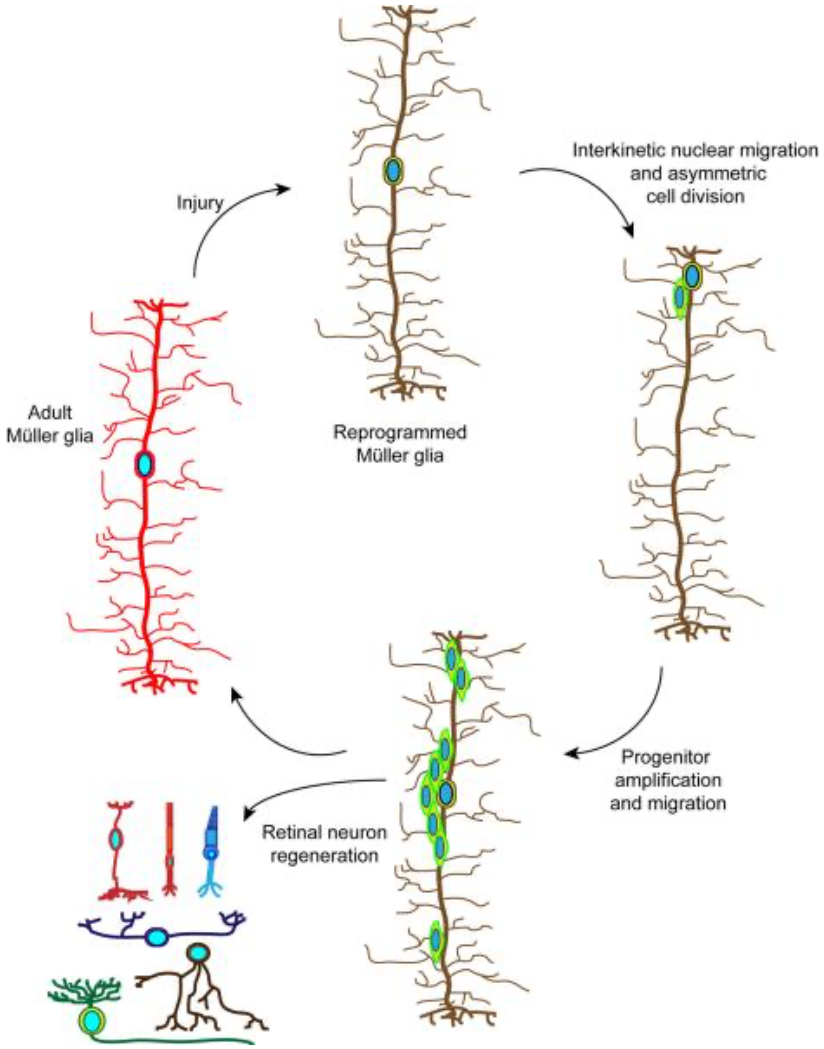

Figure 1.03: Retinal neuron regeneration from Muller glia (Goldman, 2014).

A large body of work, dating as far back as 1948, has established teleost fish as invaluable model organisms for studying retinal regeneration in a variety of damage contexts – optic nerve transection, light damage of photoreceptors, chemical ablation, and even surgical removal of whole patches of retina can be functionally restored[126-129]. A series of lineage-tracing experiments, foundationally in limited regeneration-competent chick retina and later in zebrafish, have definitively demonstrated that MG are the source of new neurons in the regenerating retina of teleosts[130-133]. In the mammalian retina, MG respond to retinal damage with hypertrophy, an upregulation of cytoskeleton genes such as GFAP, and a release of inflammatory cytokines. In zebrafish, damage initially induces a similar gliotic response in the MG, however this is transient and is followed by dedifferentiation and proliferation of the MG. These MG-derived progenitor cells then give rise to neural precursor cells that differentiate into all the major cell types of the retina (Figure 1.03)[125,134,135]. This regeneration response is complete in zebrafish, in that all retinal neurons are produced, regardless of the method of damage[136].

Signaling environment differences between the zebrafish and mouse retina

Underlying the different responses between fish and mammalian MG to retinal damage are differences in signaling and gene expression patterns. Unlike mammals, teleost fish continue to grow throughout their life, this includes constant development along the edge of the peripheral retina in the ciliary margin zone (CMZ)[137]. Perhaps due to this difference in developmental context, different signaling factors are acting on MG in the undamaged zebrafish than the fully mature MG of the adult mouse retina. One notable difference is notch signaling. In the zebrafish retina, notch signaling is active throughout adulthood and is thought to keep MG in a quiescent state – repression of notch signaling in the uninjured retina with γ-secretase inhibitor

RO4929097 is sufficient to stimulate MG to re-enter the cell cycle and give rise to some neural precursor cells[138]. Further, notch signaling is suppressed in zebrafish MG in response to injury and increases again after the regeneration response[139,140]. In mouse, notch activity is largely absent in the adult retina. Instead, notch signaling serves to maintain a pool of RPCs in the developing retina; inhibition of notch with DAPT during retinal development induces the progenitor cells to acquire a neural fate[113]. However, in later stages of postnatal development notch activity increases, peaking towards the end of neurogenesis, and is required for the postmitotic acquisition of glial gene expression[113]. Differences in signaling contexts such as this may underpin the differences observed between zebrafish and mouse MG in their response to injury.

Gene regulatory mechanisms of retinal regeneration in zebrafish

Efforts to understand the initial changes in gene expression that drive the regeneration response in zebrafish and chick MG have uncovered a few key regulatory factors that are never expressed by mammalian MG after injury. Early studies in the injured chick retina showed evidence of MG re-acquiring markers of retinal progenitor cells, such as the proneural bHLH factor Ascl1 (also known Mash1 and Cash1) as well as homeobox gene Vsx2 (also known as Chx10)[130]. Subsequently, Ascl1 was also found to be expressed in zebrafish MG after injury, and morpholino knockdown of Ascl1 prevented the regeneration response[141]. Further, with RO4929097 inhibition of notch in uninjured zebrafish retina, Ascl1 was also activated in MG prior to a proliferation response. However, this same study showed that RO4929097-induced neural precursors quickly died off unless treated with the proinflammatory cytokine TNFα, which is produced by dying retinal neurons and activated microglia[138]. Further, morpholino

knockdown of TNFα in the injured zebrafish retina inhibited Ascl1 expression and subsequent MG proliferation[142]. Taken together, this suggests that Ascl1 expression, while critical for MG dedifferentiation, may not be sufficient to drive the full regeneration response in MG without further gene regulatory events induced by additional signaling factors.

Exactly how Ascl1 expression reprograms MG into multipotent retinal progenitors is not fully understood. However, it is likely that Ascl1 co-operates with other key genes to carry out its effect. Lin28, an RNA-binder and known potency factor expressed in embryonic stem cells and neural progenitor cells, is another gene been found to be activated in MG alongside Ascl1 upon retinal damage in zebrafish[143-145]. Further, knockdown of Lin28 prevents MG proliferation in response to damage, suggesting an essential role in retinal regeneration[141]. Despite this, transgenic overexpression of Ascl1 and Lin28 in the zebrafish MG is not sufficient to drive a complete reprogramming response in uninjured retina, only limited proliferation is seen, further underlining the importance of damage-induced signaling in MG reprogramming[146].

Efforts to regenerate neurons in the mammalian retina

Knowledge gained from foundational studies into the regeneration of fish and chick retinas have in recent years been mobilized in efforts to stimulate regeneration in the mammalian retina. Much of these initial efforts were carried out in the Reh lab by former and current graduate students and postdoctoral scholars. Below I chronicle the major studies in mouse retinal regeneration that underpin my thesis work.

Reprogramming cultured MG with Ascl1

MG in zebrafish upregulate Ascl1 to drive the regeneration response to retinal injury, while mouse MG do not. To test the hypothesis that forced expression of Ascl1 can reprogram mammalian MG into neurogenic retinal progenitors, initial experiments were carried out *in vitro* in cultured mouse MG. Dissociated P12 mouse retina, after neurogenesis is complete, yields a mostly pure culture of MG when plated, with minimal surviving neurons or astrocytes. As the MG undergo some cell division in culture, EdU can be used as a method of lineage tracing for the purposes of identifying any MG-derived neurons, as EdU will not be incorporated into any surviving neurons on the plate. Using EdU-labelled cultured MG, *Pollak et al.* found lentiviral overexpression of Ascl1 reprogrammed these MG into cells that express markers of neural progenitors, like Hes6 and Olig2. Further, these cells downregulated MG genes such as Rlbp1 and Slc1a3 and expressed the neural marker beta tubulin (Tuj1). The reprogrammed MG also gave rise to cells with a neuronal morphology that co-expressed Otx2 and Isl1, indicative of bipolar cells[147].

Stimulation of retinal regeneration in young mice

Given the encouraging *in vitro* results, future studies were carried out *in vivo* to see if Ascl1 could also reprogram MG in live mice to induce a retinal regeneration response. An initial study carried out by *Ueki et al.* utilized a multi-transgenic mouse model that contained the following transgenes: a Glast-CreER knockin for conferring MG specificity, CAGG-Cat-GFP for lineage tracing (abbreviated CC-GFP; the Cat gene is flanked by loxP sites), Rosa-LNL-tTA, and TRE-Ascl1-GFP (found insufficient for lineage tracing purposes). Tamoxifen injections into these mice result in MG-specific overexpression of Ascl1-GFP and an additional GFP. In this study,

Ascl1 overexpression in MG alone did not drive neurogenesis. However, given the requirement for damage-induced signaling for retinal regeneration in zebrafish, it was hypothesized that Ascl1 overexpression may only reprogram mouse MG in the context of retinal damage. To test this hypothesis, intravitreal injections of the excitotoxin NMDA were administered after activation of Ascl1 with tamoxifen. With this treatment combination, GFP-lineage traced neurons appeared one week post treatment. These neurons were found to have a morphology reminiscent of a bipolar cell and were positive for Otx2 and the bipolar marker Cabp5. However, this effect was only seen with treatment in young mice – no neurons are regenerated in mice treated after P16. In adult mice, Ascl1 overexpression combined with either NMDA or light damage only partially reprograms MG, with a reduction in MG marker Sox9 and some Otx2+ cells observed; no markers of mature neurons were seen with this paradigm[148].

Stimulation of retinal regeneration in older mice

The team hypothesized that prohibitive changes in chromatin occur in the MG as they mature into adulthood that limit downstream gene activation during Ascl1+NMDA reprogramming. To test this hypothesis, *Jorstad et al.* introduced an additional treatment, the histone deacetylase inhibitor tricostatin-A (TSA), a class of drugs known to relax chromatin structure through increased histone acetylation. In this paradigm, TSA was injected intravitreally following Ascl1 induction and NMDA-induced damage (this treatment is referred hereafter as ANT) (Figure 1.04). This treatment successfully induced GFP-traced neurons in the INL of adult mice. As assessed by immunostaining and single-cell RNA-sequencing (scRNA-seq), the regenerated neurons showed morphologies and gene expression profiles largely indicative of bipolar cells, consistent with the MG-derived neurons generated in young mice. Further, these bipolar cells

were shown to integrate into the circuitry of the retina and respond to light stimulus with rapid changes in polarization[149].

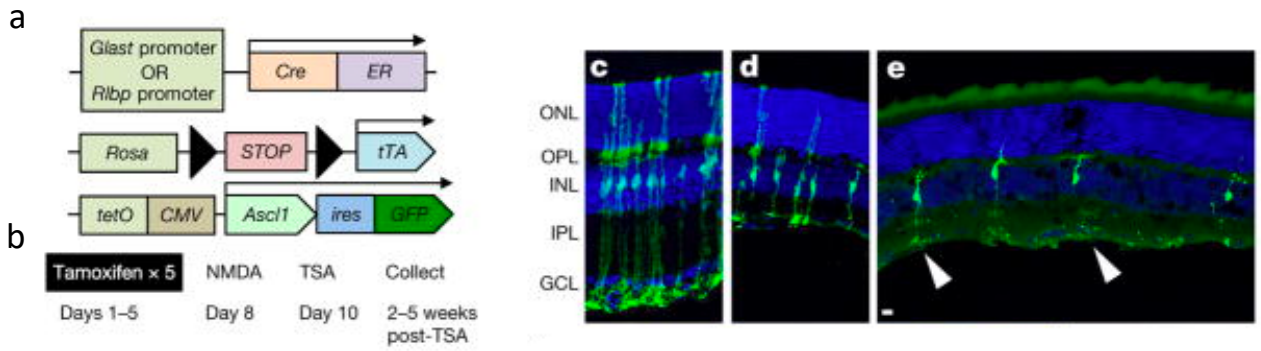

Figure 1.04: Stimulation of retinal regeneration in adult mouse. (a) Genotype of mouse. (b) Schematic of experimental paradigm. (c) Tamoxifen injection in undamaged retina does not reprogram MG. (d-e) NMDA damage with TSA treatment leads to MG-derived neurons[149].

While it is remarkable that Ascl1 can induce a regenerative response to injury in a mammalian retina, the neurons regenerated are limited to bipolar cells and overall efficiency is low. Further, it is unknown whether these regenerated neurons might help functionally restore vision in an appropriate disease model. As the most common retinal diseases result in the loss of either RGCs or photoreceptors, functional regeneration of these cell types remains an imperative. In the next chapter, I will discuss efforts to regenerate other retinal cell types, with a focus on our successful approach to regenerating RGC-like cells in the mouse retina.

Chapter 2:

Regeneration of RGC-like cells in the adult murine retina

(Text and figures modified from *Todd & Jenkins, et al., 2022)*

Introduction

In recent years many attempts have been made to improve retinal regeneration in mice. As overall efficiency of Ascl1-induced regeneration is low, one area of interest in the Reh lab has been to increase the conversion rate of MG to neurons following treatment. Three notable strategies have been found to enhance reprogramming efficiency. In *Jorstad et al., 2020* it was found that treatment with SH-4-54, an inhibitor of Stat3 phosphorylation, alongside TSA in the ANT regeneration paradigm resulted in a doubling of efficiency compared to ANT alone[150]. Stat3 signaling in MG is increased with retinal damage; in regenerative species, inhibiting this signaling pathway has been shown to reduce the number of MG that express Ascl1 and re-enter the cell cycle[151,152]. However, it has been shown in the chick retina that after induction of MG-derived progenitors with NMDA damage, inhibition of Jak/Stat signaling reduces neurogenesis and biases the MG fate[151]. These findings suggest that Jak/Stat signaling is involved with the initial MG reprogramming event in response to damage in regenerative species, but sustained Stat3 activity in mouse MG after damage inhibits neurogenesis.

Another successful approach to increasing neurogenesis during mouse retinal regeneration has been through the ablation of microglia[153]. In the chick and zebrafish retinas, microglial ablation inhibits regeneration in response to damage by reducing the number of MG-derived progenitors that appear in response to damage[154,155]. However, in *Todd et al., 2020*, it was shown that chemical ablation of microglia prior to ANT treatment doubled the efficiency of neuron conversion; a corresponding decrease of inflammation-reactive MG was also seen[153]. Further, treatment with TNFα, an inflammatory cytokine that is necessary for inducing the formation of MG-derived progenitors in fish, resulted in a reversal of the conversion efficiency mediated by

microglia ablation[153]. These findings suggest that, as with Jak/Stat signaling, microglia and inflammatory signaling may induce the formation of MG-derived progenitor cells in regenerative species but inhibit neuronal conversion in the ANT paradigm of mouse retinal regeneration.

Finally, the most successful approach at increasing regeneration efficiency has been through the combined overexpression of Ascl1 with another bHLH transcription factor, Atoh1[156]. While Atoh1 is not normally expressed in the retina, it is another Atonal family transcription factor that shares a high degree of sequence homology[35]. Further, Atoh1 has also been found to efficiently induce neural fates in cultured iPSCs[157]. In *Todd et al., 2021*, we found an 80% conversion rate from MG to neurons with simultaneous overexpression of Atoh1 and Ascl1 in adult mice; reprogramming did not require NMDA or TSA treatment. Further, few neurons were of a bipolar identity, with the majority instead showing some morphological and transcriptomic similarities to amacrine cells and RGCs. However, important markers of the RGC lineage, such as Pou4f1/2, were not found, and the neurons did not fire action potentials[156]. Nonetheless, this study demonstrated that it was possible to influence fate choice of MG-derived neurons through the overexpression of additional transcription factors, and that the need for damage signals can be bypassed – a finding of potential clinical relevance, as it is unknown whether ANT treatment would induce regeneration in the context of lower rates of chronic cell death versus acute and significant retinal damage.

In recent years, other prominent studies have taken combinatorial transcription factor overexpression or knockdown approaches in an attempt to engineer specific cell fates during mouse retinal regeneration[158-160]. Rather than utilizing transgenic mouse models for transcription

factor overexpression and lineage tracing, these studies have all relied on the use of AAVs containing promoters that confer MG specificity. This approach has recently been called into question as specificity of AAVs have been shown to be influenced by the coding sequence following the promoter, and transgenic lineage tracing approaches do not reproduce the results seen in studies employing AAV-based lineage tracing approaches, suggesting the AAVs were labeling endogenous neurons[161,162]. There have been some studies that utilize genetic knockout approaches in mice which have shown some capacity to induce a MG-mediated regeneration response without Ascl1 overexpression[163,164]. However, these approaches have not provided evidence that any neurons other than bipolar cells can be regenerated. Thus, to date, only the combination of two bHLH's, Ascl1 and Atoh1, has been convincingly demonstrated to influence cell fate in a mouse model for retinal regeneration.

In this chapter, we utilized a transgenic mouse model to test whether combining Ascl1 with transcription factors expressed in the RGC lineage during development can specifically regenerate RGCs. Specifically, we explore the effects of combining Ascl1 overexpression with two other TFs of different classes, Islet1, a LIN, Islet1, MEC3 (LIM) homeodomain TF, and Pou4f2, a class IV, Pit-Oct-Unc (POU) homeodomain TF. Both factors have been shown to be important for cell fate determination in the developing retina, with Pou4f2 necessary for RGC differentiation and Islet1 important in the development of several types of retinal neurons including RGCs[56,165].

We find that the expression of Pou4f2 and Islet1, along with Ascl1, in adult mouse MG, directs a subset of the neurons generated by the MG toward a cell fate that resembles RGCs. The MG-

derived RGC-like neurons (i) can be immunolabeled with markers of normal RGCs; (ii) have a transcriptome similar to developing RGCs by single-cell RNA sequencing (scRNA-seq); (iii) have a broader range of electrophysiological characteristics than neurons generated by Ascl1 alone, such as action potentials; and (iv) display a pattern of chromatin accessibility similar to developing RGCs. Together, our results show that neural regeneration from MG can be directed to specific cell types using combinations of developmentally relevant TFs.

Results

Pou4f2 and Islet1 increase the diversity of neurons from Ascl1-reprogrammed MG

We previously developed a mouse where Ascl1 is induced specifically in MG (*Glast-CreER:LNL-tTA:teto-mAscl1-GFP:ccGFP*) by application of tamoxifen. After Ascl1 induction, retinal injury (NMDA) followed by injection of a histone deacetylase inhibitor (TSA) induces MG to express genes associated with developing retinal progenitors and to generate new neurons in the adult mouse retina *in vivo*. Most of these newly generated neurons adopt a bipolar cell fate[149,150,153]. To examine whether expression of additional transcription factors (Pou4f2 or Islet1) can direct the MG-derived progenitors to other neuronal fates, we crossed the *Glast-CreER:LNL-tTA:teto-mAscl1-GFP* mice with a *tetO-Pou4f2-tetO-Islet1* transgenic mouse line (Figure 2.01a;tetO-IPA). This construct encodes *Pou4f2* and *Islet1* separated by two different loxP variants[64]. When exposed to Cre recombinase this cassette allows for expression of either *Pou4f2*, *Islet1*, or sometimes both.

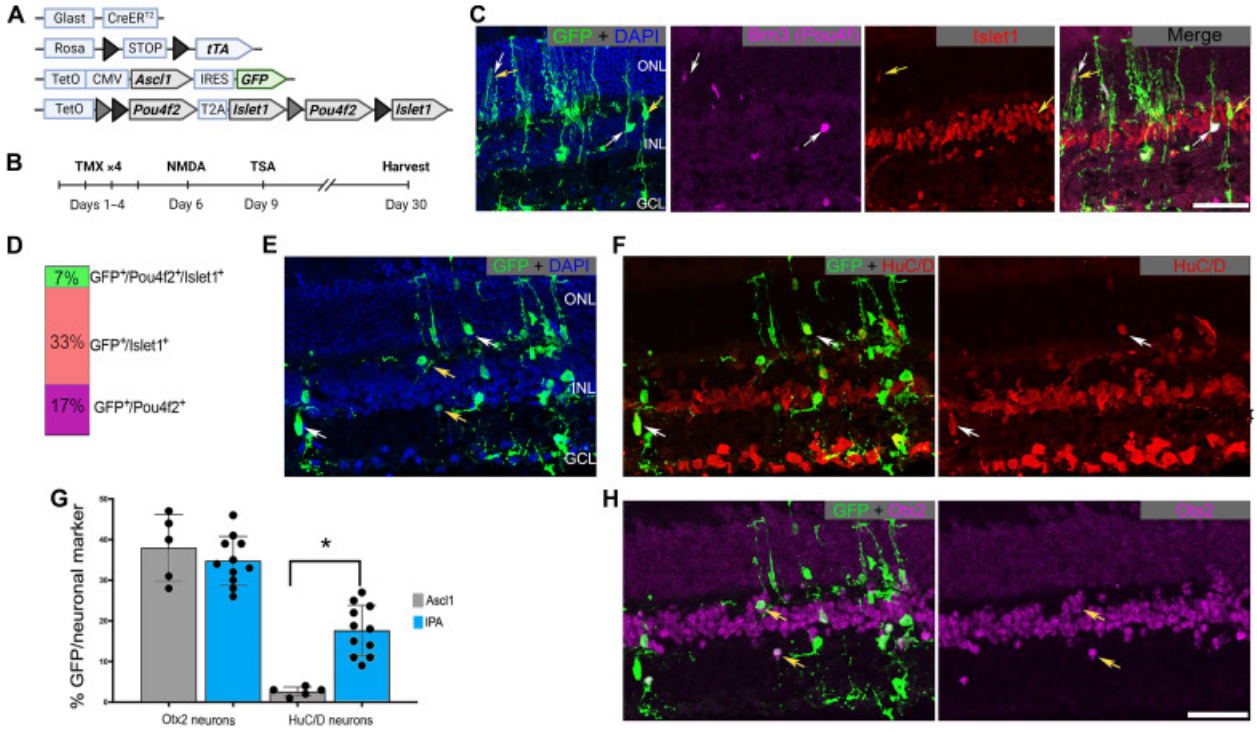

Figure 2.01: Pou4f2 and/or Islet1 stimulate regeneration of RGC-like neurons. (A) Schematic depicting the transgenic constructs used to induce Ascl1 and Pou4f2/Islet1 specifically in MG. Pou4f2/Islet1 is surrounded by mutually exclusive floxed sites, leading to expression of Pou4f2, Islet1, or both in the presence of active Cre. (B) Experimental paradigm to induce retinal regeneration in adult mice. Tamoxifen (TMX). (C) Representative sections of the retina after intravitreal NMDA damage, showing transgenic expression of Pou4f2/Brn3 (purple) and/or Islet1 (red) in GFP$^+$ lineage–traced MG. DAPI, 4′,6-diamidino-2-phenylindole. (D) Quantification of the percent of transgene-expressing MG that express Pou4f2, Islet1, or both. (E and F) Representative sections showing MG-derived neurons after the regeneration paradigm expressing HuC/D (red). (G) Quantification of the percent of GFP$^+$ MG-derived neurons that express either HuC/D or Otx2. (H) Examples of MG-derived neurons expressing Otx2 (purple). Significance of difference was determined using an unpaired t test (asterisk = $p < 0.0001$); dots represent individual animals. Scale bars, 50 μm. ONL, outer nuclear layer; INL, inner nuclear layer; GCL, ganglion cell layer. Mouse schematic was made with Biorender.com.

The tetO-IPA mouse line allows us to test whether MG-reprogramming is enhanced by treatment with Pou4f2+Ascl1, Islet1+Ascl1, or Islet1+Pou4f2+Ascl1 (hereafter IPA). After intraperitoneal application of tamoxifen to induce the transcription factors in MG, we induced a retinal injury by intravitreal injection of NMDA, followed by TSA (Figure 2.01b). The mice were then sacrificed three weeks later for immuno-fluorescence analysis to assess the fate of recombined MG (Figure

2.01c-e). Figures 1c,d show that this protocol induces the transgenes in MG and neurons derived from them (GFP+). We found GFP+ MG-derived cells expressing either Brn3 (Pou4f2) (17%), Islet1 (33%), or both TFs (7%) (Figure 2.01c,d).

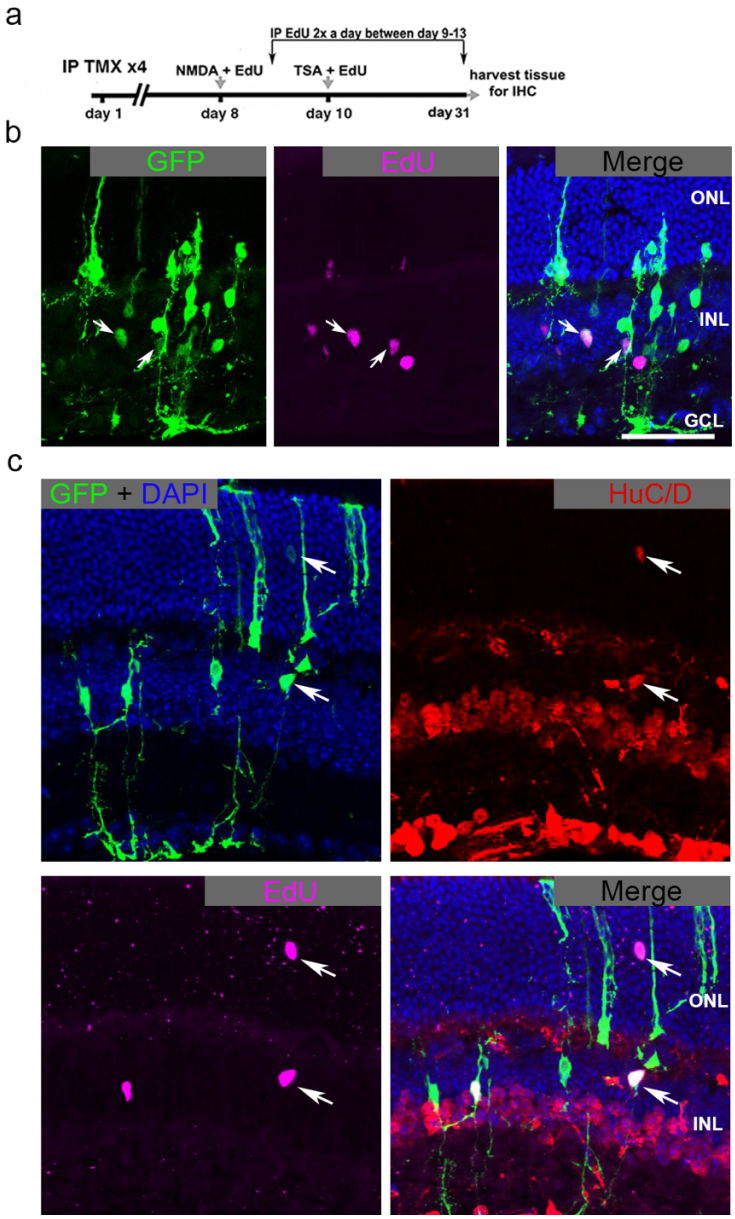

Figure 2.02: A subset of IPA-derived neurons are derived from proliferating MG. (a) Experimental paradigm to label diving cells during the regeneration experiment described in Figure 1. (b) Representative sections showing MG-derived cells (GFP+) that previously underwent cell division (EdU+). (c) Representative image showing some MG-derived neurons (GFP+/HuC/D+) are the result of proliferating MG (EdU+). Scale bars are 50µm. Abbreviations: ONL, outer nuclear layer, INL, inner nuclear layer, GCL, ganglion cell layer.

Additional IHC analysis demonstrated that the IPA combination effectively promoted neurogenesis from MG. The majority of glial-derived cells acquire a neuronal morphology three weeks post-injury (Figure 2.01e). Quantifications of MG-derived cells in retinal sections from IPA-treated mice confirmed that the MG-derived GFP+ neuronal-like cells expressed the ganglion/amacrine marker HuC/D (Figure 2.01f,g) or the bipolar marker Otx2 (Figure 2.01g,h). IPA expression significantly enhanced MG neurogenesis of HuC/D neurons compared to Ascl1 alone (Figure 2.01g). Consistent with our previous reports, a subset of the MG-derived neurons was derived from Edu^{+}, proliferating MG (Figure 2.02a-c). Taken together, these data suggest that the addition of TFs Pou4f2 and/or Islet1 enhances the neurogenic capacity and expands the resulting cell fates of Ascl1-MG *in vivo*.

We had previously found that the combination of Ascl1:Atoh1 could stimulate neurogenesis from MG in the absence of retinal damage[156]. In contrast, IPA-induction in the undamaged retina was not sufficient to stimulate neurogenesis (Figure 2.03a,b,e). We also tested whether MG could undergo neurogenic reprogramming if we activated the IPA factors in MG after NMDA injury and TSA rather than prior to NMDA and TSA as shown in Figure 1. We found that induction of IPA after injury stimulated a small amount of neurogenesis but significantly less than our original paradigm (Figure 2.03c-e).

Since a significant portion of the newly generated neurons in the damaged retina expressed the ganglion/amacrine marker HuC/D, we performed wholemount imaging of IPA-derived neurons to better assess their neuronal morphology. This revealed cells with large branching dendritic

arbors reminiscent of RGCs or wide-field amacrine cells; cells with this morphology were not previously seen with Ascl1 alone (Figure 2.04a-f).

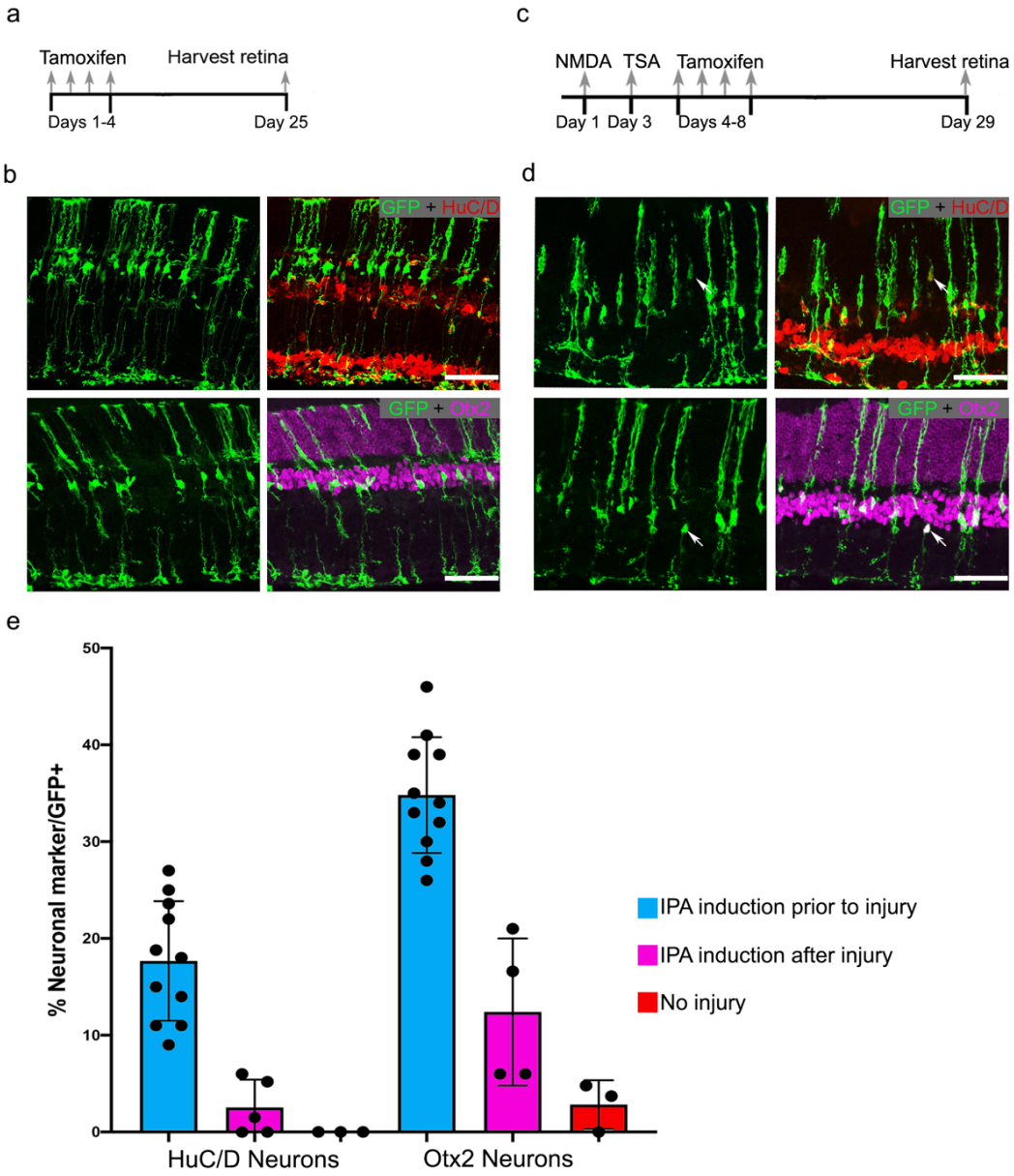

Figure 2.03: IPA-treatment is most effective at reprogramming MG if induced prior to injury. (a) Experimental paradigm using the transgenic mouse described in Figure1 to test whether Islet1/Pou4f2/Ascl1 is able to reprogram MG in the absence of retinal injury. (b) Representative pictures of GFP^+ MG showing no induction of the ganglion/amacrine marker HuC/D (red) or the bipolar marker Otx2 (purple). (c) Experimental paradigm to test whether induction of the IPA-factors after NMDA damage and TSA application can induce MGneurogenesis. (d) Representative pictures of GFP^+ MG showing some co-labeling of the neuronal markers HuC/D (red) and Otx2 (purple). (e) Quantification of the percent of MGderived cells that express HuC/D or Otx2 after IPA-induction prior to injury, after injury, or without injury. Scale bars are 50µm.

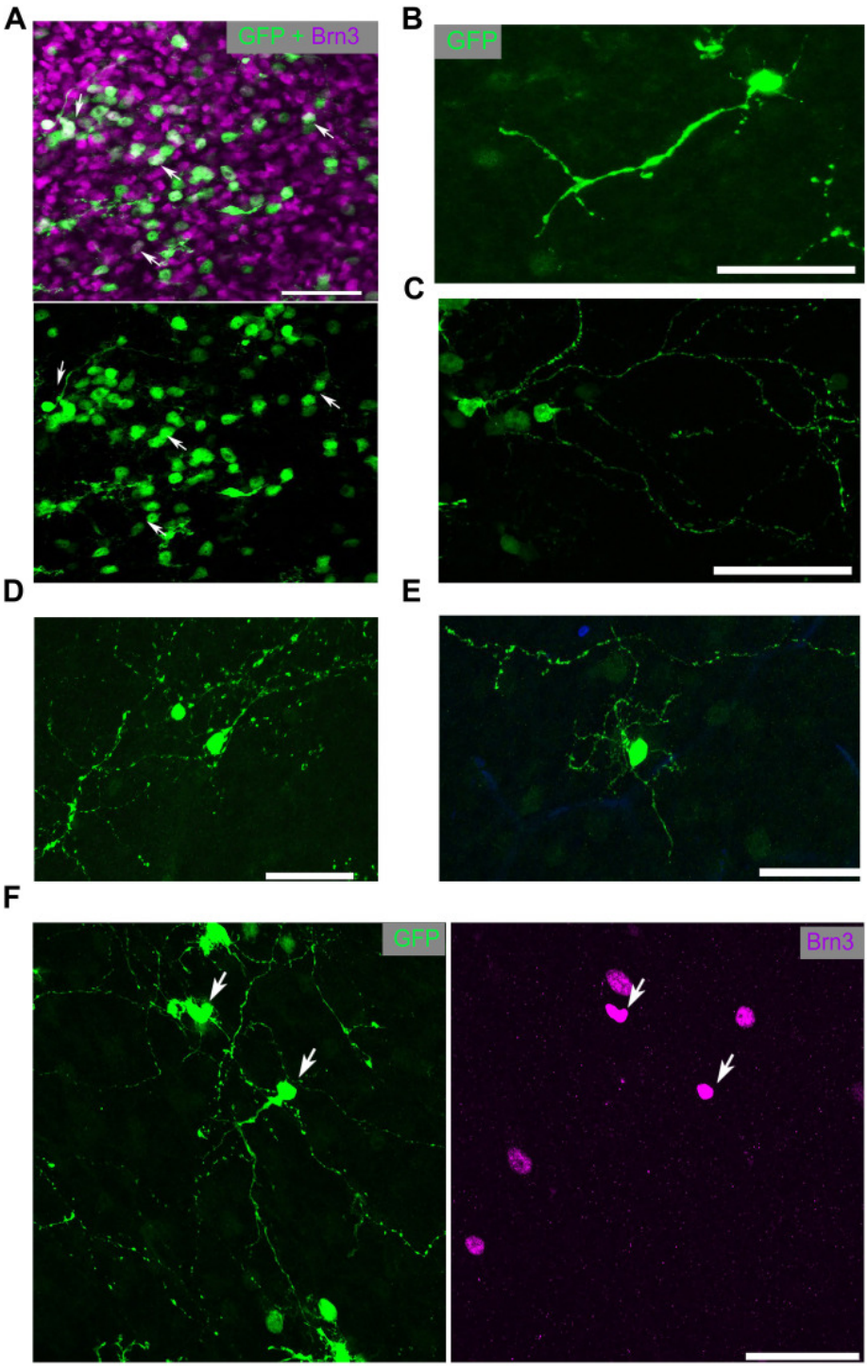

Figure 2.04: IPA-stimulated MG-derived neurons display complex neuronal morphology. (A) Retinal whole mounts stained for GFP (MG-derived cells; green) and Brn3 (purple). (B to E) Examples of the morphology of GFP^+ MG-derived cells. (F) MG-derived (GFP^+) cell with complex neurites colabeled with Brn3 (purple). Scale bars, 50 μm.

Islet1-Pou4f2-Ascl1 induces neurons with an RGC-like transcriptome

We next used single cell RNA sequencing (scRNA-seq) to analyze how Islet1 and Pou4f2 alter the phenotype of Ascl1-mediated MG reprogramming. Three weeks after initiating the IPA regeneration protocol, MG cells and their progeny were FACS-purified and processed for scRNA-seq as previously described[150,153]. To directly compare the changes in cell fates induced by IPA with those caused by expression of Ascl1 alone, we used Seurat to integrate data from IPA-treatment with previously obtained Ascl1-only reprogramming libraries[149] and clustered the cells (Figure 2.05a). The combined data from the IPA experiment and the prior Ascl1 dataset were projected onto a single UMAP plot and clusters of cell types were identified by known marker genes (Figure 2.05b).

The combined UMAP plot of Ascl1-only vs. IPA treatment contains clusters of cell types (eg. MG, progenitors, and bipolar cells) that we have previously observed during Ascl1-mediated reprogramming (Figure 2.05a). Importantly, this analysis revealed two additional phenotypes unique to the IPA condition. First, the neurogenic efficiency of MG is increased over 2-fold with IPA vs. Ascl1 only (Figure 2.05c), which is consistent with our IHC data and suggests that the combination of these three transcription factors potently stimulates neurogenesis from adult MG. Second, a novel cluster appeared after IPA-treatment that did not exist in the Ascl1-only condition (green cluster) (Figure 2.05c). While cells expressing Islet1 but not Pou4f2 were found mostly in the bipolar cluster, cells expressing Pou4f2, with or without detectable Islet1, were largely found in the novel RGC-like cluster (Figure 2.06a-c).

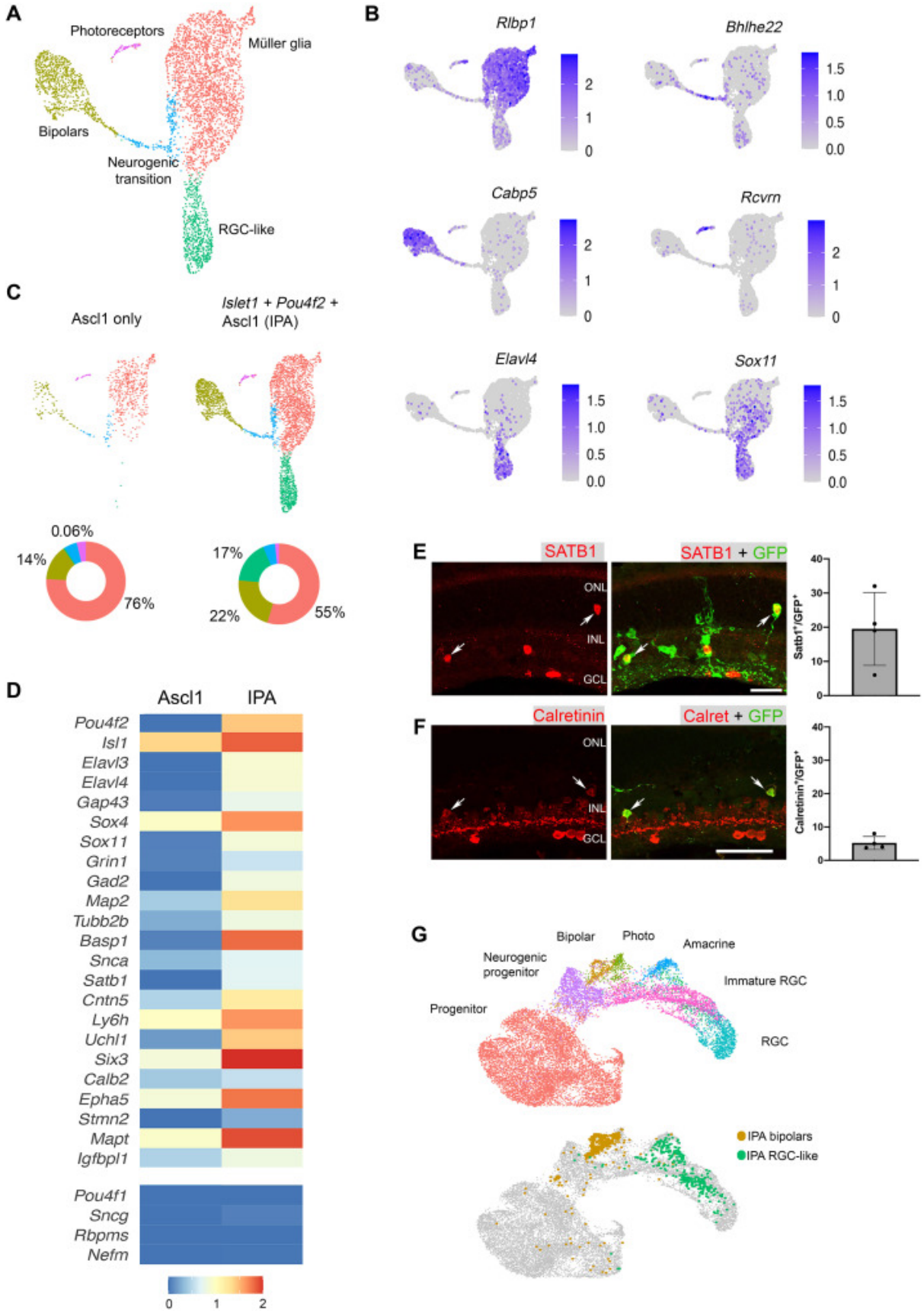
A
Photoreceptors
Müller glia
Bipolars
Neurogenic transition
RGC-like
B
Rlbp1
Bhlhe22
Cabp5
Rcvrn
Elavl4
Sox11
C
Ascl1 only
Islet1 + Pou4f2 + Ascl1 (IPA)
0.06%
14%
76%
17%
22%
55%
D
Ascl1
IPA
Pou4f2
Isl1
Elavl3
Elavl4
Gap43
Sox4
Sox11
Grin1
Gad2
Map2
Tubb2b
Basp1
Snca
Satb1
Cntn5
Ly6h
Uchl1
Six3
Calb2
Epha5
Stmn2
Mapt
Igfbpl1
Pou4f1
Sncg
Rbpms
Nefm
E
SATB1
SATB1 + GFP
ONL
INL
GCL
F
Calretinin
Calret + GFP
G
Bipolar
Photo
Amacrine
Neurogenic progenitor
Immature RGC
Progenitor
RGC
IPA bipolars
IPA RGC-like

Figure 2.05: scRNA-seq analysis of Pou4f2/Islet1-stimulated neurons reveals molecular characteristics of RGCs. (A) UMAP plot for FACS-sorted MG-derived cells after the IPA regeneration paradigm combined with a previous scRNA-seq dataset where Ascl1 only was used. (B) Feature plots highlight the major clusters of MG (*Rlbp1*), neurogenic transition (*Bhlhe22*), bipolars (*Cabp5*), photoreceptors (*Rcvrn*), and RGC-like cells (*Elavl4* and *Sox11*). (C) The distribution of cells from each treatment projected onto a split UMAP plot. Donut plots represent the percent each cluster comprises of the dataset. (D) Heatmap comparing scRNA-seq datasets of Ascl1 only versus IPA treatment. Selected genes are depicted that are associated with RGCs. (E) Retinal sections stained for MG-derived cells (GFP) with Satb1 (red), and quantifications show the percent of GFP^+ cells that are $Satb1^+$. (F) Retinal sections stained for MG-derived cells (GFP) with Calretinin (red), and quantifications show the percent of GFP^+ cells that are $Calretinin^+$. (G) UMAP of IPA-derived neurons integrated with scRNA-seq of E14 mouse retina from Clark *et al.* (21), revealing that IPA neurons cluster similarly to immature RGCs. Scale bars, 50 μm.

The new cluster of cells induced by IPA shows high expression of genes characteristic of RGCs, such as *Elavl4* and *Sox11* (Figure 2.05b)[166]. In addition, we found these IPA-neurons expressed many genes found in the gene ontology terms “axon guidance”, “axon outgrowth” and “axogenesis” (Figure 2.06d). Since Islet1 and Pou4f2 are upstream of an RGC-fate inducing regulatory network, we assayed whether this combination of factors was able to induce multiple RGC-genes in this cluster of MG-derived neurons. We used the label transfer feature of Seurat to broadly compare the transcriptome of the IPA neurons to a reference dataset of all major retinal neuron classes[33,167]. The novel cluster was classified as an RGC cluster (average prediction score = 0.74), suggesting an overall transcriptomic similarity to native RGCs (Figure 2.06e). Compared to Ascl1-induced neurons, a substantial number of RGC-associated genes were expressed in IPA-induced neurons (Figure 2.05d). These include genes such as *Sox4* and *Sox11*, which are redundantly required for RGC-fate acquisition[66,168] and the axon growth associated gene *Gap43*, which is highly expressed in developing RGCs[169]. Interestingly we found both *Satb1* and *Cntn5* were expressed in subsets of IPA-induced neurons. *Satb1* is highly expressed in the ON-OFF direction-selective subtype of RGCs where it controls *Cntn5* expression[170]. Using

IHC we were able to confirm that IPA-induced neurons expressed Satb1 protein (Figure 2.05e). Additionally, the RGC and amacrine marker Calretinin (*Calb2*), was also detected at the RNA and protein level (Figure 2.05c, f).

Despite this large suite of RGC-genes expressed by the MG-derived RGC-like neurons, these cells fail to express some canonical RGC-markers such as *Pou4f1*, *Sncg*, *Rbpms*, and *Nefm* (Figure 2.05d). This suggests that the newborn neurons do not fully differentiate into mature RGCs. Consistent with this observation, when we integrated the scRNA-seq data of IPA-induced neurons with a dataset from E14 embryonic mouse retina[33], we find that the MG-derived RGC-like neurons most closely resemble immature RGCs (Figure 2.05g). We compared the IPA induced neurons from a 3-week endpoint with a longer survival time point (6 weeks) and found the regenerated RGC-like neurons were a stable population and did not show evidence of increased cell death or stress over this period (Figure 2.07a-d).

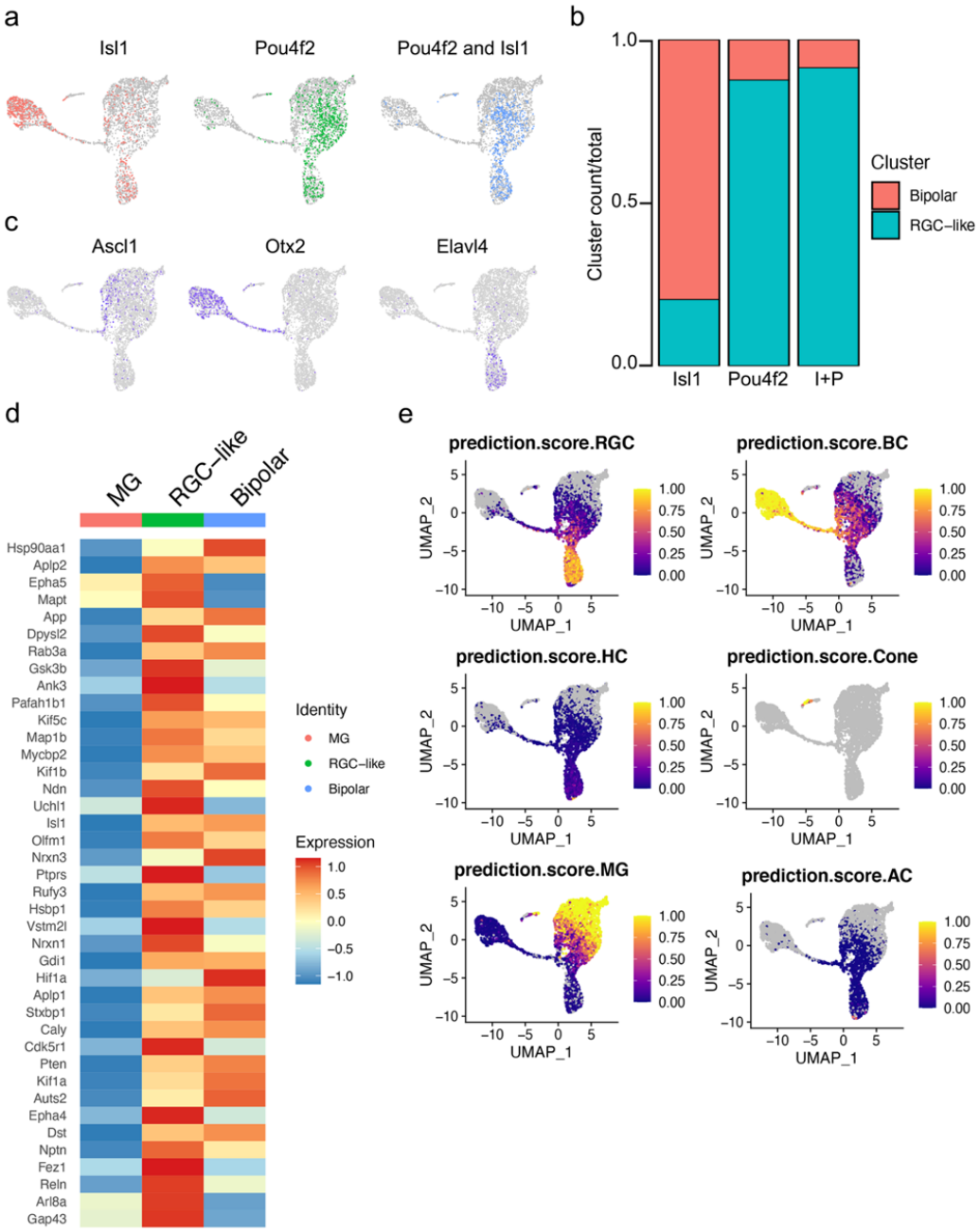

Figure 2.06: scRNA-seq analysis showing Pou4f2 biases MG-production towards RGC-like neurons. (a) UMAPs of integrated IPA and Ascl1-only reprogrammed MG highlighting cells expressing either Isl1, Pou4f2, or the combination of both. (b) Stacked bar graph quantifying the percent of Islet1-only, Pou4f2-only, or Islet1/Pou4f2 double-positive cells that end up as MGderived bipolars or RGC-like neurons. (c) Feature plots highlighting Ascl1-expressing cells which get downregulated as they differentiate into bipolar neurons (Otx2+) or RGC-like neurons (Elavl4+). (d) Heatmap of the top 40 differentially expressed genes between MG and MGderived neurons found in the GO-terms “axon guidance”, “axonogenesis”, and “axon outgrowth”. (e) Feature plots of prediction scores from Seurat’s label transfer using a reference dataset of randomly sampled cells of each major retinal neuron class and MG, subsetted from mouse retinal development scRNA-seq data23.

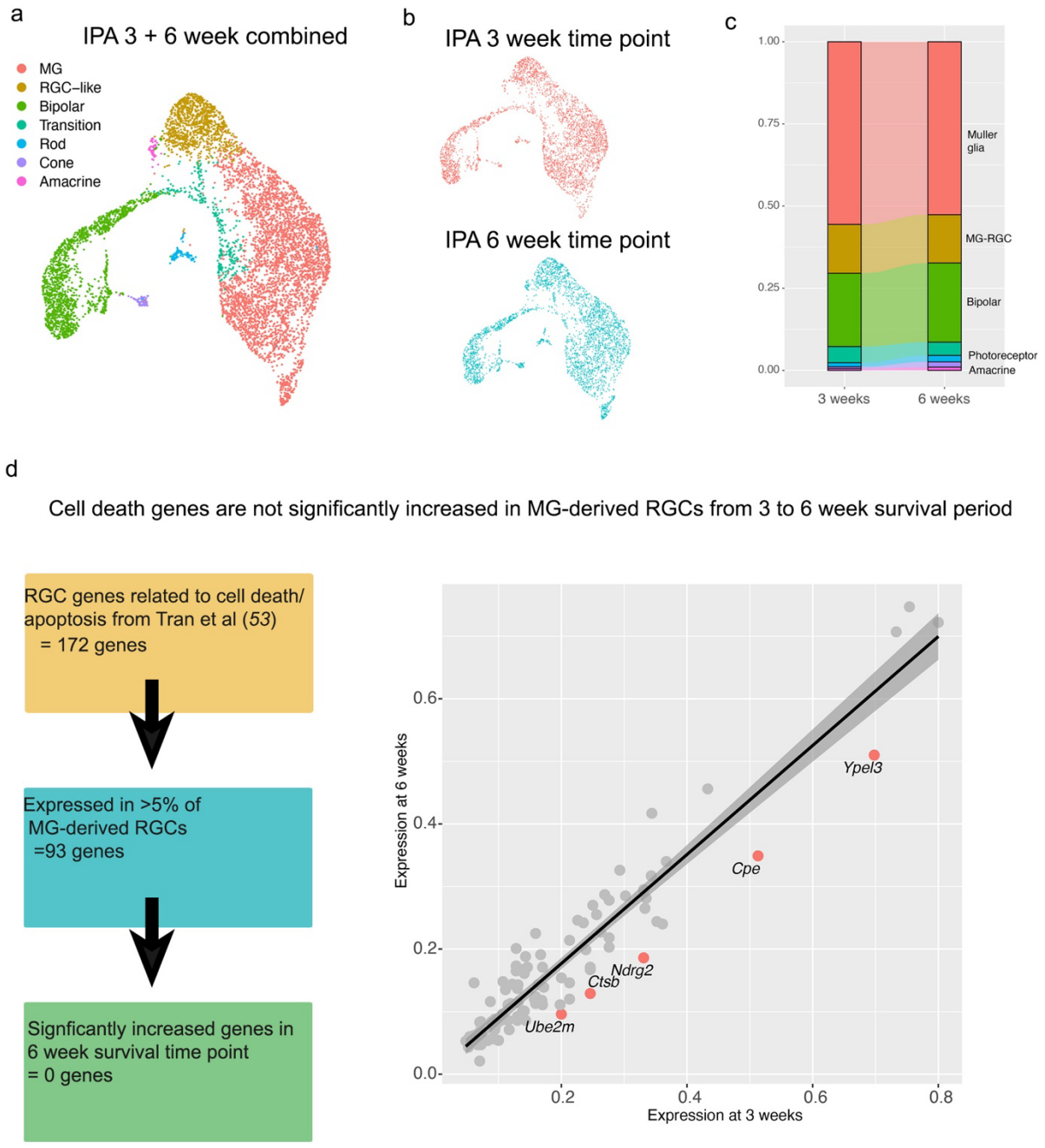

Figure 2.07: MG-derived RGCs are a stable population over time. (a) Combined UMAP of IPA-treated MG from a three and six week end point. (b) Split UMAP showing the distribution of cells in the UMAP in (a) from each time point. (c) Stacked bar graph showing the percentages of each cluster of MG and MG-derived neurons from the three week and six week time point. (d) Analysis of cell death genes found in MG-derived RGC-like neurons.

Simultaneous expression of Islet1-Pou4f2 with Ascl1 more uniformly induces an RGC-state from MG *in vitro*

Because the tetO- Pou4f2 and Islet1 transgenic construct contains mutually exclusive loxP sites, most of the Cre-expressing MG *in vivo* expressed Ascl1 and either Pou4f2 or Islet1. While a small number of cells co-labelled for both Pou4f2 and Islet1 *in vivo* (Figure 2.01c,d), to better assess the effect of overexpressing all three transgenes uniformly we bred mice containing the tetO-Pou4f2-Islet1 and tetO-Ascl1-GFP cassettes to a germline Rosa26-rtTA line, and then performed *in vitro* MG-reprogramming experiments (Figure 2.08a,b). MG were cultured from P11 mice for 7 days before passaging as previously described[147]. The cultures obtained in this way are largely composed of MG, though some surviving neurons are observed[147]. EdU was added to the medium to determine which cells are derived from proliferating MG and which cells were likely surviving neurons from the initial dissociation. After passage, doxycycline was added to the medium to induce transgene expression and then cells were assayed with immunofluorescence and scRNA-seq (Figure 2.08b).

Analysis of the cultures after five days of treatment confirmed that the cells express the transgenes. Immunolabeling for the transgenes showed that cells co-express Pou4f2, Islet1, and Ascl1 (Figure 2.09a). The cells largely adopted a neuronal morphology and immunolabeling demonstrated Edu+ cells that were co-labelled with neuronal markers Tuj1 (Figure 2.08c), Neurofilament (Figure 2.08d), and Calbindin (Figure 2.08e).

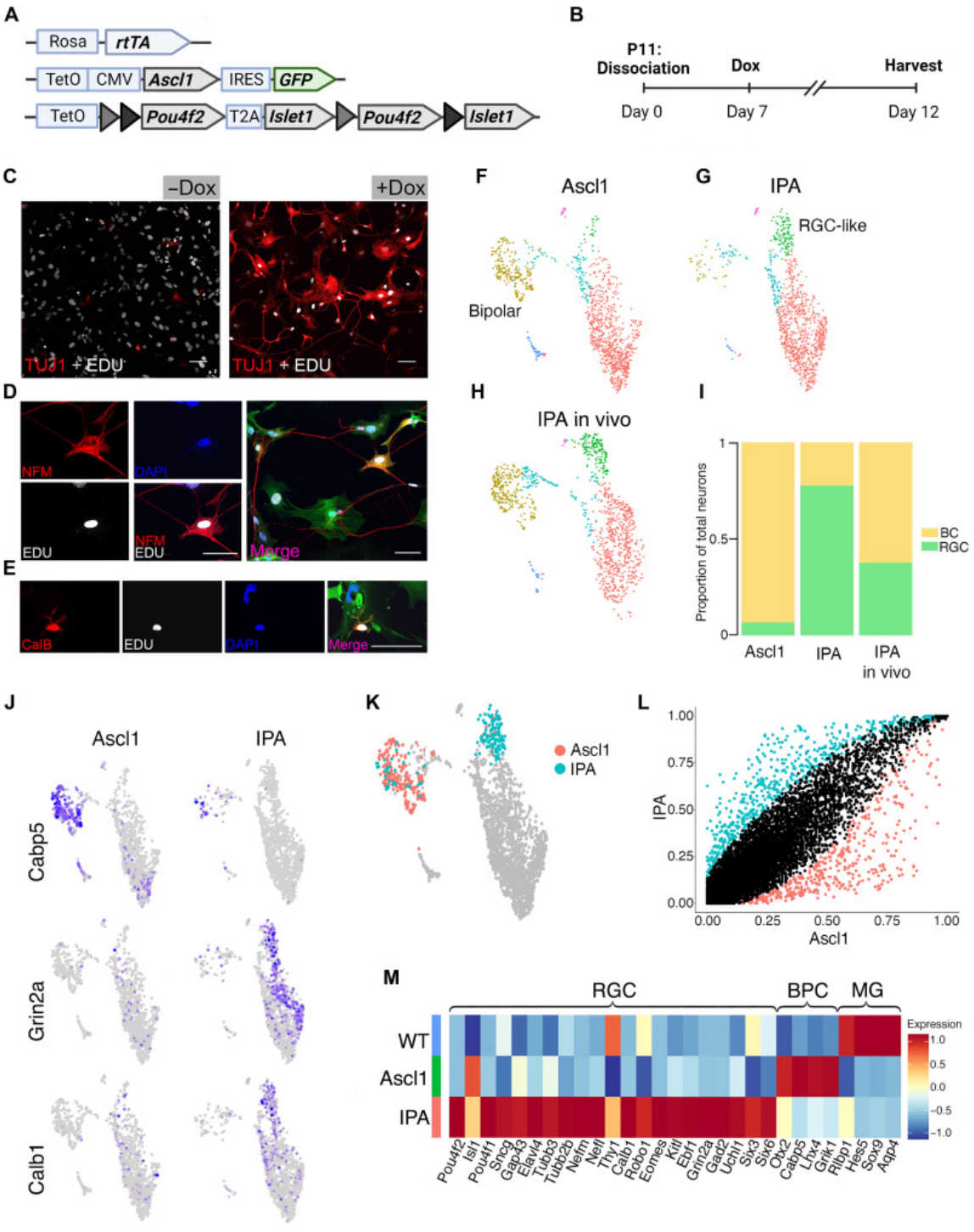

Figure 2.08: Islet1 and Pou4f2 coinduction stimulates RGC-like neurons from MG in vitro. (A) Schematic of transgenic construct to induce IPA in all primary MG in vitro by doxycycline. (B) Paradigm for inducing Ascl1-mediated neurogenesis in vitro. (C to E) Representative images of EdU$^+$ MG-derived neurons expressing neuronal markers.) (C) EdU$^+$ (white) MG-derived cell expressing Tuj1 (red). (D) MG-derived neuron expressing EdU (white), Neurofilament M (NFM;

red), and the GFP transgene reporter (GFP). ((E) MG-derived neuron expressing Calbindin (red) colabeling with EdU (white), DAPI, and GFP. (F to H) UMAP plots of cultured MG reprogrammed with Ascl1 (F) and IPA (G), integrated with cells from in vivo IPA regeneration model (H) as reference. (I) Stacked bar plot showing composition of neuronal clusters in each sample. BC, bipolar cell. (J) Feature plots highlighting differentially expressed genes in neuronal clusters of either reprogramming strategy. (K) Highlighted cells of the Ascl1 and IPA datasets used for downstream DGE analysis in (L). (M) Heatmap of genes differentially expressed in either the Ascl1 or IPA condition. WT, untreated cultured MG included for baseline values. Statistics for differential gene analysis: Wilcoxon Mann-Whitney test for significance ($P < 0.05$). Scale bars, 50 μm. Mouse schematic was made with Biorender.com.

To determine how the overexpression of IPA differed from Ascl1 alone, we repeated the reprogramming experiment as described above, alongside sister MG cultures from tetO-Ascl1;Rosa26-rtTA mice, either with or without dox treatment to activate transgene expression. We carried out scRNA-seq as described above for each sample. The untreated MG were largely homogenous, with one glial cluster and a small cluster containing only a few surviving neurons (Figure 2.09b,c). To compare the cluster composition between the treatment conditions, as well as to the *in vivo* IPA dataset, we integrated all three together (Figure 2.08f-i, 2.09d). We identified cells in both the Ascl1-only *in vitro* and IPA-reprogrammed MG *in vitro* that mapped to the neuron clusters from the IPA *in vivo* dataset. However, each treatment stimulated one main neuron cluster from MG; in the Ascl1 culture, the neurons most closely resembled bipolar cells (Figure 2.08f,i), while in the IPA cultures, the neurons acquired an RGC-like fate (Figure 2.08g,i), with a minority differentiating into bipolar cells. This differed from our observations *in vivo*, in which the bipolar cluster did not differ significantly in proportion from the Ascl1-only sample (Figure 2.01d and 2.07fh).

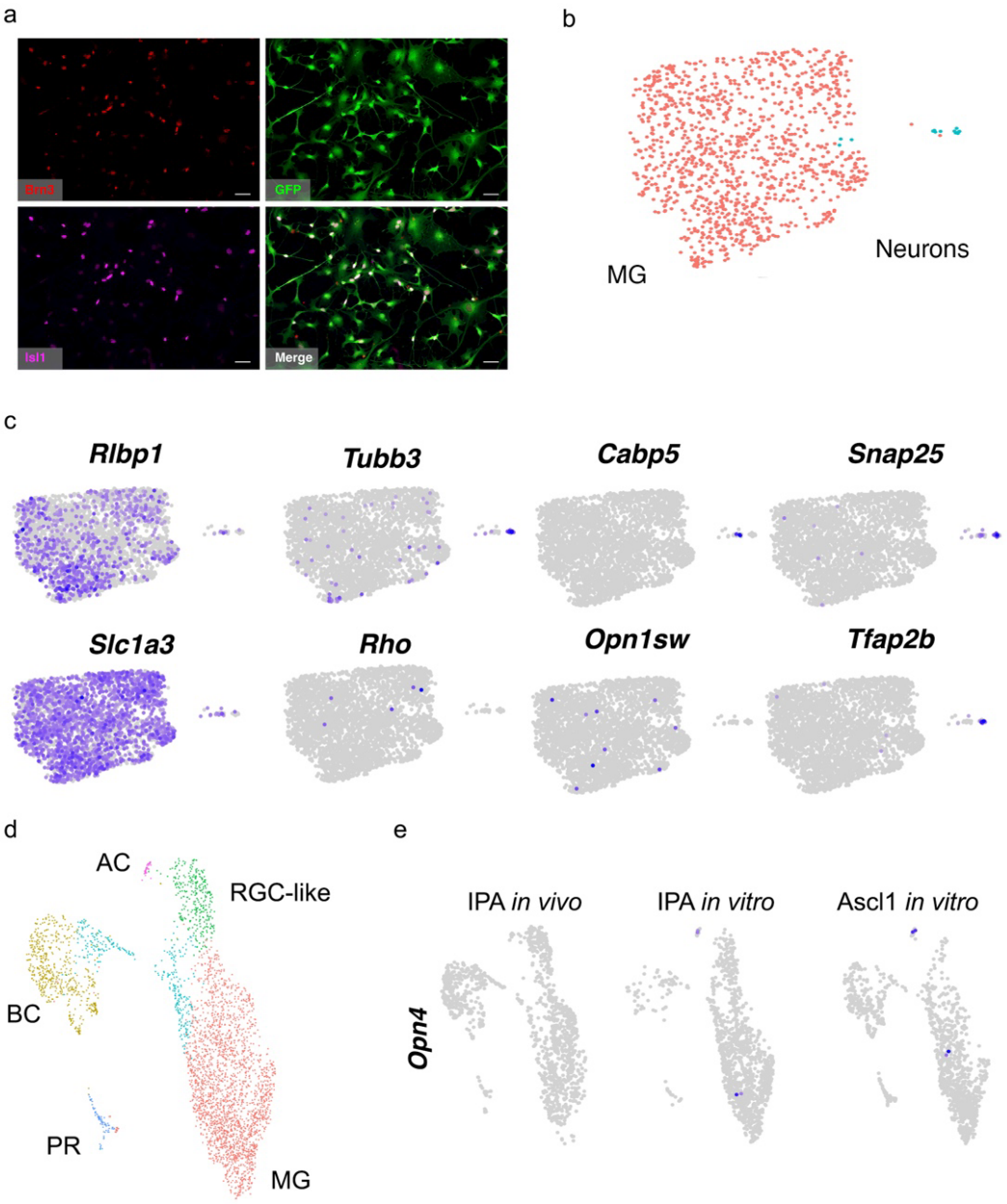

Figure 2.09: MG from IPA mice express reprogramming factors. (a) Immunofluorescence of IPA MG treated with doxycycline for 5 days showing Ascl1-IRES-GFP, Brn3, and Isl1 colabeling in most cells (b) UMAP of untreated cultured MG with glial and neuronal cell populations labeled. (c) Markers of MG and various retinal neurons reveal a small population of bipolar and amacrine cells survived dissociation. (d) UMAP of integrated datasets from IPA overexpression in vivo and in vitro, with Ascl1overexpression in vitro. (e) Expression of melanopsin (Opn4) in three datasets featured in (d). Scale bars are 50µm. Abbreviations: MG, Müller glia; AC, amacrine cells; BC, bipolar cells; PR, photoreceptors; RGC, retinal ganglion cells.

Next, we compared the gene expression profiles of the induced neurons in the IPA and Ascl1-only *in vitro* datasets. We observed that bipolar genes, such as *Cabp5*, were largely restricted to the Ascl1-only neuron cluster. RGC genes, such as *Grin2a* and *Calb1*, were found only in the IPA neurons (Figure 2.08j). To identify unique marker genes expressed in the IPA neurons, we made a subset of all neuron populations in the IPA and Ascl1-only integrated dataset (Figure 2.08k) and performed a differential gene expression (DGE) analysis (Figure 2.08l). We identified a number of RGC genes enriched in the IPA neurons, while bipolar genes were enriched in the Ascl1 neurons. Additionally, we found some canonical markers of the RGC-lineage that were not induced *in vivo*, such as *Sncg*, *Nefm*, and *Pou4f1* were induced *in vitro* (Figure 2.07m). We also failed to detect cells expressing the intrinsic photosensitive RGC marker *Opn4* (Figure 2.09e). These results collectively suggest that concurrent overexpression of all three IPA factors biases MG-derived neurons to an RGC-like fate and induces more uniform RGC gene expression.

IPA induces neurons with diverse electrical properties

We found previously that Ascl1 can stimulate MG-derived neurons that have physiological characteristics of endogenous retinal neurons, particularly bipolar cells [149,156]. Because IPA-treatment leads to a different molecular and morphological neuronal phenotype compared to Ascl1 alone, we characterized the light responses and electrical properties of these cells. We performed patch-clamp electrophysiology on GFP+ cells in retinal slices and whole mounts after our IPA-*in vivo* regeneration paradigm. We measured responses to current and voltage steps and responses to light stimuli. We plotted the membrane resistance and resting potential of IPA-induced neurons compared to GFP- MG, endogenous neurons, and neurons from our previous

regeneration strategies using Ascl1 or Ascl1:Atoh1[149,150,156] (Figure 2.10a). Glial cells have low membrane resistance, hyperpolarized resting potentials and little in the way of voltage-activated conductance. Neurons have higher resistance, less negative resting potential, and express voltage-activated conductance.

Most of the IPA-induced neurons displayed resting potential and membrane resistance profiles similar to endogenous neurons, however some of these cells still had glial-like hyperpolarized membrane potentials (Figure 2.10a). This is consistent with our IHC and scRNA-seq analysis where a portion of glia do not reprogram after IPA-treatment (see Figure 2.01 and 2.05). Figure 2.10b shows examples of responses to families of current or voltage steps recorded from IPA-treated GFP+ cells. These cells exhibit a range of characteristics. Some have a neuronal phenotype and appear to express voltage-activated K+ conductance that limit the extent of depolarization to current steps, while others retain features of glia (Figure 2.10b). Six of sixteen recorded cells responded to brief light flashes, indicating that they established synaptic connections with other components of the retinal circuitry (Figure 2.10c). Remarkably, some cells responded to current steps by generating action potentials and others generated spiking activity likely representing Ca2+ spikes (Figure 2.10d). This diversity of the physiological properties is consistent with the phenotypes observed in Figures 2.01 and 2.05. Notably, we did not observe action potentials, a distinct feature of RGCs, in our previous strategies to stimulate MG-derived neurons [149,150,156]. Thus, IPA increases the diversity of the electrical properties of the MG-derived neurons, including generating some cells that can produce Na^+ and/or Ca^{2+} action potentials.

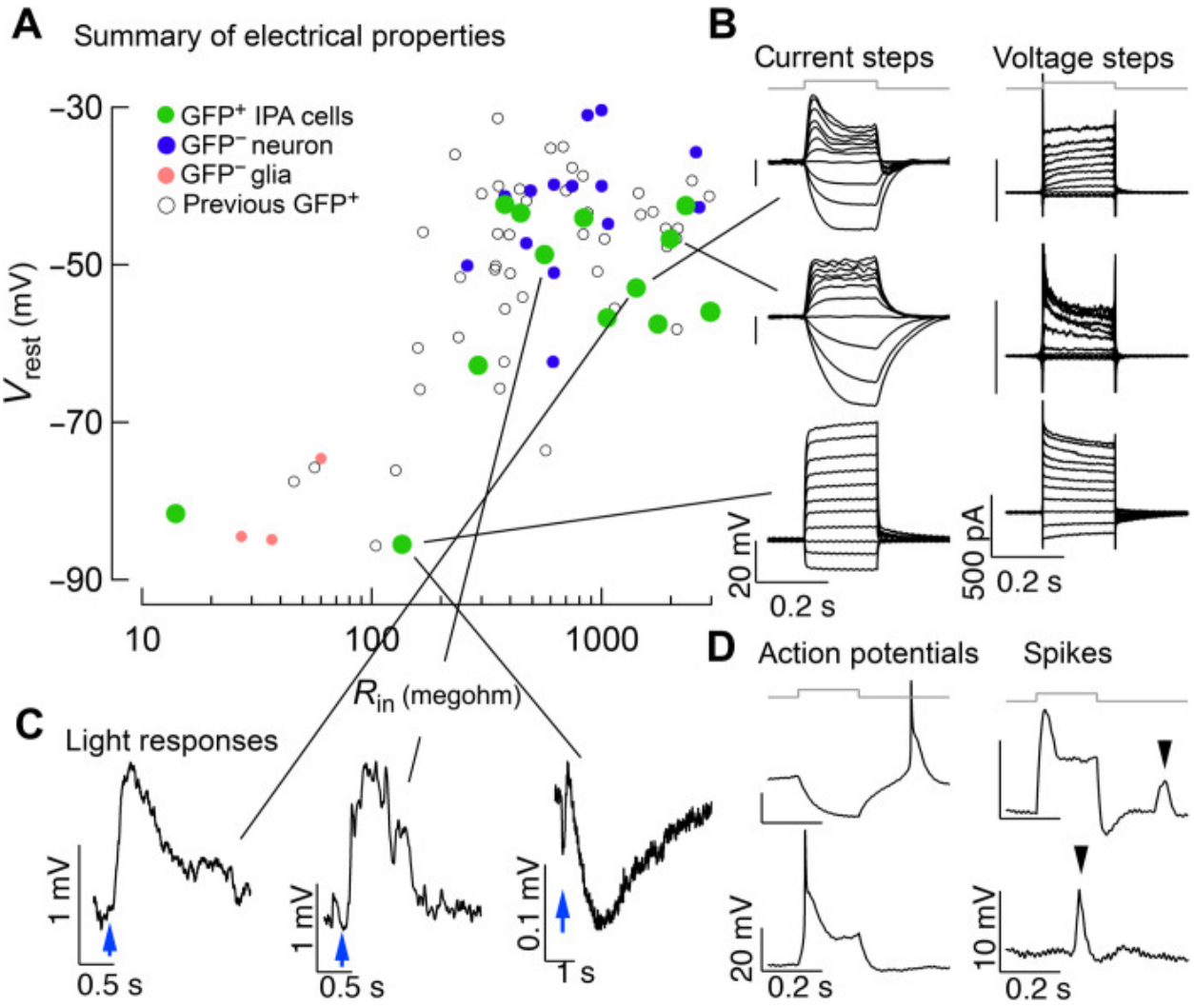

Figure 2.10: Physiological profiling of IPA-induced neurons. (A) Summary of electrical properties of cells in this study compared to endogenous neurons, endogenous glia, and MG-derived neurons from previous regeneration protocols (*4*, *5*, *13*). Resting potential and input resistance were estimated from current clamp recordings. (B) Examples of responses to current (left) and voltage (right) steps for three cells. (C) Three examples of cells that responded to light stimulus. (D) Examples of cells that displayed action potentials or similar events. The two left panels are responses to hyperpolarizing and depolarizing current steps from a cell that generated apparent Na^{+} spikes. The right two panels are responses from a cell that generated smaller discrete events, likely Ca^{2+} spikes.

IPA-expression remodels MG chromatin to an imperfect RGC-like fate

We next carried out single cell Assay for Transposase-Accessible Chromatin (scATAC-seq) on Ascl1 vs. IPA-reprogrammed MG to gain a better understanding of the mechanistic differences between these two reprogramming strategies. Mice were treated with the same *in vivo* retinal regeneration paradigm described in Figure 2.05 but were processed for scATAC-seq instead of scRNA-seq. 1,692 nuclei from Ascl1 only and 2,451 nuclei from IPA-treatment passed our quality control metrics (see Methods). Single cells from these two treatments were then integrated and plotted as a UMAP to identify cell types (Figure 2.11a-c). Cell type clusters were identified by the pattern of accessible chromatin near genes identified with specific retinal cell types. Coverage plots show representative peaks for the groups we identified, MG (*Rlbp1*+), neurogenic transition (*Islet1*$^{+}$), MG-derived bipolar cells (*Crx*$^{+}$), induced RGC-like cells (*Pou4f2*$^{+}$), and photoreceptors (*Arr3*$^{+}$) (Figure 2.11d). When the UMAP is split between the two treatment groups, it is clear while a large cluster of cells retain a MG-phenotype, both the Ascl1 and the IPA conditions lead to MG-derived bipolar neurons (Figure 2.11b-c). However, the IPA treatment induces a unique cluster of cells that have accessible chromatin that most closely resemble RGCs (green cluster) (Figure 2.11c). Consistent with accessibility patterns, the motif for Otx2 is enriched in the bipolar cluster while the Pou4f2 motif is highly represented in the accessible chromatin of the IPA-unique cluster (Figure 2.11f). This is consistent with our scRNA-seq findings and demonstrates that these MG-derived neurons have patterns of cis-regulatory regions consistent with their transcriptomic identity.

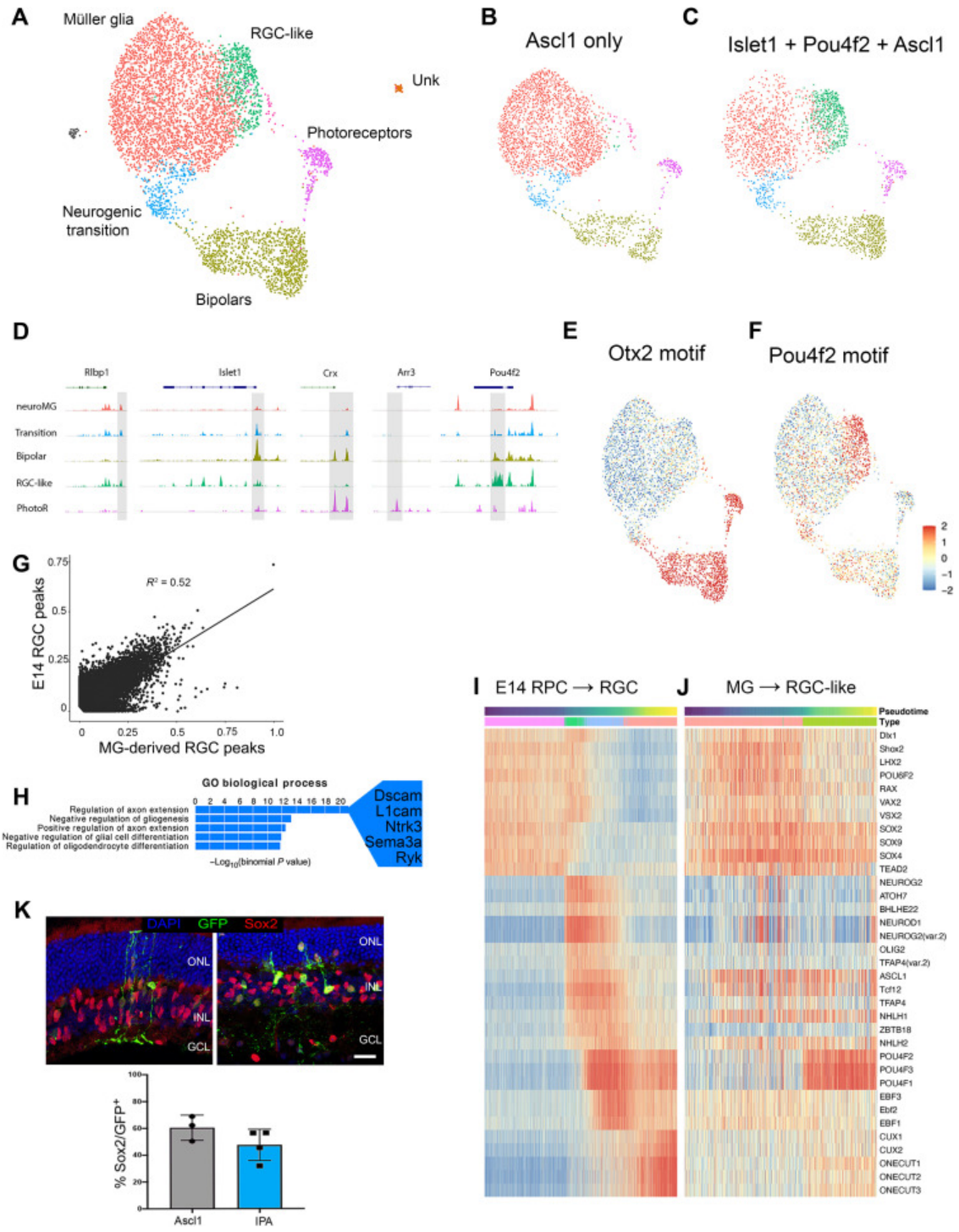

Figure 2.11: scATAC reveals MG remodel chromatin to an RGC-like state in response to IPA treatment. (A) Combined UMAP of GFP^{+} sorted MG and their progeny from the in vivo regeneration paradigm with Ascl1-only (B) or IPA treatment (C). (D) Coverage plots for known marker genes used to identify clusters. (E and F) chromVAR scores of Otx2 and Pou4f2 to highlight differential accessibility of their respective motifs. (G) Scatterplot comparing accessible motifs in E14 RGCs versus IPA-induced RGCs. (H) Top "GO biological process"

results for peaks specific to E14 RGCs compared to IPA-derived RGC-like neurons. (I) Heatmap of the chromVAR activity scores of the top variable motifs for TFs found on the pseudotime lineage of E14 progenitor cells to RGCs. (J) Heatmap of the same chromVAR activity scores of the E14 motifs plotted on pseudotime from MG to RGC-like neuron after IPA treatment. (K) Retinal sections showing GFP^+ MG-derived cells costained with the MG nuclei marker Sox2 (red) and quantification of GFP^+ cells expressing Sox2. Scale bars, 50 μm.

To determine how closely the chromatin of MG-derived RGCs resembles that of normal, developing RGCs we generated a scATAC-library from the E14 developing mouse retina to compare with the MG-derived RGCs (Figure 2.12a-f). The scatterplot in Figure 2.11g shows that there is significant correlation between the accessible peaks in E14 RGCs and the MG-derived neurons, however there are clearly many regions that are differentially accessible between cell types (Figure 2.11g). When we assayed for gene ontology (GO) enrichment to understand the types of genes that are more highly represented in nearby accessible chromatin in E14 RGCs than in MG-derived RGCs, many of the top terms were related to axon growth (Figure 2.11h; Table 2.T). This is consistent with the fact that many MG-derived RGCs do not extend long axons.

The current model of retinal development suggests a cascade of transcription factors are sequentially activated when cells transition through multipotent progenitors, to neurogenic precursors, to their ultimate neuronal cell fate[22]. Therefore, we sought to examine whether neurogenesis induced in MG recapitulates developmental cascades at the chromatin level. We used pseudotime to order cells in a projected lineage from the progenitor cells to RGCs in the E14 retina and compared this with a similar analysis of MG-derived RGCs, and then analyzed the motif enrichment in accessible chromatin over pseudotime in a “cascade plot” (Figure 2.11i-j)[171]. This analysis reveals key differences in the process of RGC-development vs. RGC

production from MG. Normal development of RGCs shows down regulation of progenitor TF motifs (Rax, Sox2) in accessible regions followed by a transient increase in regions with bHLH motifs (Atoh7) then finally induction of regions with mature RGC TF motifs (Pou4f1-3, Ebf1, Onecut). This has recently been described in both mouse and human[171,172]. By contrast, the sequential changes in motif representation in accessible chromatin in MG reprogrammed to generate neurons with IPA show clear differences from normal development. Although there is a reduction in progenitor gene motifs as cells acquire an RGC-like identity, the progenitor TFs are apparently never fully down-regulated, since their motifs persist in the accessible regions of MG-derived RGCs (Figure 2.11j). In addition, although MG-derived RGCs show an increase in accessible bHLH motifs and a robust increase in Pou4f1/2/3 motif representation in accessible chromatin, the TFs that are presumably downstream of Pou4f1/3, such as Onecut and Ebf, are not sequentially activated (Figure 2.11j). This epigenomic analysis suggests RGC-like generation is imperfect from IPA-treated MG, in part because of the maintenance of accessibility at glial and progenitor regulatory regions. Consistent with this notion the progenitor/MG marker Sox2 is still detectable by immunofluorescence 3 weeks after IPA reprogramming in GFP+ cells with neuronal morphology (Figure 2.11k).

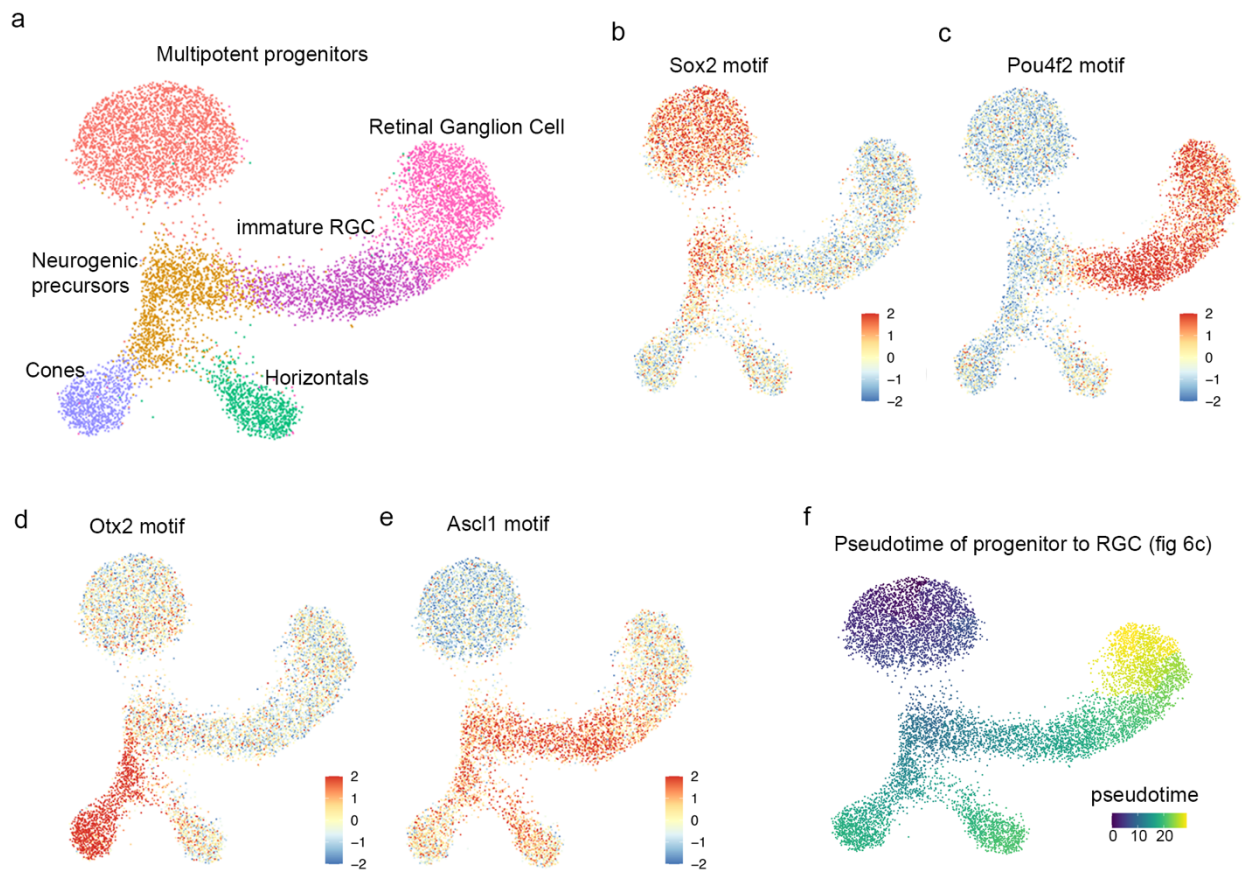

Figure 2.12: scATAC-seq of the E14 embryonic mouse retina. a. UMAP plot of scATAC-seq from E14 embryonic mouse retina. Chromvar scores show the motif accessibility used to identify the clusters of progenitors (b. Sox2), retinal ganglion cells (c. Pou4f2), cones (d. Otx2), and neurogenic precursors (e. Ascl1). f. Pseudotime subset of the transition of retinal progenitor cells to retinal ganglion cells that is further analyzed in Fig 2.11.

Discussion

Non-mammalian adult vertebrates can regenerate neurons in many regions of their CNS. For example, after tail amputation in larval frogs and some adult urodeles, the radial glial cells of the spinal cord acquire a pattern of gene expression similar to neuronal precursors and go on to proliferate and regenerate an apparently normal spinal cord[173]. Similarly, in the retina and brain of zebrafish, glia respond to injury by activating a progenitor-like gene expression program of TFs[174]. These glia-derived progenitor cells undergo multiple rounds of mitotic cell divisions and

the progeny differentiate into the range of neuron types that can restore function in the brain and retina[135].

Re-expressing developmentally active TFs in adult mammalian glia can trigger a regenerative process in these cells that in many ways resembles what is found in fish and amphibians. For example, after retinal injury, the transgenic overexpression of the proneural TF Ascl1, combined with HDAC inhibition, can stimulate MG to acquire a progenitor-like state with the capacity of generating bipolar neurons[149]. The MG-derived neurons differentiate to the point that they make synapses with the surrounding neuronal circuitry and respond to light. In addition to lineage tracing the neurons to validate their glial derivation, we have used EdU labeling to show their adult origin, and have profiled the cells using scRNA-seq, and scATAC-seq, to observe intermediate states between glial-progenitor and regenerated neurons[150,153,156]. Taken together, this validates that TFs can reprogram glia in the adult CNS to generate neurons.
Although Ascl1 induces MG to adopt many features of retinal progenitors, including proliferative neurogenesis and a transcriptional and epigenetic landscape similar to developmental progenitors, not all of developmentally appropriate Ascl1 targets are induced in MG-derived progenitor cells and the neuronal output from Ascl1-MG is restricted to primarily bipolar neurons[150]. Thus, we reasoned that additional TFs might be required to properly steer MG-derived progenitors to specific types of neurons. This is particularly important for endogenous regeneration strategies because most blinding diseases are the result of deficits in a particular neuronal subtype. For example, glaucoma is primarily caused by the death of RGCs.

RGCs are generated during development by a cascade of transcription factors, characterized by the initial expression of Atoh7 and the downstream expression of additional TFs, such as Pou4f1/2 and Islet1[50]. Atoh7 is necessary for proper RGC fate by inducing these downstream stabilizing TFs[41,47,49]. Two of these downstream TFs, Pou4f2 and Islet1, are required for proper RGC-fate specification [56,61,63] and ectopic expression of Pou4f2 and Islet1 in the Atoh7 null retina is sufficient to rescue the RGC fate[64]. By taking advantage of the wealth of knowledge of normal transcriptional regulation of the RGC fate, we were able to test whether members of this TF cascade can re-initiate the genesis of these cells from the Ascl1-induced MG-derived progenitors.

We report here that the RGC fate-inducing factors, Islet1 and Pou4f2, along with Ascl1, can induce MG-neurogenesis towards an RGC-like fate. Using IHC we show that the MG-derived neurons, from IPA expressing MG, express protein markers and morphological features of RGCs. At the physiological level these IPA-induced, MG-derived neurons display neuronal resting membrane potentials and a subset generated voltage gated action potentials consistent with an RGC-like fate. Finally, our molecular analysis using scRNA-seq and scATAC-seq show that at the transcriptomic and epigenetic level IPA-induced MG-derived neurons most closely resemble immature RGC cells.

Although the expression of the IPA transgenes in MG collectively reprograms a subset of the cells to an RGC-like fate, this combination does not activate the full complement of TFs required for mature RGCs. We find both in the scRNA-seq and scATAC-seq datasets that some mature RGC genes fail to be induced; instead, the MG-derived neurons retain expression of some

progenitor/glial genes and a resulting chromatin landscape intermediate between progenitors and RGCs.

It is interesting that the RGC-like neurons derived from MG are most frequently found in the INL, instead of the GCL. Although a small percentage of RGCs is normally found in the INL in mice, the majority migrate to the GCL. It is possible, that the inner plexiform layer provides a barrier to migration of the RGC-like cells, or alternatively, they may lack the cues for appropriate migration. Although the scRNAseq data show MG-derived RGC-like cells express many RGC genes, they may lack some critical migration program. Nevertheless, some of these cells connect with the existing neural circuitry and respond to light, and it may be that appropriate connectivity can be established without proper somal location.

Although we also did not observe robust axonal outgrowth directed to the optic nerve, we find that many genes important for axon growth and guidance are expressed in the RGC-like cells. It is possible that some key guidance factors are not expressed in these cells, or alternatively, that the adult retinal environment no longer expresses the guidance factors needed to direct axons to the optic nerve head. RGC transplant experiments have found that in some cases the RGC axons project ectopically, suggesting that the microenvironment of the adult retina may not fully reflect that of the developing retina; future studies will be needed to better understand the interplay between cell-autonomous factors and non-autonomous factors in regeneration.

Over the past decade, a number of reports have suggested that other developmental TFs such as Sox2, Pax6, NeuroD1, Neurog2, and Ascl1 can stimulate neurogenesis from glia both in vitro and in the brain[175]. However, the interpretation of many of these reports has been clouded by the

finding that lineage tracing new neurons is unreliable using existing AAV paradigms, and often leads to endogenous neurons being misidentified as glial-derived [161,176]. Nevertheless, some of the earlier studies that used alternative methods to trace glial-derived neurons were able to show that reprogramming of astrocytes to neurons is possible, and proneural TFs, including Ascl1, are among the neurogenic stimulants[177 178,179 180]. Thus, it is possible that the strategy of combining TFs from a specific neuronal lineage, as we have employed for the retina, will have applicability throughout the CNS.

Overall, this study provides a proof of concept that TFs used to specify cell fate in development can be harnessed to initiate similar fate acquisition from reprogrammed glia cells in the adult CNS. The re-engineering process of cell fate acquisition during endogenous regeneration strategies will be key in guiding neural replacement appropriate for specific neurodegenerative diseases.

Genes associated with peaks enriched in E14 RGCs vs. MG-derived RGC-like cells negative regulation of glial cell differentiation
Ctnnb1
Dab1
Dlx1
Dlx2
Drd3
Dusp10
Hes1
Hes5
Hmga2
Id2
Id4
Kdm4a
Lin28a
Lingo1
Mycn
Nkx6-1
Nkx6-2
Nog
Ntrk3
negative regulation of gliogenesis
Abcc8
Adcyap1
Ascl2
Ctnnb1
Dab1
Dicer1
Dlx1
Dlx2
Drd3

Dusp10
Hes1
Hes5
Hmga2
Id2
Id4
Idh2
Kdm4a
Lin28a
Lingo1
Mycn
Nkx6-1
Nkx6-2
Nog
Ntrk3
Pitx3
Ptn
Ski
Sox10
Sox11
positive regulation of axon extension
Adnp
Cdh4
Disc1
Dscam
Fn1
Islr2
L1cam
Limk1
Map1b
Mapt

Ndel1
Nrg1
Nrp1
Ntn1
Ntrk3
Pafah1b1
Pou4f2
Rab11a
Rufy3
Sema5a
Sema7a
Srf
Vegfa
regulation of axon extension
Abl1
Adnp
Barhl2
Cdh4
Cdk5
Cdk5r1
Clasp2
Cttn
Disc1
Draxin
Dscam
Fn1
Islr2
L1cam
Limk1
Map1b
Mapt
Mgll

Ndel1
Nkx6-1
Nrg1
Nrp1
Ntn1
Ntrk3
Olfm1
Pafah1b1
Plxna1
Plxna2
Plxna4
Pou4f2
Ptprs
Rab11a
Rtn4
Rtn4r
Rufy3
Ryk
Sema3a
Sema3f
Sema3g
Sema4f
Sema5a
Sema7a
Srf
Tnr
Vegfa
Wdr36
Wnt3
Wnt5a
regulation of oligodendrocyte differentiation
Ctnnb1

Cxcr4
Dicer1
Dlx1
Dlx2
Drd3
Dusp10
Dusp15
Hes1
Hes5
Id2
Id4
Lingo1
Olig2
Rheb
Shh
Tcf7l2
Tenm4
Tnfrsf21
Zfp365
Zfp488

Table 2.T: Genes associated with peaks enriched in E14 RGCs vs. MG-derived RGC-like cells

Chapter 3:

Identification of additional transcription factors that improve maturation of Müller glia-derived RGCs

(Some text and figures modified from *Todd & Jenkins, et al., 2022)*

Introduction

Thus far have we have established proof-of-principle of a combined TF overexpression approach to regenerating RGCs in the adult mammalian retina. However, these new neurons exhibit a number of features that suggest a lack of maturation. The success of a future RGC regeneration-based therapy will ultimately require the regenerated neurons to function similarly to their endogenous counterparts. With this in mind, we chose to explore methods for improving the maturation of IPA-induced regenerated RGCs. In this chapter, I discuss our approach to identifying additional TFs that may synergize with IPA to improve RGC maturity, and the overexpression studies we carried out to assess their ability to do so.

In the RGC-like cells derived from IPA overexpression we have observed both sustained activity of glial and progenitor transcription factors as well as lack of activity of several TFs involved in the differentiation of RGCs (Figures 2.05 and 2.11). This leads to two non-mutually exclusive hypotheses: i) persistent glial and progenitor gene activity is preventing maturation of the RGC-like cells, or ii) overexpression of additional RGC developmental transcription factors is needed to promote full maturation of MG-derived RGC-like cells. To address both of these hypotheses, we carried out experiments both *in vivo* and in cultured MG to express additional TFs alongside IPA. In the above chapter, we identified multiple candidate TFs that could potentially shut down glial and progenitor genes or turn on additional genes involved with the maturation of RGCs, such as those that regulate axon outgrowth and the ability to fire action potentials. While IPA RGCs express many genes involved with neurite outgrowth and extend long processes *in vivo* (Figures 2.04 and 2.05), these processes are not seen at the optic nerve head, suggesting limitations in axon outgrowth or targeting. Additionally, though we observed action potential-

like spikes in the IPA-derived RGCs in some cells (Figure 2.10), they were rarely seen firing spontaneously as endogenous RGCs do, suggesting an incomplete expression profile of voltage-gated sodium channels. Thus, in the studies below, we chose to assess maturation primarily through measurements of morphology, expression of glial and progenitor genes, and expression of neurite outgrowth and sodium channel genes. We quantified cell morphology using the Sholl and Strahler methods[181-185]. The former assesses the size and complexity of neurons by centering an overlay of concentric circles over the soma and counting neurite intersections at each radius. The latter, originally developed for quantifying the geomorphology of rivers, assigns an order to each neurite branch based on the order of other branches with a shared node – generally, the outermost branches are order 1 and increase towards the soma depending on the number of forks. Broadly, RGCs have characteristic radial arborizations and they extend long axons[186]. Using the above measurement techniques we assessed the degree of neurite outgrowth, branching, and length.

To narrow down a list of candidate TFs, we referenced both our own scRNA-seq and scATAC-seq data, as well as the literature on RGC development. The transcription factors we chose to test were Atoh1, Neurod2, Irx2, Irx5, Ebf1, and Tcf3. Due to the lack of availability of mouse models for conditional overexpression of most of these factors, the bulk of these factors were overexpressed in cultured IPA MG as a small screen. However, we generated one additional mouse model to assess the combined overexpression of Atoh1 with IPA *in vivo*.

We found overexpression of Atoh1 alongside IPA to be sufficient for reducing the expression of glial and progenitor genes, improving the overall rate of RGC regeneration. We also found two

additional factors, Neurod2 and Irx2, promoted RGC maturation by increasing neurite outgrowth and gene expression.

Results

Atoh1 can improve the ability of IPA to induce RGC-like cells from MG

The scRNA and scATAC-seq analysis revealed that although IPA-induced neurons resembled RGCs, these cells lack some features of mature RGCs. One hypothesis for why this is the case is the persistence of glial and progenitor genes and chromatin accessibility (i.e., Sox, Rax, Vsx2, etc.) in the MG-derived neurons. Recently, we have reported that the Atoh-class of TFs, when combined with Ascl1, can potently stimulate neurogenesis[156]; the combination of Ascl1:Atoh1 results in nearly 80% of transgene-expressing MG acquiring a neural identity. Therefore, we tested whether combining Atoh1 with IPA reprogramming could improve the regeneration of RGCs from MG *in vivo.*

We crossed mice containing a tetracycline-inducible Atoh1 to the IPA strain and carried out the regeneration paradigm as described in Figure1; we then performed scRNA-seq and immunohistochemistry analysis of MG-progeny as described above (Figure 3.01a-b). Consistent with our previous findings using Atoh1, the expression of IPA and Atoh1 in MG caused the majority of MG-progeny to acquire a neuronal identity[156].

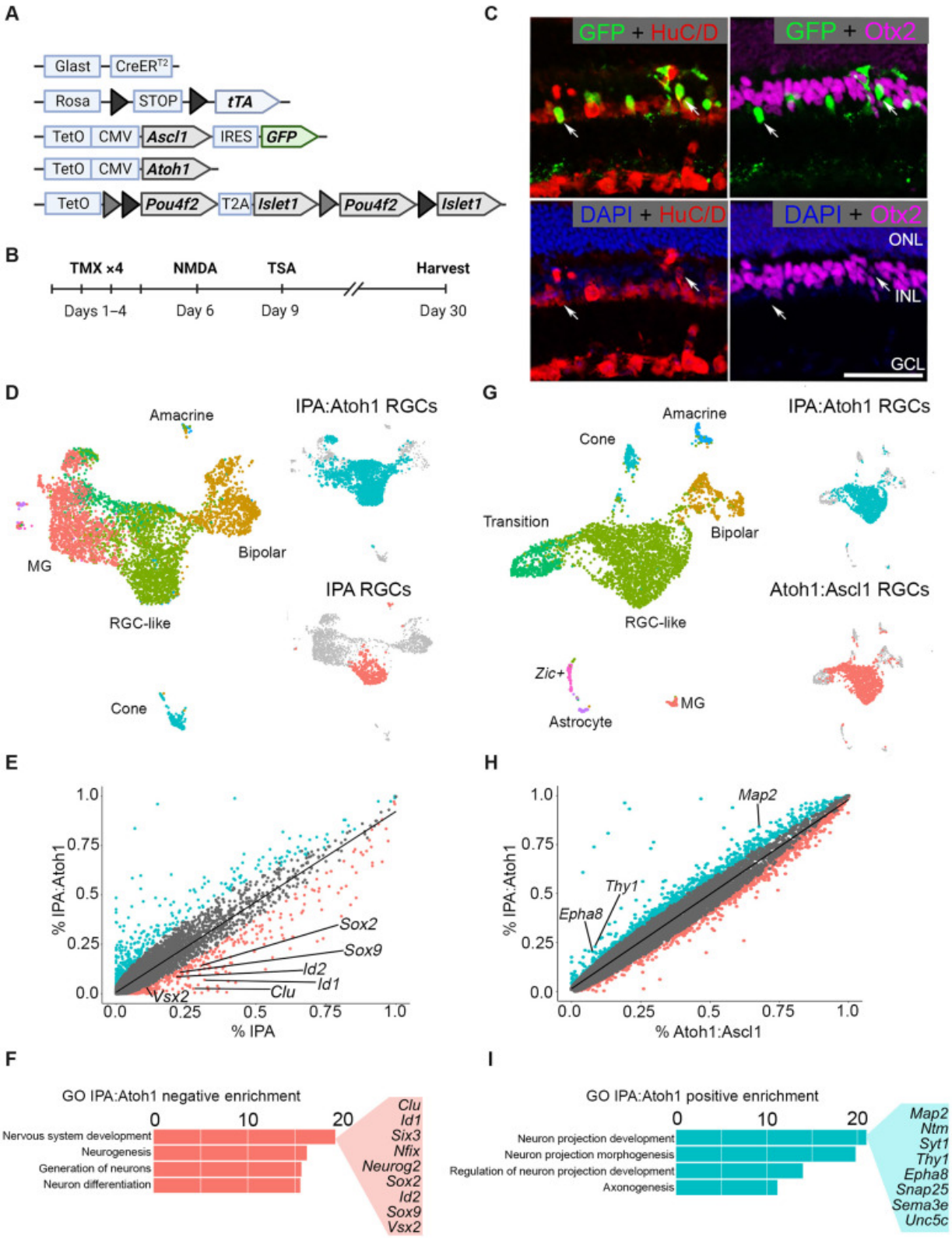
A
Glast
CreER^{T2}
Rosa
STOP
tTA
TetO
CMV
Ascl1
IRES
GFP
TetO
CMV
Atoh1
TetO
Pou4f2
T2A
Islet1
Pou4f2
Islet1
B
TMX ×4
NMDA
TSA
Harvest
Days 1–4
Day 6
Day 9
Day 30
C
GFP + HuC/D
GFP + Otx2
DAPI + HuC/D
DAPI + Otx2
ONL
INL
GCL
D
Amacrine
IPA:Atoh1 RGCs
MG
Bipolar
IPA RGCs
RGC-like
Cone
G
Amacrine
Cone
IPA:Atoh1 RGCs
Transition
Bipolar
Atoh1:Ascl1 RGCs
RGC-like
Zic+
MG
Astrocyte
E
% IPA:Atoh1
% IPA
Sox2
Sox9
Id2
Id1
Clu
Vsx2
H
% IPA:Atoh1
% Atoh1:Ascl1
Map2
Thy1
Epha8
F
GO IPA:Atoh1 negative enrichment
Nervous system development
Neurogenesis
Generation of neurons
Neuron differentiation
Clu
Id1
Six3
Nfix
Neurog2
Sox2
Id2
Sox9
Vsx2
I
GO IPA:Atoh1 positive enrichment
Neuron projection development
Neuron projection morphogenesis
Regulation of neuron projection development
Axonogenesis
Map2
Ntm
Syt1
Thy1
Epha8
Snap25
Sema3e
Unc5c

Figure 3.01: The addition of Atoh1 to the IPA paradigm facilitates transition from a progenitor state to a differentiated neuron. (A) Schematic of transgenic construct to express IPA with Atoh1 in MG. (B) Regeneration paradigm for inducing IPA:Atoh1 expression in MG in the damaged retina. (C) Representative immunofluorescence images of regenerated neurons from IPA:Atoh1 mice demonstrating MG-derived neurons (GFP^+) are HuC/D^+ (red) and not $Otx2^+$ (purple). (D) Integrated UMAP of FACS-sorted MG-derived cells after regeneration paradigm with either IPA:Atoh1 or IPA-only overexpression. Highlighted in either blue or red are the RGC-like cells from each dataset that were subsetted for further comparative analysis. (E) Scatterplot highlighting differentially expressed genes between the RGC-like cells of the IPA:Atoh1 (blue) and IPA-only (red) regeneration paradigms. (F) GO analysis revealed that neurodevelopmental terms containing many retinal progenitor genes were down-regulated in the IPA:Atoh1 dataset versus IPA only. (G) Integrated UMAP of IPA:Atoh1 data as described above with previously generated Ascl1:Atoh1 dataset (*13*). Blue or red highlighting denotes RGC-like cells from each dataset compared in further analysis. (H) Scatterplot highlighting differentially expressed genes between the RGC-like cells of the IPA:Atoh1 and Ascl1:Atoh1 regeneration paradigms. (I) Bar plot of GO terms relating to neurite outgrowth enriched in the IPA:Atoh1 data. Known neuron projection genes listed are up-regulated with IPA:Atoh1 versus Ascl1:Atoh1. Mouse schematic was made with Biorender.com.

Immunohistochemistry revealed the majority of GFP^+ MG-derived neurons expressed the ganglion/amacrine marker HuC/D and lacked expression of the bipolar marker Otx2 (Figure 3.01c). Adding Atoh1 to the combination of IPA factors also bypasses the requirement for retinal injury to induce MG-neurogenesis (Figure 3.02a-d). We next performed scRNA-seq on regenerated cells treated from the IPA:Atoh1 condition and integrated them with cells from the IPA-only treatment group to determine whether the addition of Atoh1 may improve RGC generation after retinal damage (Figure 3.01d). This analysis revealed that MG-derived neurons from the IPA:Atoh1 mice were most similar to the MG-derived RGCs from the IPA condition, while a smaller proportion of bipolar, cone, and amacrine cells were also present (Figure 3.01d; Figure 3.02e-f).

To assess whether Atoh1 overexpression reduces the progenitor signature of MG-derived neurons after IPA expression, we formed a subset of the RGC-like cells from each dataset for

comparison. A differential gene expression (DGE) analysis showed that the in the IPA:Atoh condition, the RGC-like cells showed a greater decrease in expression of progenitor and glial genes than similar cells from the IPA only condition (Figure 3.01e). This was further confirmed with (GO) analysis, where IPA:Atoh1 reduced genes associated with neural progenitors compared to the IPA-only condition (Figure 3.01f), consistent with the hypothesis that Atoh1 promotes maturation of the RGC-like cells.

We have previously shown Ascl1:Atoh1 generates immature RGC-like cells from MG[156]. We hypothesized that the addition of IPA-factors to Atoh1 might induce markers of more mature RGCs. We compared IPA:Atoh1 with previously-generated Ascl1:Atoh1 datasets and found a similar composition of cell types (Figure 3.01g; Figure 3.02e-h). However, we found the addition of IPA to Atoh1 increased RGC-like cells by 15% and resulted in a corresponding decrease in bipolar and progenitor-like cells (Figure 3.02g-h). DGE analysis revealed that the addition of IPA to Ascl1:Atoh1 leads to an enrichment of RGC genes such as *Map2* and *Thy1* (Figure 3.01h). Furthermore, we found the top GO terms enriched in the IPA:Atoh1 were related to neuron projection development and axonogenesis (Figure 3.01i), with many genes specifically related to axon guidance (eg.*Epha8*, *Sema3e*) and synaptogenesis (e.g. *Syt1*, *Snap25*).

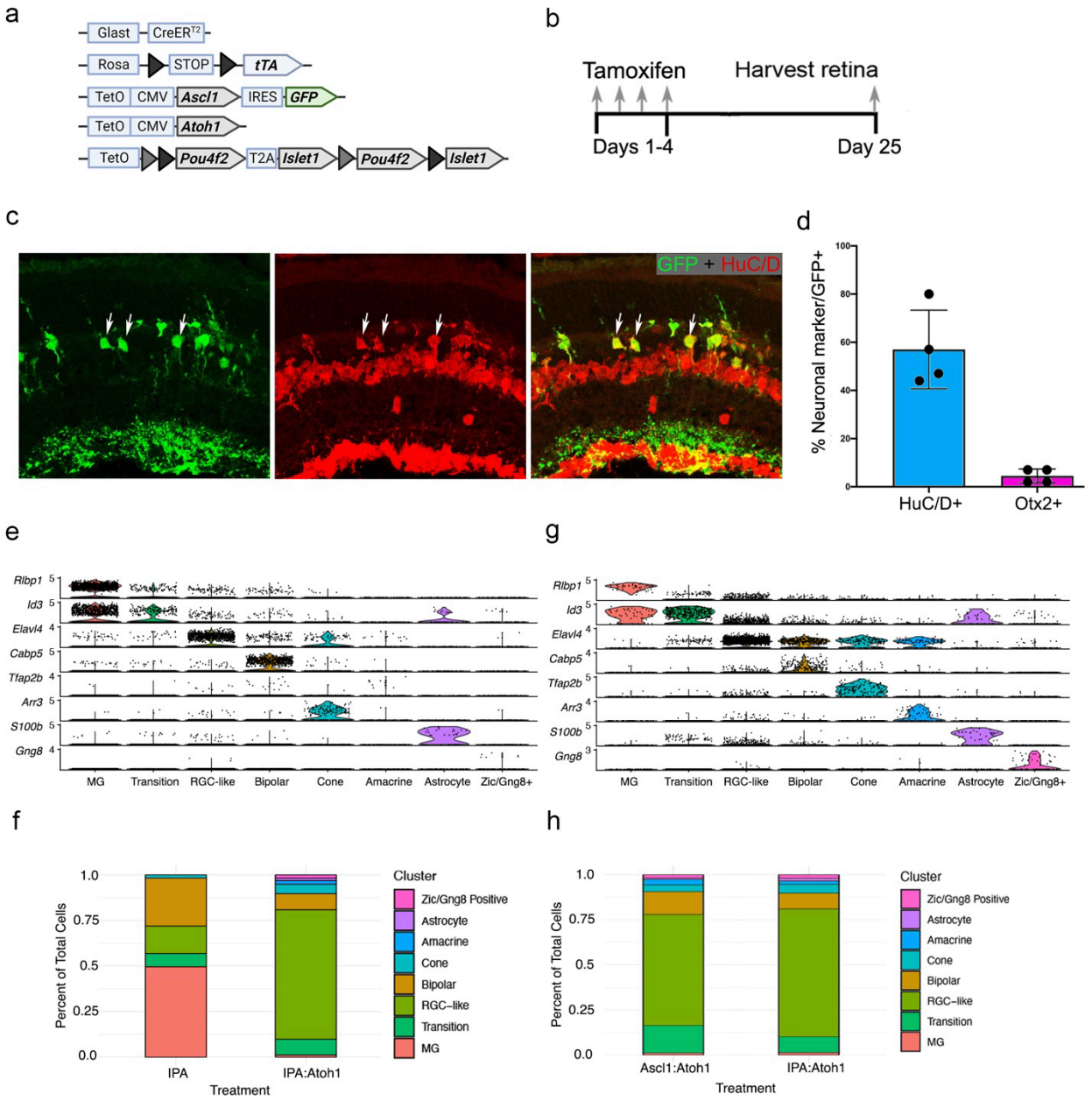

Figure 3.02: The addition of Atoh1 to IPA significantly induces MG-derived RGC-like cells and does not require retinal damage. (a) Transgenic mouse construct used for induction of Ascl1, Atoh1, Pou4f2, and Islet1. (b) Paradigm to assay whether induction of all four transcription factors can induce MG-neurogenesis in the absence of retinal injury. (c) Representative section of a retina after IPAA treatment showing MG-derived (GFP+) cells express the neuronal marker HuC/D (red). (d) Quantification of the percent of MG-derived cells that express the RGC-like marker HuC/D or the bipolar marker Otx2 after IPAA treatment without injury. (e-h) Violin plots of markers used to define clusters, and bar plots showing cluster composition of IPA-IPA:Atoh1 (e-f) and Ascl1:Atoh1-IPA:Atoh1 (g-h) integrated scRNAseq data.

RGC-like cells lack expression of definitive subtype markers

While IPA:Atoh1 overexpression resulted in a marked increase in the efficiency of RGC regeneration, we observed only a subtle improvement in maturation in the transcriptomics data, with the main phenotype being a reduction of glial and progenitor genes. This led us to hypothesize that the expression of additional factors is needed to drive the terminal differentiation of RGCs. Recent studies by Joshua Sane's group have expanded our knowledge of both RGC subtypes and of the transcription factors involved with promoting the differentiation of different sets of subtypes. In *Tran et al., 2019* the team used a computational approach for *de novo* subtype identification using scRNA-seq data from sorted adult RGCs[16]. While our RGCs express some of these subtype markers, they are not present in any combination indicative of a specific subtype (Figure 2.05). Likewise, to explore the similarity between the IPA-induced RGC-like cells and the diversity of endogenous RGC subtypes we used Seurat's label transfer feature with the sorted RGC dataset assigned as a reference and the RGC-like cells as the query; low prediction scores were seen for any given subtype, with most subtypes having a prediction score of zero – further evidence that the RGC-like cells are failing to reach a state of terminal differentiation (Figure 3.03a-b).

In *Shekhar et al., 2022* the team performed scRNA-seq on mouse RGC precursor cells at different time points to study the transcriptomic changes that occur during the diversification of subtypes. They discovered that early RGCs are both multipotent and heterogeneous; expression of a small set of transcription factors was shown to discriminate these early RGC populations and can be used to predict sets of fully differentiated RGC subtypes[9]. While this study lacked experimental validation that these genes drive the differentiation of different RGC subtypes,

another study carried out in zebrafish did ablate at least one gene identified by both studies (Eomes) and observed a corresponding loss of the computationally predicted subtypes[187]. Notably, the IPA-induced RGC-like cells lack expression of any of these putative subtype fate-driving transcription factors (Figure 3.03b).

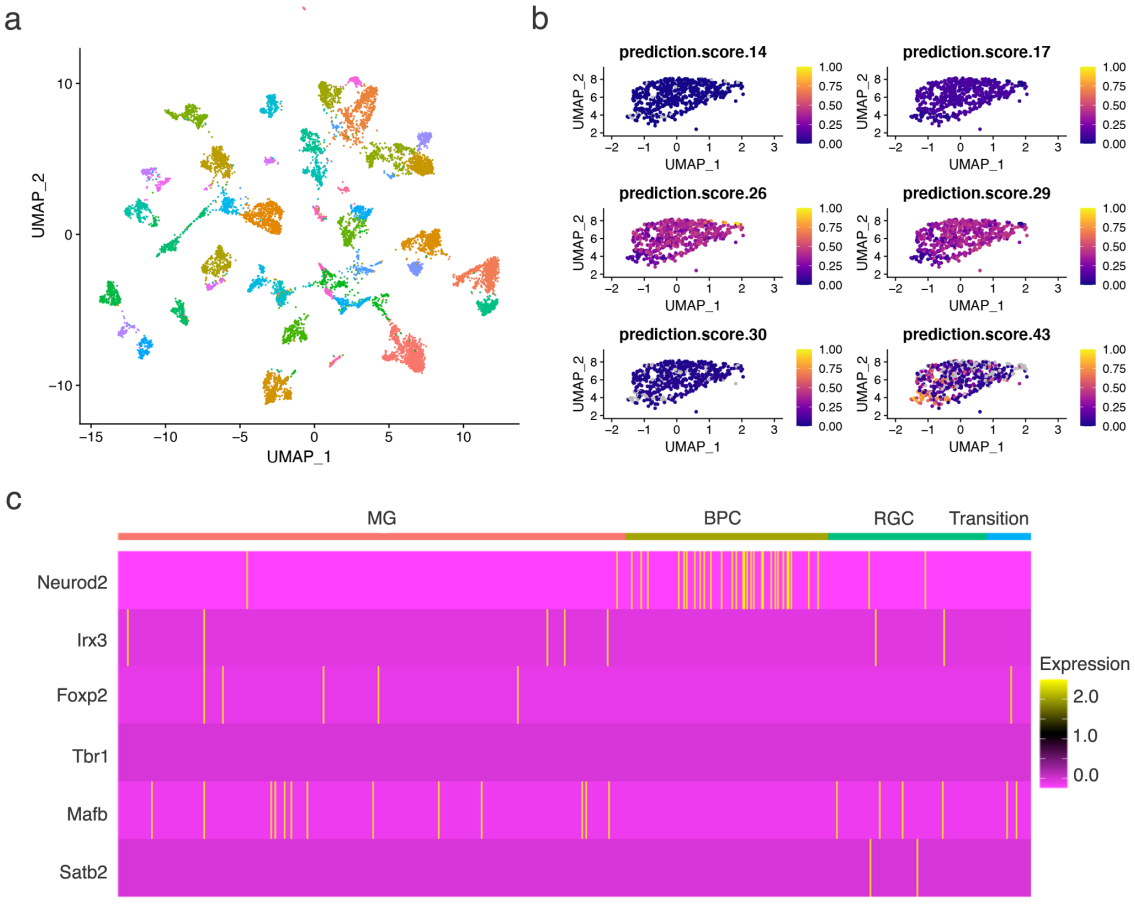

Figure 3.03: IPA RGCs lack many lineage-defining subtype markers. (a) UMAP showing cluster of RGC subtypes (data from: *Tran et al., 2015*). (b) Feature plot showing Seurat label-transfer prediction scores for IPA RGCs. (c) Heatmap of normalized expression values in IPA data for subtype-specifying transcription factors identified in *Shekhar et al., 2022*; genes with a value of zero throughout the dataset are not shown.

Overexpression of Neurod2 and Irx2 improves neurite outgrowth *in vitro*

We hypothesized that overexpression of additional fate-driving transcription factors may improve the maturation of the RGC-like cells derived from IPA overexpression. As the IPA RGCs and progenitor cells lack expression of any of the putative fate-driving factors identified in both mice and zebrafish, we filtered these lists of genes by factors we have identified through our analyses of transcription factor activity cascades across the developing RGC lineage (described in Ch.2) to narrow down a list of five factors for overexpression alongside IPA: NeuroD2, Irx2, Irx5, Ebf1, and Tcf3. As transgenic mouse models capable of conditional overexpression of any of these genes were not readily available, we used a TRE-based lentiviral approach to overexpress each gene concomitantly with IPA in cultured MG and assayed the phenotype of each, relative to IPA alone, through IF profiling and cell morphology analysis. MG cultured from 3-5 mice were pooled and experiments were carried out with 3 replicates. Lentivirus was added to the cultured MG for two days before adding doxycline to activate IPA and the additional TFs, and then the cells were allowed to reprogram for another 5-7 days (Figure 3.04a-b). One factor, Tcf3, was toxic to the cells upon overexpression and was subsequently eliminated from the analyses.

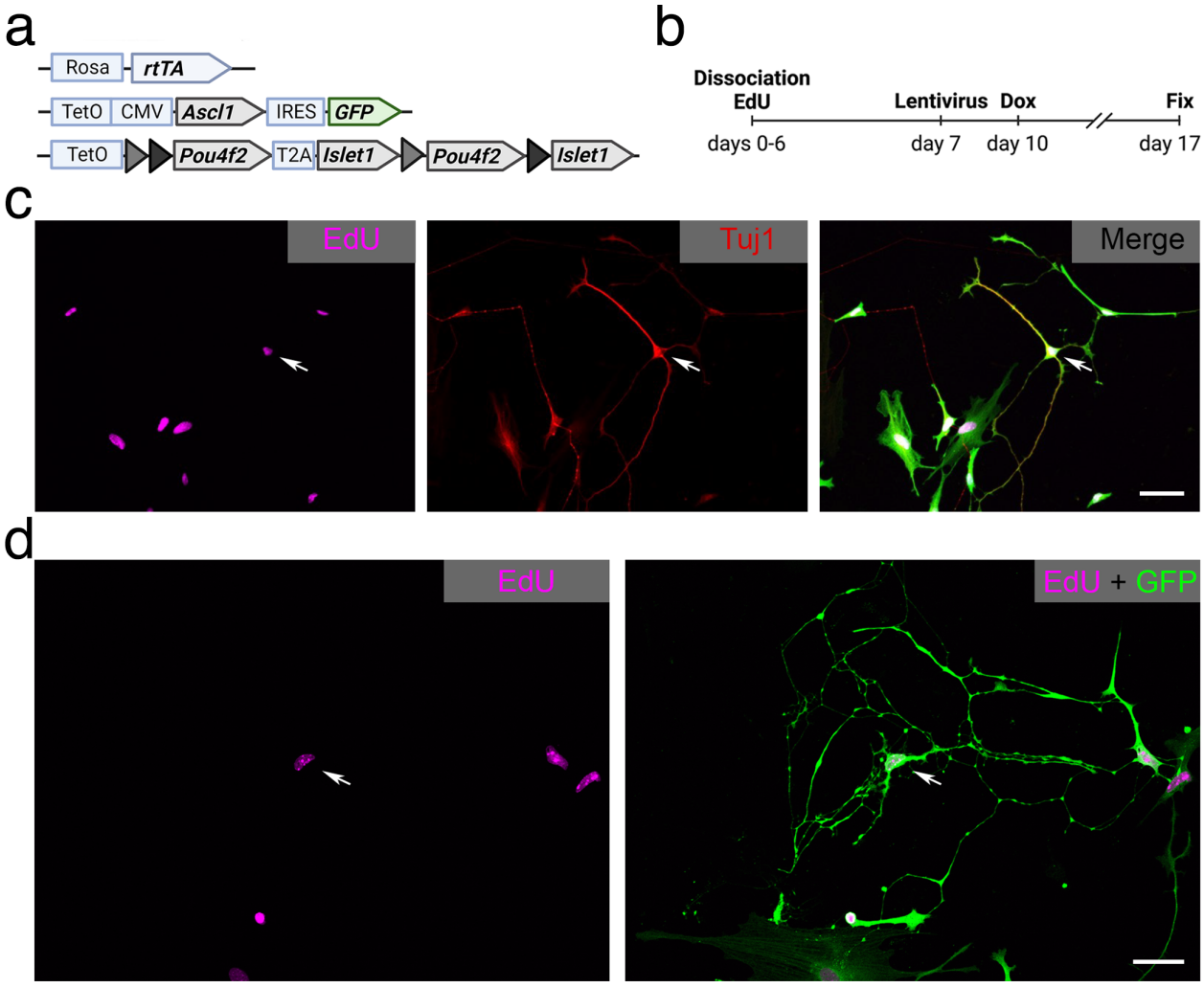

Figure 3.04: Overexpression of IPA with additional transcription factors for improved maturation of RGC-like cells. (a) Genotype of cultured MG. (b) Schematic of reprogramming paradigm. (c-d) Representative immunofluorescence images of MG reprogrammed with co-expression of IPA and lentivirus of either (c) Irx2 or (d) NeuroD2. Scale bars, 50 μm.

While no condition gave rise to neurons with increased expression of the markers of terminal RGC differentiation we assayed via immunofluorescence (Rbpms, Sncg, and Nfm – data not shown), we saw similar staining of markers we observed in our previous IPA overexpresson studies in cultured MG, such as Tuj1. However, we noticed a striking difference in cell morphology in some treatments, characterized by larger cells with long branched processes (Figure 3.04c-d). To better assess size and neurite complexity, we made neurite traces in ImageJ

(n=23-40 cells per condition) and carried out a Sholl analysis. A Sholl profile was obtained for each condition and the number of intersections at each radii was compared to the IPA-only control (Figure 3.05a).

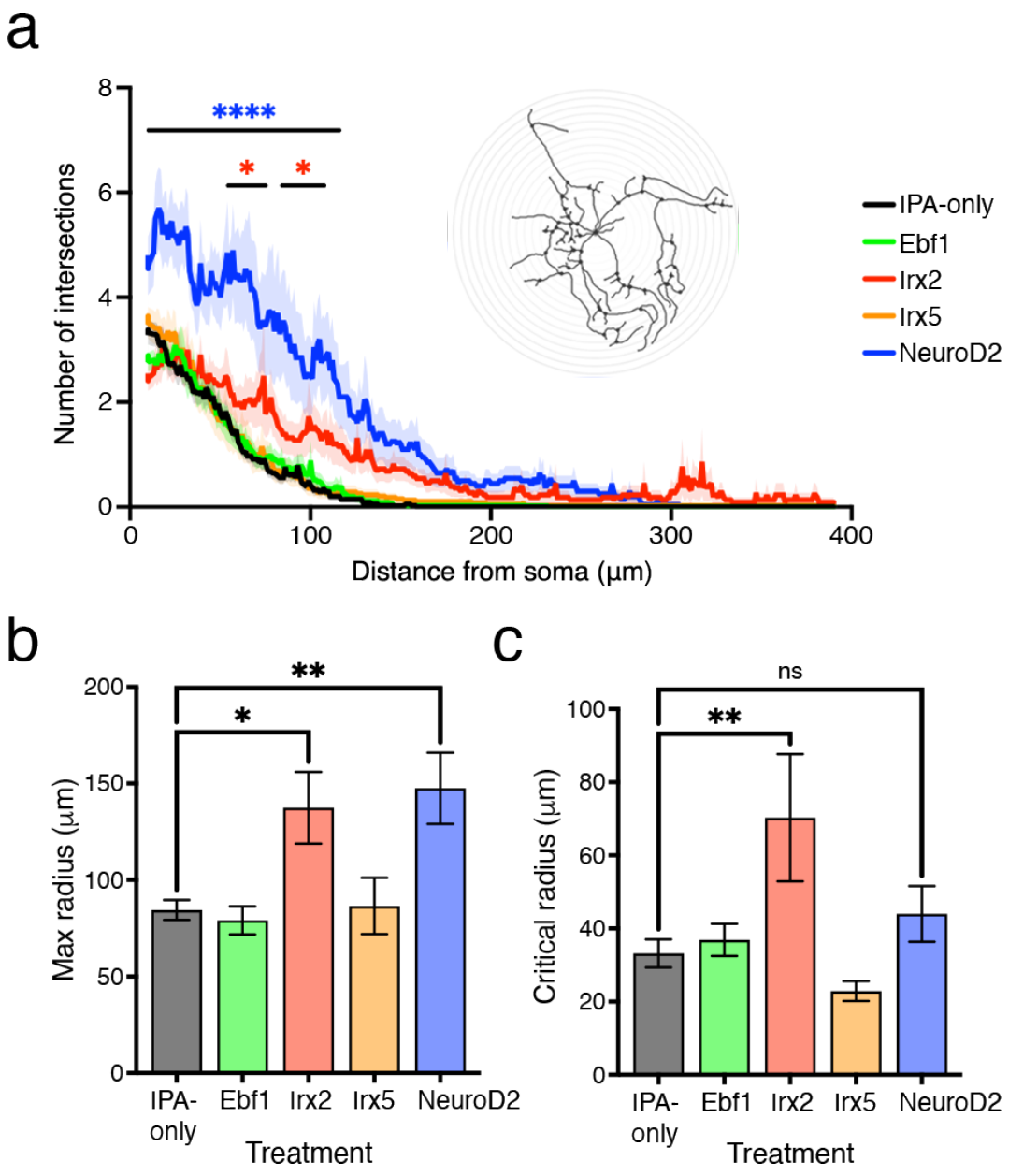

Figure 3.05: Neurod2 and Irx2 increase neurite complexity when co-expressed with IPA in cultured MG. (a) Sholl profiles of MG-derived neurons from IPA overexpression combined with either Ebf1, Irx2, Irx5, or NeuroD2 expression. (b) The average maximum radius for each condition. (c) The average critical radius for each condition. Significance of difference was determined by two-way Anova followed by Dunnett's multiple comparison (* $p < 0.01$, ** $p < 0.01$; *** $p < 0.001$; **** $p < 0.0001$).

Two TF treatments resulted in distinct profiles. NeuroD2 induced cells with a significant increase in neurite intersections starting at radii near the soma, while Irx2 cells had a more modest increase that began around 70μm out from the soma (Figure 3.05a). Each of these two conditions also resulted in an overall increase in cell length, as assessed by the average maximum radius at which intersections occurred (Figure 3.05b). While NeuroD2 stimulated the most overall neurite outgrowth, Irx2 had the highest average critical radius – the point at distance at which most neurite intersections occur (Figure 3.05c). This matched with qualitative observations of the cells, which often appeared to project long thin processes that began branching further out from the soma (Figure 3.04c). To better assess the differences in neurite branching patterns between NeuroD2 and Irx2, we carried out a Strahler analysis to assign an order to each neurite branch and quantified the length of each branch. While both NeuroD2 and Irx2 had higher-order branching than IPA alone (we observed no Strahler order 4 cells in this condition), only Irx2 had significantly longer branches with an order greater than 1 (Figure 3.06a-d). These observations are consistent with cells that extend long axons with arbors further out from the soma than those of dendrites.

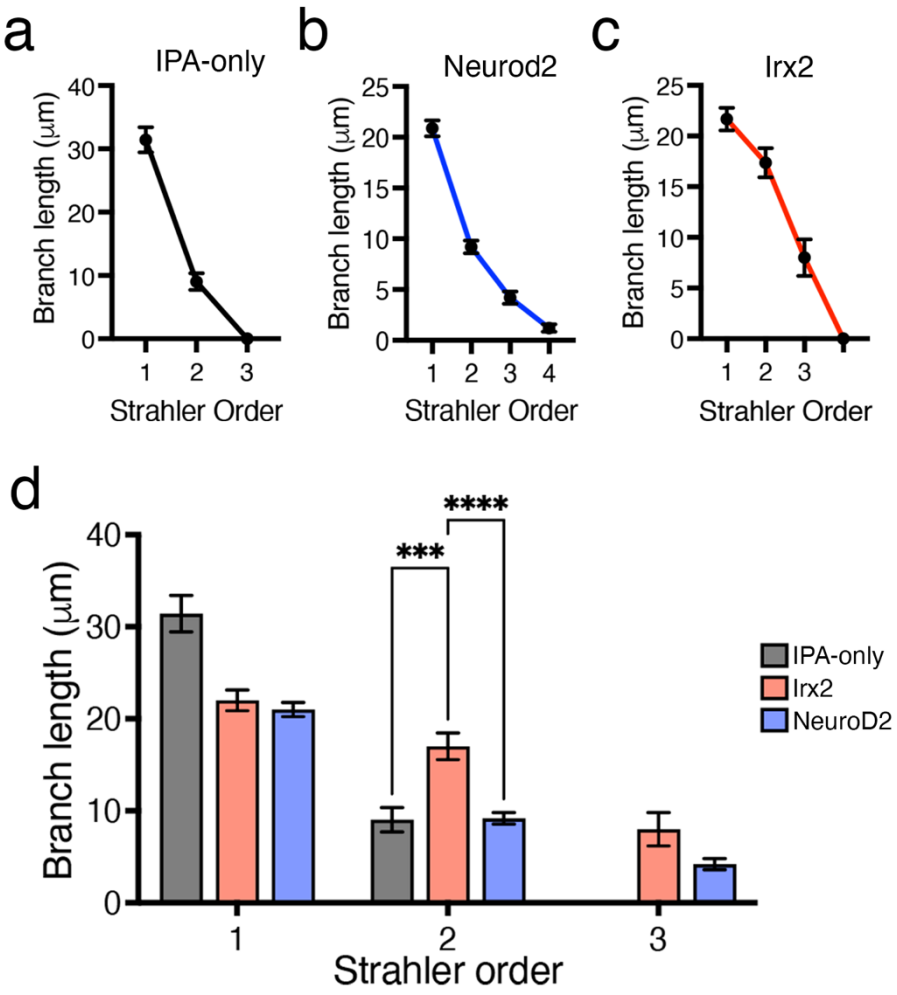

Figure 3.06: Neurod2 and Irx2 induce different neurite morphologies in cultured IPA MG. (a-c) Average branch length by Strahler order for (a) IPA, (b) IPA+NeuroD2, and (c) IPA+Irx2. (d) Statistical comparison of the average branch length for branches of Strahler orders 1-3. Significance of difference was determined by two-way Anova followed by Dunnett's multiple comparison (*** $p < 0.001$; **** $p < 0.0001$).

To examine whether the NeuroD2 or Irx2 conditions lead to an increased expression of dendrite and axon-associated genes, we repeated the lentiviral overexpression experiments with these two TFs and then processed the reprogrammed MG with the 10x genomics platform for scRNA-seq. Unfortunately, due to technical issues resulting in low read quality for the Irx2 sample, we only analyzed the data from the NeuroD2 sample. The overall data structure of the IPA+NeuroD2

condition is similar to IPA-alone when integrated together (Figure 3.07a). Interestingly, however, we observed more bipolar cells with a reduction in the number of cells in the transition population, which resulted in an overall increase in the percentage of neurons in the NeuroD2 sample (21% in IPA+NeuroD2 vs 17% in IPA-only), albeit with a slight reduction in the number of RGCs. To determine if NeuroD2 is promoting maturation of the RGCs, we made a subset of only the RGCs from each condition and performed a DGEA (Figure 3.07b). We noted an increase in expression of many RGC marker genes (Gal and Robo1), as well as an enrichment of GO terms relating to neurons and neurodevelopment, including neuron projection development (Figure 3.07b-c). We also observed an increase in voltage-gated sodium channel component genes which were expressed both throughout the population as well as specifically in the RGCs (Figure 3.07d).

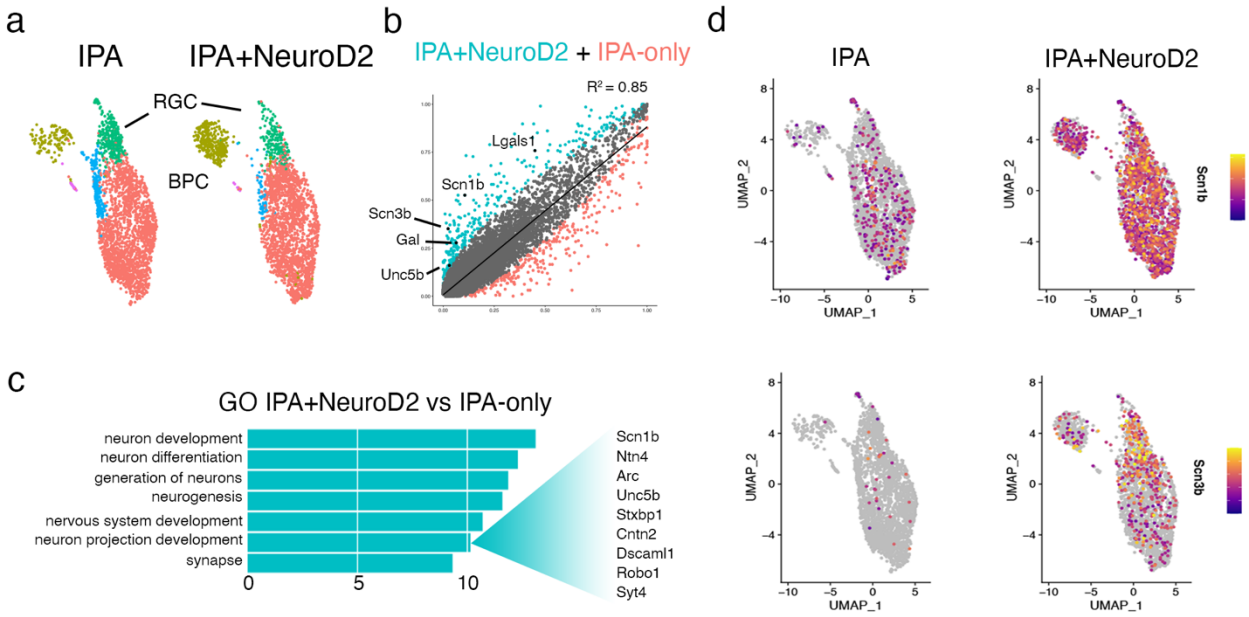

Figure 3.07: IPA:Neurod2 induces expression of more neural projection genes than IPA alone. (a) UMAP of scRNA-seq data from IPA and IPA+NeuroD2 reprogrammed MG. (b) Differentially expressed genes between the RGCs from IPA+NeuroD2 versus IPA-only conditions with labelled RGC genes. (c) GO analysis depicting terms relating to neurons and neurogenesis that are enriched in RGCs from the IPA+NeuroD2 condition. (d) Sodium channel expression between IPA and IPA+NeuroD2 conditions.

Discussion

While we have shown that overexpression of developmental TFs in MG can stimulate the regeneration of RGC-like neurons, these cells fail to fully mature. We found that some TFs that are normally active in the RGC lineage during development were not expressed in IPA-reprogrammed cells. These genes mostly consisted of bHLH and homeobox TFs that are expressed either upstream (Atoh, NeuroD, Tcf families) or alongside/downstream of Pou4f2 and Isl1 (Ebf, Irx families). We hypothesized that one or more of these genes may be necessary for the full maturation of regenerated RGCs. Interestingly, we found different TFs promoted different components of maturation.

The progenitor state in MG can be repressed by the expression of Atoh1 in addition to IPA, consistent with the role for Atonal TFs in promoting neuronal differentiation, and this allows further differentiation of the MG-derived RGCs. In cultured MG, co-expression of IPA with either Neurod2 or Irx2 yielded neurons with greater and more complex neurite outgrowth. The most dramatic change in terms of overall complexity was seen in the Neurod2 condition, however, both conditions increased the number of cells with long, branching neurites. While there was less overall neurite outgrowth in the Irx2 condition, these cells exhibited a significant increase in order 2 branch length. While branches that are part of a higher order chain could contribute to this, it is consistent with single long neurites extending from the soma with either small outgrowths along the neurite or single branch points at the end of the neurite. The Irx2 Sholl profile also shows an increase in neurite complexity versus IPA alone does not occur until around 70-100μm from the soma. Collectively, these findings suggest Irx2 overexpression may be activating genes involved with axon outgrowth.

In the scRNA-seq analysis from the NeuroD2 condition we noted several genes involved with neurite outgrowth and neuronal signaling were upregulated. For instance, we saw increased expression of netrin signaling components (Ntn4, Unc5b), which is involved with RGC axon guidance during development and has been demonstrated to regulate branching[188,189]. We also saw expression of genes involved with neurite structure, such as activity-regulated cytoskeleton associated-protein (Arc) and the actin-binding protein Twf2. Finally, we saw genes involved with various aspects of neuronal signalling, such as sodium channels and intracellular transport and synaptic signaling (Syt4, Stxbp1, Twf2)[190-192]. Collectively, this suggests Neurod2 overexpression activates various gene modules governing neurite development and function.

Neurod-family TFs are known regulators of cell fate in the retina, and forced expression in neonatal progenitors has been shown to lead to RGC production[88]. However, little is known about the precise role of Irx genes in retinal development. While deletion of some genes in this family have been shown to not result in loss of RGCs, all 6 Irx-family genes are expressed by developing RGCs so they may function in a redundant fashion[33,193-195]. However, they are expressed early in development in the GCL and are downstream of Atoh7 and Pou4f2, suggesting they likely play an important role in the RGC development[52,196]. The results presented here suggest a role for Irx2 in neurite outgrowth.

In this chapter we have demonstrated that regenerated RGCs can be improved through overexpression of additional developmental TFs that are not activated with IPA-induced reprogramming. We have discovered that the combined overexpression of Atoh1 with IPAs

efficiently reprograms MG to regenerate RGCs at a much higher rate than what we observed with IPA overexpression alone. We also identified two additional transcription factors that further mature IPA-reprogrammed MG in culture by promoting extensive neurite outgrowth. It remains to be seen if Neurod2 and Irx2 will improve RGC maturation in the adult mouse. As these results, collectively, suggest that a larger cocktail of TFs may be warranted for robust and complete RGC regeneration, breeding additional transgenic mice for this purpose is not practical. The future development of AAV technology combined with transgenic lineage tracing approaches will be essential to exploring additional TF combinations and their potential to synergize with the IPA model. This may also pave the way for an eventual path to the clinic where these studies may form the bedrock of novel regenerative therapeutics for restoring sight.

Chapter 4:

Summary and future directions

Synopsis of results

The ultimate goal of the work presented in this thesis was to regenerate ganglion cells in the mammalian retina. To this end, the overexpression of transcription factors normally expressed in developing RGCs has proven to be a fruitful approach to re-directing the fate of regenerated neurons in an Ascl1-overexpression model of mammalian retinal regeneration. The cells regenerated through this approach exhibit many features of RGCs, such as extension of long axon-like neurites, the ability to fire action potentials, and overall transcriptomic similarity to endogenous RGCs. While the regenerated RGCs appear to be only partially differentiated, we have discovered additional transcription factors that can both increase the efficiency and uniformity of RGC regeneration as well as improve the maturity of regenerated RGCs. While much work remains to be done, the results presented here represent significant strides towards this future endeavor.

Overexpression of Isl1, Pou4f2, and Ascl1 in murine MG gives rise to bipolar and RGC-like cells

Since the discovery that Ascl1 overexpression can induce the regeneration of bipolar cells in an adult mouse retina, a major interest in the field has been whether other types of retinal neurons can also be regenerated[149]. In retinal development, neural diversity is generated from a common pool of progenitor cells by the differential expression of various fate-specifying TFs[22]. Thus, we hypothesized that the concurrent overexpression of Ascl1 with additional RGC lineage-specifying TFs could redirect the fate of regenerated neurons to RGCs. To test this, we bred transgenic mice capable of driving MG-specific expression of Ascl1 with two additional shown to be sufficient to drive the RGC fate in development, Pou4f2 and Isl1[64]. We carried out

experiments both in cultured mouse MG and in live adult mice, following a previously established paradigm of retinal injury and regeneration[148,149]. By profiling regenerated neurons with immunofluorescence, scRNA-seq, scATAC-seq, and patch-clamp electrophysiology we identified two populations: bipolar and RGC-like cells. While bipolar cells can be induced with Ascl1 alone, the RGC-like population was a novel finding. Immunofluorescence staining revealed this population to be positive for RGC marker genes HuC/D, Satb1, and Calretinin *in vivo* and Tuj1, Nfm, and Calbindin *in vitro*. The scRNA-seq and scATAC-seq experiments revealed both transcriptome and accessibility similarity to endogenous RGCs. Patch-clamp electrophysiology experiments revealed that these cells responded to light, indicating integration within the retinal circuitry; they were also capable of firing action potential-like spikes when injected with current – a feature absent in retinal neurons other than RGCs.

We noted some interesting differences between the cell culture and mouse experiments. Due to the nature of the transgenic Pou4f2-Isl1 expression cassette, most cells express only Pou4f2 or Isl1 when activated in the Ascl1-overexpression and lineage-tracing mouse model bred for experiments to be carried out *in vivo*. However, the mouse line bred for our cell culture experiments could reliably express all three transgenes. We found that when all three transgenes were expressed *in vitro,* the relative number of bipolar cells produced was much lower. We hypothesize that this difference is due to the more uniform expression of Pou4f2, specifically, for two reasons: i) Isl1 is normally expressed in bipolar cells, both endogenous and regenerated, and ii) The vast majority of Pou4f2+ neurons in the scRNA-seq data are found in the RGC-like cluster rather than the bipolar cluster. Due to the well-known issue of UMI "drop-out" in scRNA-seq data, it is not possible to reliably determine which cells are triple versus double-

positive, and thus whether Ascl1 and Pou4f2 overexpression are sufficient to drive the novel RGC-like cluster without necessitating Isl1. Nonetheless, we don't see a notable difference in the contribution of Pou4f2+/Isl1- cells vs Pou4f2+/Isl1+ cells to the RGC-like cluster.

We also noted the expression of more canonical RGC marker genes in the cultured MG-derived neurons compared to what we observed *in vivo*. Genes such as Pou4f1 (a downstream target of Pou4f2), Sncg, and Rbpms are exclusively expressed by RGCs in the mouse retina, all of which were seen activated at a higher rate in the cell culture experiments, albeit still in a relatively small percentage of the total RGC-like cells. It is possible that the more reliable activation of all three transgenes induced the expression of more RGC genes. However, we cannot rule out the influence of cell culture conditions contributing to these observed differences in gene expression. Further, some marker genes were activated at a higher rate in the RGC-like cells *in vivo*, such as Elavl4 (HuD) and Calb2 (Calretinin), implying that RGC gene induction wasn't simply more robust *in vitro*. Finally, attempts at integrating the scRNA-seq data from the cell culture experiments with the E14 retina data proved unsuccessful – while some cells clustered with the progenitor and RGC populations from the E14 data, largely the two datasets did not integrate well, with most cells forming sample-dependent clusters (data not shown). This suggests that the cell culture conditions influence the overall transcriptome of the MG-derived progenitors and their neural progeny sufficiently so to make direct comparisons to endogenous cells difficult.

RGC-like cells derived from IPA-induced regeneration do not fully mature

The RGC-like population from the scRNA-seq data of the *in vivo* experiments clustered with immature RGCs when integrated with the E14 retina development data. We also observed

sustained accessibility of progenitor and glial TF motifs, such as those of Ascl1 and Sox genes, in the scATAC-seq data. When compared to endogenous RGCs, the MG-derived RGCs lacked accessibility around genes which regulate axon extension and repress gliogenesis. While we did observe some MG-derived neurons extending long neurites both *in vivo* and *in vitro*, most did not – nor were GFP+ axons observed at the optic nerve head.

One hypothesis for why the MG-derived RGCs failed to reach a state of terminal differentiation is insufficient time was allowed post-treatment. The mice were all given 3 weeks after the final treatment, TSA administration, before harvesting the tissue. To see if increasing the time between treatment and tissue harvest would allow the MG-derived RGCs to mature further we repeated the experiments, harvesting the tissue 6-weeks post-treatment. We repeated the same scRNA-seq analyses as were done with the 3-week timepoint and the results were largely equivalent in regard to gene expression, clustering with the development dataset, and cluster composition. This suggests the MG-derived RGCs do not mature further with additional time.

We also investigated another hypothesis: the MG-derived RGCs die off before they can fully mature. If this were the case, the relative number of cells assigned to the RGC cluster at the 6-week timepoint would be lower than at the 3-week timepoint. An integration of the scRNA-seq datasets of each timepoint revealed this not to be the case – the percent of cells assigned to each cluster was nearly identical between each timepoint. However, it could be that new RGC-like cells are continually being produced and then are lost to apoptosis, creating a stable population size through time. As the regeneration response requires both retinal damage and TSA treatment, this is not likely to be the case. Further, we compared the expression of genes

associated with dying RGCs between the 6-week and 3-week timepoint and saw no significant increase; most genes were expressed at low levels regardless of the timepoint.

Collectively, the above suggest that IPA overexpression can stimulate the production of RGCs that are stable over time but fail to fully mature. While we are uncertain whether these MG-derived RGCs provide any functional recovery of vision after ablation of endogenous RGCs with NMDA, this is not likely to be the case as they do not extend axons to the optic nerve, nor do they fire spontaneous action potentials. Further, the transgenes are only activated in a small number of the total MG in the retina, and of this number < 20% give rise to RGCs.

Atoh1 overexpression increases the number of MG-derived RGCs

The issues stated above present significant translational challenges. In an effort to improve the RGC regeneration model, we sought additional TFs with the potential to increase RGC number and maturity. We focused on a few key gene families that are expressed in the RGC lineage during development but not during IPA-induced regeneration – Atoh, Ebf, Irx, Tcf, and NeuroD. We have previously shown that Ascl1 overexpression with Atoh1 greatly increases the efficiency of reprogramming and reduces glial and progenitor genes[156]. We hypothesized that overexpressing Atoh1 with IPA may repress glial signatures, allowing the MG-derived RGCs to differentiate more fully. When compared to IPA alone, this combination greatly increased the number of RGC-like cells we observed while also reducing the relative number of bipolar cells and MG. We also observed a corresponding decrease in the expression of glial and progenitor genes. When compared to the Ascl1:Atoh1 model, we again noticed an increase in RGC-like cells relative to bipolar cells, however this effect was much more subtle than when compared to

IPA alone. The IPA:Atoh1 RGCs showed some increase in the expression of neurite outgrowth genes as well as axon guidance genes, such as components of ephrin and semaphorin signaling – despite this we did not see much difference in the morphology of the neurons or in their ability to project axons to the optic nerve head. We also did not see expression of Pou4f1, Rbpms, or Sncg with this combination.

Neurod2 and Irx2 overexpression increases neurite outgrowth of MG-derived RGCs

The main phenotype associated with adding Atoh1 to the TF overexpression cocktail was the dramatic increase in the efficiency of RGC regeneration. In an effort to identify TFs that may induce more mature RGCs with increased neurite outgrowth, we continued to screen through the additional candidate TFs. Due to the lack of availability of additional transgenic mice for this purpose, we took a lentivirus-based approach in cultured IPA MG. When co-expressed with IPA, we found two TFs significantly increased neurite outgrowth in cultured MG: Neurod2 and Irx2. Interestingly, the overexpression of these two factors led to two distinct phenotypes. Neurod2 induced more neurite outgrowth overall, with more radial projections from the soma, and longer and more highly branched processes than IPA alone. IPA:Irx2 neurons also produced longer processes with more branching, but less radial projections from the soma. Instead, these cells tended to project long neurites with arbors further out from the soma, as evidenced by the significant increase in the critical radius and order 2 branch lengths versus IPA:Neurod2 and IPA alone.

To see if these TFs also induced genes indicative of further maturation of the MG-derived RGCs, we repeated these experiments and processed the cells of each combination with scRNA-seq.

Unfortunately, the quality of the Irx2 data was low, with less than 70% of total reads mapping to cells so we proceeded to analyze only the Neurod2 sample. The overall cluster composition was similar to IPA alone, however we noted an increase in total neurons, largely due to an increase in bipolar cells, and a decrease in the transition population. This suggests that Neurod2 may aid in differentiation. It is unclear why more bipolar cells were generated. However, we noticed Pou4f2 was not expressed highly in this population, as is seen *in vivo*, suggesting Neurod2 may be aiding in the differentiation of Pou4f2-negative MG to bipolar cells. The RGC-like cells exhibited an increase in many neural projection-related genes compared to IPA alone, including an increase in sodium channels. Some of these genes were increased only in the RGC-like cells, while others were found to be increased in the total population.

Significance of results

To date, there have been many attempts to restore RGC numbers in damaged retinas via transplantation or AAV-based MG reprogramming. Earlier transplantation studies of photoreceptors were initially met with enthusiasm – GFP-labelled photoreceptors transplanted into the subretinal space could migrate to the ONL, form proper outer segments, and establish synaptic connections with the bipolar cells[197-200]. These studies were followed by similar studies involving transplantation of stem cell-derived RGCs[201-204]. The results from the photoreceptor transplantation studies have since been called into question, however, as it was demonstrated that transplanted photoreceptors can transfer either protein, mRNA, or both to endogenous photoreceptors – a phenomenon now referred to as "material transfer"[205-210]. While the results of these various RGC transplantation experiments were quite encouraging, material transfer could not be ruled out entirely in any of these studies. Although it is not clear whether retinal cells

other than photoreceptors are capable of material transfer, this remains an important consideration of all future studies involving retinal neuron transplantation and rigorous controls must be included to rule this possibility out. For instance, experiments involving cross-species transplant can utilize species-specific antibodies and FISH probes to look for instances of cells which co-label for two species.

AAV-based MG-reprogramming has also been attempted as a method to induce RGC regeneration in mice[159,160,211,212]. However, this approach has also been called into question, largely due to demonstrated leakiness of glial-specific promoters in a cell-specific and insert-dependent fashion[161,162,213]. This discovery has rendered AAV-based lineage tracing unreliable and future AAV-based cell reprogramming experiments must demonstrate lineage using a more faithful approach, such as EdU/BrdU labeling or transgenic Cre-based systems.

In this thesis, regeneration of RGC-like cells has been convincingly demonstrated using a combined approach of transgenic lineage-tracing mouse models, cultured MG labeled with EdU, and scRNA-seq data demonstrating transitional states. Further, we compared the MG-derived RGCs to endogenous RGCs using both scRNA-seq and scATAC-seq approaches – the regenerated RGCs maintain features of glial and progenitor cells not present in the endogenous RGCs, further evidence that the cells were indeed generated *de novo*.

The results presented in this thesis also indicate the fate of regenerated neurons can be steered towards a specific cell type though overexpression of lineage-specific drivers of that fate in development. This finding has implications for future studies in the retina that seek to regenerate

other clinically important cell types, such as rods and cones. More broadly, this approach may also hold significance for the regeneration of other tissues, such as brain via astrocyte reprogramming.

Considerations for the functional restoration of vision by RGC regeneration

Ultimately, if the regenerated RGCs are to restore vision they must function sufficiently like endogenous RGCs. While IPA-induced RGCs do not appear to fully differentiate, we have discovered additional transcription factors that may induce further maturity. Neurod2 and Irx2 overexpression resulted in a promising increase in neurite formation. The increase in voltage-gated sodium channels seen in the IPA:Neurod2 cells is also encouraging; the electrophysiological recordings of IPA cells suggest there is a sufficient density of sodium channels to induce an action potential with current injection, but the cells did not fire spontaneously. An important next step towards regenerating functional RGCs is to test these additional TFs *in vivo*. As there are no transgenic mice available for overexpressing either TF, a new transgenic mouse could be established. However, the most forward-looking approach may be to develop an efficient AAV delivery system for targeting MG. When used in conjunction with the transgenic IPA mouse, this would allow for faithful lineage tracing as well as require fewer transgenes to be delivered via AAV. For this approach to be viable, sufficiently efficient targeting needs to be achieved such that enough IPA-GFP+ cells are transduced to enable quantification with immunostaining and cell sorting for -omics experiments. Further, expression levels from the AAV need to be high enough for the TFs to exert an effect. If these two benchmarks are achieved, many more TFs can be screened *in vivo* for their potential to improve retinal regeneration. Additionally, this approach is more amenable to experimentation in human

tissue systems, such as retinal organoids, as developing new iPSC lines and growing out mature organoids are time-intensive procedures. Finally, despite the technical challenges faced so far in the field, viral-based approaches ultimately have the most clinical relevance and will be necessary to develop for their translational potential.

In addition to triggering axon outgrowth from the regenerated RGCs, axon pathfinding may be another hurdle to overcome. Axons from regenerated RGCs in the adult retina have a great distance to cover and must locate the optic nerve head, exit, and eventually find their appropriate targets in the brain. In regenerative species such as zebrafish, this is clearly possible. However, it is unclear whether the appropriate cues exist in the adult mammalian retina to enable proper axon pathfinding.

Additionally, there are over 40 subtypes of RGCs in the mouse retina[16]. The TFs we overexpressed alongside IPA were largely found to drive specific sets of RGC subtypes in development[9]. IPA alone was not sufficient to drive the regeneration of any particular RGC subtype, let alone a diversity of subtypes. Continued experimentation with the TFs identified in this thesis may yield RGCs that can more cleanly be classified as a specific subtype or types. While the ideal treatment would induce regeneration of all RGC subtypes, the regeneration of some subtypes may take precedent over others in terms of the clinical benefit they may offer; for instance, vision-forming RGCs versus non-vision forming RGCs, such as ipRGCs. Thus, a notable restoration of vision may be possible through only partial regeneration of all the possible RGCs. Ultimately, functional restoration will have to be established empirically through

behavioral tests of visual acuity in mice – a feat which has yet to be convincingly demonstrated in any mammalian model of retinal regeneration.

Concluding remarks

The state of the field is currently at an exciting inflection point. A door to regeneration in the adult mammalian retina has been opened with the discovery that Ascl1 overexpression can stimulate the regeneration of bipolar cells[149]. The path forward is now steered by questions which aim to leverage this insight to advance the field towards future clinical applications: *Can the regenerated neurons functionally restore vision? Can other retinal neurons, such as photoreceptors be regenerated? Can neurons in the human retina be restored with this approach?* For the hundreds of millions suffering retinal-related vision loss worldwide, this is a hopeful sign of what lies in wait at the horizon of future discovery. While this field is still in its infancy, the results presented in this thesis represent a major step forward towards the regeneration of retinal neurons lost to degenerative disease.

Materials and Methods

Animals

All animals were treated and housed with University of Washington Institutional Animal Care and Use Committee approved protocols (UW-IACUC). The (1) *Glast-CreER:LNL-tTA:tetO-mAscl1-ires-GFP,* (2) *Glast-CreER:LNL-tTA:tetO-P&I:tetO-mAscl1-ires-GFP*, (3) *Glast-CreER:LNL-tTA:tetO-Atoh1:tetO-P&I: tetO-mAscl1-ires-GFP* mice, (4) rtTa:tetO-Ascl1-ires-GFP, (5) rtTa:tetO-P7I:tetO-Ascl1-ires-GFP are from mixed backgrounds of C57BL/6 and B6SJF1. The Glast-CreER, LNLtTA, and rtTa mice are from Jackson labs. The tetO-mAscl1-GFP mice were a gift from M. Nakafuku (University of Cincinnati), the tetO-Atoh1 mice were a gift from P. Chen (Emory University), and the tetO-P&I mice were a gift from X. Mu (University of Buffalo). Males and females were both used in experiments at equal frequencies. All *in vivo* experiments were performed on adult mice that were over 40 days old.

Primary cell culture

Retinas from tetO-Ascl1-GFP;Rosa-rtTA or tetO-Pou4f2-Islet1-Ascl1-GFP;Rosa-rtTA mice of both sexes were harvested at P12 for MG-cultures. For dissociation, the retinas were incubated in a solution of papain and DNase (Worthington) for 10min at 37ºC, followed by trituration. To stop the reaction, an equal volume of ovomucoid (Worthington) was added. Cells were then spun at 4ºC at 300g for 10min and resuspended in growth medium consisting of Neurobasal (Gibco), 10% FBS (Clontech), N2 (Invitrogen), 1mM L-glutamine (Invitrogen), 1% Penicillin-Streptomycin (Invitrogen) and 100ng/mL mEGF (R&D). Cells were plated at a density of two retinas per 10cm^2 in a 6-well dish and incubated at 37ºC. The media was changed every two days until confluent (~7 days). At confluence, cells were passaged with TrypLE (Gibco),

resuspended in a freezing medium consisting of 50% growth medium, 40% FBS, and 10% DMSO and stored at least one day in liquid $N0_2$ for at least 24 hours. After thawing, cells were grown in FBS-reduced growth medium (1%) and treated with doxycycline to induce tetO-mediate genes.

Immunohistochemistry

After CO2 mediated euthanasia corneas were removed and eye globes were fixed for 30 minutes in 4% PFA in PBS. Fixed eyes were then incubated overnight in 30% sucrose at 4ºC. Retinas were then frozen in O.T.C. and cryosectioned at 18 um. For immunostaining, sections were washed 2 times for 10 minutes in PBS and then incubated in primary antibody in 0.5% Triton X-10 and PBS overnight. Slides were then washed in PBS and incubated in secondary antibodies for one hour. Finally, slides were washed again in PBS and cover slipped with Fuoromount-G (SouthernBiotech). See Table M.T for antibody and concentration information.

Cultured MG were plated on glass coverslips with FBS-reduced growth medium (described above). To activate the transgenes, doxycycline was added at a concentration of 3 ug/mL every 24 hrs for a period of 5 days for scRNA-seq and 7 days for some immunofluorescence experiments. For lentiviral infections, cells were first treated with lentivirus containing both a TRE expression cassette for the transcription factor to be overexpressed and a separate CMV-GFP; two days later the media was replaced as above with added doxycycline. The coverslips were washed with PBS and then fixed with 4% PFA for 10 min at RT, followed by 3x 5min washes with PBS. Primary antibody incubation was done in 0.5% Triton X-10 and 10% NHS in PBS overnight at 4ºC. Coverslips were washed in PBS and then click chemistry was used to

label EdU (Click-iT EdU Assay, Invitrogen), followed by incubation with secondary antibodies and DAPI at RT for 1 hr. After staining, the coverslips were washed 3 more times and placed onto slides with Fluoromount-G (SouthernBiotech).

Analysis of neurite morphology

Three separate pools of tetO-Pou4f2-Islet1-Ascl1-GFP;Rosa-rtTA MG from 3-5 mice were treated with lentivirus and infection rate was assessed two days later as the percentage of cells expressing GFP (only wells with > 90% infection rate were used). Doxycycline was added to activate transgenes and cells were processed for immunofluorescence staining as above. Neurons from each condition (n=25-45) were selected for analysis based on their isolation from nearby cells and presence of at least one neurite. Neurites of each cell were traced and then analyzed with Sholl and Strahler methods in ImageJ using Simple Neurite Tracer (SNT) version 4.1. For the Sholl analysis, fixed radius steps of 1μm were used, beginning with 10μm to exclude soma. Parameter means, statistics, and plots were generated in Prism 9 GraphPad. Significance of difference was determined by two-way AOVA followed by Dunnett's multiple comparison.

Fluorescence-activated cell sorting (FACS)

Following euthanasia, retinas were dissociated into single cells as described for cell culture, after pelleting at 300g at 4 ºC, cells resuspended in Neurobasal solution and passed through a 35 um filter. Using a BD FACSAria III Cell Sorter (BD Bioscience) FACS was performed on GFP+ cells.

Injections

Intravitreal injections were performed with a 32-gauge Hamilton syringe on mice anesthetized with isoflurane. Injections of NMDA were done in a volume of 1uL at a concentration of 100mM in PBS. TSA (Sigma) was administered via intravitreal injections in DMSO at a concentration of 1ug per ul. Intraperitoneal injections of tamoxifen (1.5mg per 100 □L of corn oil) were administered to adult mice for 4 consecutive days to induce expression of the tetO-mAscl1-ires-GFP, the tetO-P&I and the tetO-Atoh1 gene.

Microscopy/cell counts

Images were taken on a Zeiss LSM880 confocal microscope. For quantification of cell counts, a minimum of four images per retina with a 20x objective were taken at the same magnification.

Electrophysiology

Recordings were performed identical to our previous reports [149,150]. Mice were dark-adapted prior to recordings. After euthanasia, retinas were sliced into 200 μm slices for recording. Tissue recordings were performed in Ames medium at 32°C and oxygenated with 95% O_2 / 5% CO_2. GFP+ cells were targeted for recording using video DIC with infrared light and confocal microscopy. Light responses were measured under infrared conditions and the tissue was exposed to full-field illumination via blue and green LEDs. Recordings were performed using pulled glass pipettes and filled with solution containing (in mM): 123 K-aspartate, 10 HEPES, 1 $MgCl_2$, 10 KCl, 1 $Cacl_2$, 2 EGTA, 0.5 Tris-GTP, 4 MG-ATP and 0.1 Alexa-695 hydrazide.

Single cell RNA library construction

For *in vivo* datasets, following FACS purification of GFP+ MG, cells were centrifuged at 300 g at 4 ºC and resuspended at a concentration of 1000 cells per □l. Library construction was done using 10x genomics 3' single cell RNA V3 or V3.1 sequencing kits as described by the manufacturer. Cells were encapsulated in gel beads and given unique barcodes using the 10x chromium controller and 10x genomics chip type G. Libraries were multiplexed using single and dual index kits (10x genomics).

For *in vitro* experiments, MG cultures from 3-5 mice were used. Following 5 days of doxycycline treatment, cells were dissociated using a mix of Accutase (Sigma Aldrich, Saint-Louis, MS) and DNAse (Worhington, Lakewood, NJ) for 2 min and then spun down at 400 RCF for 7 min at 4 ºC. The pellet was resuspended in culture medium to reach a targeted concentration of 1000 cells per µL. Cells were passed through a strainer and loaded into a 10x Genomics Chromium Single Cell chip G following the protocol of Chromium Single Cell 3′ Reagents Kits v3.1 (10X Genomics, Pleasanton, CA).

Single cell RNA sequencing, mapping and data analysis

Libraries were sequenced using an Illumina NextSeq500, in most cases using multiplexed libraries using high output 150 kits. Data were demultiplexed and aligned to the mm10 genome using CellRanger version 3.0. Filtered output files were further analyzed in R using Seurat version ≥ 3.0, ggplot2, data.table, dplyr, tidyr and other commonly used R packages. Low quality cells (identified as having low read depth or high mitochondrial content, >10 %) were removed from datasets. Microglia, as well as any astrocytes or endothelial cells present (for *in vitro*

experiments) were identified and removed from the data prior to downstream analysis. Additionally, prior to analysis, gene expression data were normalized, scaled and cells were clustered using Principal Component Analysis (PCA) and Uniform Manifold Approximation Projection (UMAP), using the tools available in the Seurat R package version ≥ 3.0. Comparisons between datasets were done by canonical correlation analysis as described by the Satija lab vignette[214] (https://satijalab.org/seurat/archive/v3.0/integration.html).

Integration with development data

For comparison to developing retina, data were first downloaded from GEO[16,33]. The label transfer was carried out in Seurat using a reference dataset composed of either RGC subtypes or 432 randomly sampled cells of each major cell class in the developing retina dataset (Rod, Cone, Bipolar, Amacrine, Horizontal, Retinal Ganglion, and Müller Glia cells), for a total of 3024 cells, as identified by canonical markers. Reads were downsampled to a common average depth before analysis. Additionally, the IPA neurons were integrated directly with a subset composed only of E14 cells from the development dataset.

Single cell ATAC-sequencing

The Cellranger ATAC pipeline (2.0.0) was used to preprocess the data resulting from sequencing[215]. First 'cellranger-atac mkfastq' was used to convert BCL files to fastqs and demultiplex reads. Next 'cellranger-atac count' was run to map Tn5 sites to mm10 (mouse genome), remove duplicate reads, and remove background cells. This returned peak by cell matrices and barcoded fragment files which were loaded into Signac[216] , a R (4.0.4) (R core team, 2021) package. Macs2 was then run on the Signac object and barcoded fragment files to

call peaks using Signac's 'CallPeaks' function[217]. Fragments were mapped to the peaks called by Macs2 and assigned to cells using Signac's 'FeatureMatrix' function. Further QC metrics were measured in Signac using the 'NucleosomeSignal' and 'TSSEnrichment' functions. Cells who were outliers in the QC metric categories were removed as per Signac's standard processing guidelines. Latent semantic indexing (LSI) was performed in Signac using the 'RunTFIDF' and 'RunSVD' functions. Signac's 'DepthCor' was used to identify LSI dimensions that were highly correlated with read depth, these LSI dimensions were excluded from downstream analysis. Signac/Seurat's 'RunUMAP' function was run to compute the UMAP embedding. To identify clusters Signac/Seurat's 'FindClusters' was then run at varying resolutions. Clusters were assigned to known retinal cell types by inspecting Tn5 insertions within 100 kb of known marker genes using Signac's 'CoveragePlot' and further supported using chromvar scores for known lineage specific transcription factors. Clusters of the same type were grouped for visualization purposes. Vertebrate motifs were acquired from the Jaspar 2020 database. Signac's 'AddMotifs' function was used to map these motifs to peaks within the Signac object. Signac's 'RunChromvar' function was used to calculate motif accessibility z-score across all cells.

scATAC-seq dataset integration

Before integrating Signac objects, we first ran all previous computational steps on each sample independently. Next we created a shared peak set for all objects that were to be integrated using BEDOPS (-m)[218]. Signac's 'FeatureMatrix' function was run on each sample with the merged peak set to put all samples in the same featurespace. Samples were next downsampled to the same average read depth using DropletUtils 'downsampleMatrix' function. Samples were merged using Signac/Seurat's 'merge' function, and standard Signac normalization, dimensional

reduction, clustering and visualization was performed on the merged object as described above. The object was then split by samples and the samples were integrated together. Anchors between samples were calculated using 'FindIntegrationAnchors' an integrated embedding space was then calculated using Signac's 'IntegrateEmbeddings' function. UMAP and clustering for the integrated object were performed as previously described.

Pseudotime analysis

To calculate psuedotime, and identify trajectory branches samples were loaded into Monocle 3[219] using SeuratWrapper's 'as.cell_data_set' function. Clustering was performed and partitions were defined using Monocle 3's 'cluster_cells'. Monocle 3's 'learn_graph' was then run to define the principal trajectory graph. The pseudotime root was placed in the progenitor-like or Müller glia-like cluster using Monocle 3's 'order_cells'. Branches were selected using Monocle 3's 'choose_graph_segments'. Pseudotime and branch data was transferred back to the Seurat object for later analysis.

Scatterplots

To create the scatterplots Signac/Seurat's 'FindMarkers' function was run between cell groups of interest, using the top 25% most accessible peaks in those cell groups. A scatterplot was then made showing the percent of cells in each group that had accessibility of each peak. Peaks with an average log base 2 fold change greater than .05 were selected for each group. For GO analysis, these peak sets were then loaded into GREAT (Genome Regions Enrichment of Annotations Tool)[220]; or analyzed with gprofiler2 package in R for scRNA-seq data.

Cascade heatmaps

To construct the Cascade heatmaps, motif names were translated to mouse gene names using R and biomart's 'getLDS' function. Pseudotime lineage branches for the RGCs were subset from the RNA and ATAC data from E14 samples. Variable motifs were identified by running Chromvar's 'addGCBias', 'getBackgroundPeaks', 'computeDeviations', and 'computeVariability' functions. Peaks with a verbality score greater than 1.2 were kept for further analysis. This motif list was then subset again, only motifs corresponding to transcription factors expressed by more than 10% of cells in the RGC branch were kept. Lastly conjoined motifs were dropped. Motifs enrichment scores for selected motifs were ordered over pseudotime in the E14 RGC branch in the scATACseq data by fitting their Chomvar scores to a third order polynomial function and ordering motifs by the maximum value of this function within our pseudotime range. To create the heatmaps chromvar motif accessibility Z-scores were plotted in the previously derived order over pseudotime within the RGC lineage. RNA heatmaps were created by plotting the genes whose binding sites were in the final motif list in the same order across pseudotime in the RNA object within RGC lineage. The cascade heatmap for the reprogrammed cells was created by plotting motifs and factors identified in the developmental data.

REAGENT or	SOURCE	IDENTIFIER	CONCENTRATION
Antibodies			
Goat anti-Brn3	Santa Cruz	Cat#: SC-6026 RRID: AB_673441	1:300
Rabbit anti-Calbindin	Millipore	Cat#:AB1778 RRID:AB_2068336	1:1000
Rabbit anti-Calretinin	SW Ant	Cat#:7699 RRID: AB_10000321	1:500
Chicken anti-GFP	Abcam	Cat#: Ab13970 RRID: AB_300798	1:1000
Mouse anti-HUC/D	Invitrogen	Cat#: A-21271 RRID: AB_221448	1:500
Mouse anti-Islet1	DSHB	Cat#: 40.2D6 RRID: AB_528315	1:50
Mouse anti-Neu/N	Millipore	Cat#: MAB377 RRID: AB_2298767	1:1000
Rabbit anti-Neurofilament	Chemicon	Cat#: AB1982 RRID:AB_2313731	1:500
Goat anti-OTX2	R&D Systems	Cat#: BAF1979 RRID: AB_2157171	1:250
Rabbit anti-SATB1	Abcam	Cat#: Ab109122 RRID:AB_10862207	1:300
Goat anti-Sox2	Santa Cruz	Cat#: SC-17320 RRID:AB_2286684	1:1000
Rabbit anti-Tuj1	Covance	Cat#: MRB-435p RRID: AB_2313773	1:500
Secondaries			
Donkey anti-chicken 488	Jackson Immuno	Cat#:703-545-155	1:1000
Donkey anti-goat 568	Life Technologies	Cat#: A11057	1:1000
Donkey anti-goat 647	Jackson Immuno	Cat#: 705-605-147	1:1000
Donkey anti-mouse 568	Life Technologies	Cat#: A10037	1:1000
Donkey anti-mouse 647	Jackson Immuno	Cat#: 715-605-150	1:1000
Donkey anti-rabbit 568	Life Technologies	Cat#: A100042	1:1000
Donkey anti-rabbit 647	Thermo Fisher Scientific	Cat#: A-31573	1:1000

Table M.T: List of antibodies used in the study. Columns identify the antibody, source, catalogue number, RRID, and concentration used for immunohistochemistry.

References

1. Blindness, G.B.D., Vision Impairment, C., and Vision Loss Expert Group of the Global Burden of Disease, S. (2021). Causes of blindness and vision impairment in 2020 and trends over 30 years, and prevalence of avoidable blindness in relation to VISION 2020: the Right to Sight: an analysis for the Global Burden of Disease Study. Lancet Glob Health *9*, e144-e160. 10.1016/S2214-109X(20)30489-7.
2. Dowling, J.E. (1987). The retina : an approachable part of the brain (Belknap Press of Harvard University Press).
3. Gramage, E., Li, J., and Hitchcock, P. (2014). The expression and function of midkine in the vertebrate retina. Br J Pharmacol *171*, 913-923. 10.1111/bph.12495.
4. Hoon, M., Okawa, H., Della Santina, L., and Wong, R.O. (2014). Functional architecture of the retina: development and disease. Prog Retin Eye Res *42*, 44-84. 10.1016/j.preteyeres.2014.06.003.
5. Hubbard, R., and Wald, G. (1952). Cis-trans isomers of vitamin A and retinene in the rhodopsin system. J Gen Physiol *36*, 269-315. 10.1085/jgp.36.2.269.
6. Lamb, T.D. (2013). Evolution of phototransduction, vertebrate photoreceptors and retina. Prog Retin Eye Res *36*, 52-119. 10.1016/j.preteyeres.2013.06.001.
7. Shichida, Y., and Matsuyama, T. (2009). Evolution of opsins and phototransduction. Philos Trans R Soc Lond B Biol Sci *364*, 2881-2895. 10.1098/rstb.2009.0051.
8. Volland, S., Esteve-Rudd, J., Hoo, J., Yee, C., and Williams, D.S. (2015). A comparison of some organizational characteristics of the mouse central retina and the human macula. PLoS One *10*, e0125631. 10.1371/journal.pone.0125631.
9. Shekhar, K., Lapan, S.W., Whitney, I.E., Tran, N.M., Macosko, E.Z., Kowalczyk, M., Adiconis, X., Levin, J.Z., Nemesh, J., Goldman, M., et al. (2016). Comprehensive Classification of Retinal Bipolar Neurons by Single-Cell Transcriptomics. Cell *166*, 1308-1323 e1330. 10.1016/j.cell.2016.07.054.
10. Mangel, S.C. (1991). Analysis of the horizontal cell contribution to the receptive field surround of ganglion cells in the rabbit retina. J Physiol *442*, 211-234. 10.1113/jphysiol.1991.sp018790.
11. Murakami, M., Shimoda, Y., Nakatani, K., Miyachi, E., and Watanabe, S. (1982). GABA-mediated negative feedback from horizontal cells to cones in carp retina. Jpn J Physiol *32*, 911-926. 10.2170/jjphysiol.32.911.
12. Piccolino, M., and Neyton, J. (1982). The feedback effect from luminosity horizontal cells to cones in the turtle retina: a key to understanding the response properties of the horizontal cells. Prog Clin Biol Res *113*, 161-179.
13. Thoreson, W.B., and Mangel, S.C. (2012). Lateral interactions in the outer retina. Prog Retin Eye Res *31*, 407-441. 10.1016/j.preteyeres.2012.04.003.
14. Yan, W., Laboulaye, M.A., Tran, N.M., Whitney, I.E., Benhar, I., and Sanes, J.R. (2020). Mouse Retinal Cell Atlas: Molecular Identification of over Sixty Amacrine Cell Types. J Neurosci *40*, 5177-5195. 10.1523/jneurosci.0471-20.2020.
15. Demb, J.B., and Singer, J.H. (2012). Intrinsic properties and functional circuitry of the AII amacrine cell. Vis Neurosci *29*, 51-60. 10.1017/S0952523811000368.

16. Tran, N.M., Shekhar, K., Whitney, I.E., Jacobi, A., Benhar, I., Hong, G., Yan, W., Adiconis, X., Arnold, M.E., Lee, J.M., et al. (2019). Single-Cell Profiles of Retinal Ganglion Cells Differing in Resilience to Injury Reveal Neuroprotective Genes. Neuron *104*, 1039-1055 e1012. 10.1016/j.neuron.2019.11.006.
17. Agte, S., Junek, S., Matthias, S., Ulbricht, E., Erdmann, I., Wurm, A., Schild, D., Kas, J.A., and Reichenbach, A. (2011). Muller glial cell-provided cellular light guidance through the vital guinea-pig retina. Biophys J *101*, 2611-2619. 10.1016/j.bpj.2011.09.062.
18. Casey, M.A., Lusk, S., and Kwan, K.M. (2021). Build me up optic cup: Intrinsic and extrinsic mechanisms of vertebrate eye morphogenesis. Dev Biol *476*, 128-136. 10.1016/j.ydbio.2021.03.023.
19. Young, R.W. (1985). Cell differentiation in the retina of the mouse. Anat Rec *212*, 199-205. 10.1002/ar.1092120215.
20. La Vail, M.M., Rapaport, D.H., and Rakic, P. (1991). Cytogenesis in the monkey retina. J Comp Neurol *309*, 86-114. 10.1002/cne.903090107.
21. Prada, C., Puga, J., Perez-Mendez, L., Lopez, R., and Ramirez, G. (1991). Spatial and Temporal Patterns of Neurogenesis in the Chick Retina. Eur J Neurosci *3*, 559-569. 10.1111/j.1460-9568.1991.tb00843.x.
22. Bassett, E.A., and Wallace, V.A. (2012). Cell fate determination in the vertebrate retina. Trends Neurosci *35*, 565-573. 10.1016/j.tins.2012.05.004.
23. Reh, T.A., and Kljavin, I.J. (1989). Age of differentiation determines rat retinal germinal cell phenotype: induction of differentiation by dissociation. J Neurosci *9*, 4179-4189. 10.1523/JNEUROSCI.09-12-04179.1989.
24. Sparrow, J.R., Hicks, D., and Barnstable, C.J. (1990). Cell commitment and differentiation in explants of embryonic rat neural retina. Comparison with the developmental potential of dissociated retina. Brain Res Dev Brain Res *51*, 69-84. 10.1016/0165-3806(90)90259-2.
25. Belliveau, M.J., and Cepko, C.L. (1999). Extrinsic and intrinsic factors control the genesis of amacrine and cone cells in the rat retina. Development *126*, 555-566. 10.1242/dev.126.3.555.
26. Gomes, F.L., Zhang, G., Carbonell, F., Correa, J.A., Harris, W.A., Simons, B.D., and Cayouette, M. (2011). Reconstruction of rat retinal progenitor cell lineages in vitro reveals a surprising degree of stochasticity in cell fate decisions. Development *138*, 227-235. 10.1242/dev.059683.
27. Cayouette, M., Barres, B.A., and Raff, M. (2003). Importance of intrinsic mechanisms in cell fate decisions in the developing rat retina. Neuron *40*, 897-904. 10.1016/s0896-6273(03)00756-6.
28. Cepko, C.L., Austin, C.P., Yang, X., Alexiades, M., and Ezzeddine, D. (1996). Cell fate determination in the vertebrate retina. Proc Natl Acad Sci U S A *93*, 589-595. 10.1073/pnas.93.2.589.
29. Reh, T.A., and Cagan, R.L. (1994). Intrinsic and extrinsic signals in the developing vertebrate and fly eyes: viewing vertebrate and invertebrate eyes in the same light. Perspect Dev Neurobiol *2*, 183-190.

30. Elliott, J., Jolicoeur, C., Ramamurthy, V., and Cayouette, M. (2008). Ikaros confers early temporal competence to mouse retinal progenitor cells. Neuron *60*, 26-39. 10.1016/j.neuron.2008.08.008.
31. Georgi, S.A., and Reh, T.A. (2011). Dicer is required for the maintenance of notch signaling and gliogenic competence during mouse retinal development. Dev Neurobiol *71*, 1153-1169. 10.1002/dneu.20899.
32. Reh, T.A., and Hindges, R. (2018). MicroRNAs in Retinal Development. Annu Rev Vis Sci *4*, 25-44. 10.1146/annurev-vision-091517-034357.
33. Clark, B.S., Stein-O'Brien, G.L., Shiau, F., Cannon, G.H., Davis-Marcisak, E., Sherman, T., Santiago, C.P., Hoang, T.V., Rajaii, F., James-Esposito, R.E., et al. (2019). Single-Cell RNA-Seq Analysis of Retinal Development Identifies NFI Factors as Regulating Mitotic Exit and Late-Born Cell Specification. Neuron *102*, 1111-1126 e1115. 10.1016/j.neuron.2019.04.010.
34. Ohsawa, R., and Kageyama, R. (2008). Regulation of retinal cell fate specification by multiple transcription factors. Brain Res *1192*, 90-98. 10.1016/j.brainres.2007.04.014.
35. Brown, N.L., Dagenais, S.L., Chen, C.M., and Glaser, T. (2002). Molecular characterization and mapping of ATOH7, a human atonal homolog with a predicted role in retinal ganglion cell development. Mamm Genome *13*, 95-101. 10.1007/s00335-001-2101-3.
36. Brown, N.L., Kanekar, S., Vetter, M.L., Tucker, P.K., Gemza, D.L., and Glaser, T. (1998). Math5 encodes a murine basic helix-loop-helix transcription factor expressed during early stages of retinal neurogenesis. Development *125*, 4821-4833. 10.1242/dev.125.23.4821.
37. Kanekar, S., Perron, M., Dorsky, R., Harris, W.A., Jan, L.Y., Jan, Y.N., and Vetter, M.L. (1997). Xath5 participates in a network of bHLH genes in the developing Xenopus retina. Neuron *19*, 981-994. 10.1016/s0896-6273(00)80391-8.
38. Yang, Z., Ding, K., Pan, L., Deng, M., and Gan, L. (2003). Math5 determines the competence state of retinal ganglion cell progenitors. Dev Biol *264*, 240-254. 10.1016/j.ydbio.2003.08.005.
39. Feng, L., Xie, Z.H., Ding, Q., Xie, X., Libby, R.T., and Gan, L. (2010). MATH5 controls the acquisition of multiple retinal cell fates. Mol Brain *3*, 36. 10.1186/1756-6606-3-36.
40. Brzezinski, J.A.t., Prasov, L., and Glaser, T. (2012). Math5 defines the ganglion cell competence state in a subpopulation of retinal progenitor cells exiting the cell cycle. Dev Biol *365*, 395-413. 10.1016/j.ydbio.2012.03.006.
41. Brown, N.L., Patel, S., Brzezinski, J., and Glaser, T. (2001). Math5 is required for retinal ganglion cell and optic nerve formation. Development *128*, 2497-2508. 10.1242/dev.128.13.2497.
42. Wang, S.W., Kim, B.S., Ding, K., Wang, H., Sun, D., Johnson, R.L., Klein, W.H., and Gan, L. (2001). Requirement for math5 in the development of retinal ganglion cells. Genes Dev *15*, 24-29. 10.1101/gad.855301.
43. Brzezinski, J.A.t., Brown, N.L., Tanikawa, A., Bush, R.A., Sieving, P.A., Vitaterna, M.H., Takahashi, J.S., and Glaser, T. (2005). Loss of circadian photoentrainment and abnormal retinal electrophysiology in Math5 mutant mice. Invest Ophthalmol Vis Sci *46*, 2540-2551. 10.1167/iovs.04-1123.

44. Prasov, L., and Glaser, T. (2012). Pushing the envelope of retinal ganglion cell genesis: context dependent function of Math5 (Atoh7). Dev Biol *368*, 214-230. 10.1016/j.ydbio.2012.05.005.
45. Hufnagel, R.B., Riesenberg, A.N., Quinn, M., Brzezinski, J.A.t., Glaser, T., and Brown, N.L. (2013). Heterochronic misexpression of Ascl1 in the Atoh7 retinal cell lineage blocks cell cycle exit. Mol Cell Neurosci *54*, 108-120. 10.1016/j.mcn.2013.02.004.
46. Mao, C.A., Wang, S.W., Pan, P., and Klein, W.H. (2008). Rewiring the retinal ganglion cell gene regulatory network: Neurod1 promotes retinal ganglion cell fate in the absence of Math5. Development *135*, 3379-3388. 10.1242/dev.024612.
47. Brodie-Kommit, J., Clark, B.S., Shi, Q., Shiau, F., Kim, D.W., Langel, J., Sheely, C., Ruzycki, P.A., Fries, M., Javed, A., et al. (2021). Atoh7-independent specification of retinal ganglion cell identity. Sci Adv *7*. 10.1126/sciadv.abe4983.
48. Farah, M.H., and Easter, S.S., Jr. (2005). Cell birth and death in the mouse retinal ganglion cell layer. J Comp Neurol *489*, 120-134. 10.1002/cne.20615.
49. Kay, J.N., Finger-Baier, K.C., Roeser, T., Staub, W., and Baier, H. (2001). Retinal ganglion cell genesis requires lakritz, a Zebrafish atonal Homolog. Neuron *30*, 725-736. 10.1016/s0896-6273(01)00312-9.
50. Wu, F., Bard, J.E., Kann, J., Yergeau, D., Sapkota, D., Ge, Y., Hu, Z., Wang, J., Liu, T., and Mu, X. (2021). Single cell transcriptomics reveals lineage trajectory of retinal ganglion cells in wild-type and Atoh7-null retinas. Nat Commun *12*, 1465. 10.1038/s41467-021-21704-4.
51. Liu, W., Mo, Z., and Xiang, M. (2001). The Ath5 proneural genes function upstream of Brn3 POU domain transcription factor genes to promote retinal ganglion cell development. Proc Natl Acad Sci U S A *98*, 1649-1654. 10.1073/pnas.98.4.1649.
52. Ge, Y., Chen, X., Nan, N., Bard, J., Wu, F., Yergeau, D., Liu, T., Wang, J., and Mu, X. (2023). Key transcription factors influence the epigenetic landscape to regulate retinal cell differentiation. Nucleic Acids Res *51*, 2151-2176. 10.1093/nar/gkad026.
53. Mao, C.A., Cho, J.H., Wang, J., Gao, Z., Pan, P., Tsai, W.W., Frishman, L.J., and Klein, W.H. (2013). Reprogramming amacrine and photoreceptor progenitors into retinal ganglion cells by replacing Neurod1 with Atoh7. Development *140*, 541-551. 10.1242/dev.085886.
54. Zhang, X.M., Hashimoto, T., Tang, R., and Yang, X.J. (2018). Elevated expression of human bHLH factor ATOH7 accelerates cell cycle progression of progenitors and enhances production of avian retinal ganglion cells. Sci Rep *8*, 6823. 10.1038/s41598-018-25188-z.
55. Gan, L., Wang, S.W., Huang, Z., and Klein, W.H. (1999). POU domain factor Brn-3b is essential for retinal ganglion cell differentiation and survival but not for initial cell fate specification. Dev Biol *210*, 469-480. 10.1006/dbio.1999.9280.
56. Gan, L., Xiang, M., Zhou, L., Wagner, D.S., Klein, W.H., and Nathans, J. (1996). POU domain factor Brn-3b is required for the development of a large set of retinal ganglion cells. Proc Natl Acad Sci U S A *93*, 3920-3925. 10.1073/pnas.93.9.3920.
57. Mu, X., Beremand, P.D., Zhao, S., Pershad, R., Sun, H., Scarpa, A., Liang, S., Thomas, T.L., and Klein, W.H. (2004). Discrete gene sets depend on POU domain transcription factor

Brn3b/Brn-3.2/POU4f2 for their expression in the mouse embryonic retina. Development *131*, 1197-1210. 10.1242/dev.01010.
58. Mu, X., Fu, X., Sun, H., Beremand, P.D., Thomas, T.L., and Klein, W.H. (2005). A gene network downstream of transcription factor Math5 regulates retinal progenitor cell competence and ganglion cell fate. Dev Biol *280*, 467-481. 10.1016/j.ydbio.2005.01.028.
59. Qiu, F., Jiang, H., and Xiang, M. (2008). A comprehensive negative regulatory program controlled by Brn3b to ensure ganglion cell specification from multipotential retinal precursors. J Neurosci *28*, 3392-3403. 10.1523/JNEUROSCI.0043-08.2008.
60. Badea, T.C., Cahill, H., Ecker, J., Hattar, S., and Nathans, J. (2009). Distinct roles of transcription factors brn3a and brn3b in controlling the development, morphology, and function of retinal ganglion cells. Neuron *61*, 852-864. 10.1016/j.neuron.2009.01.020.
61. Mu, X., Fu, X., Beremand, P.D., Thomas, T.L., and Klein, W.H. (2008). Gene regulation logic in retinal ganglion cell development: Isl1 defines a critical branch distinct from but overlapping with Pou4f2. Proc Natl Acad Sci U S A *105*, 6942-6947. 10.1073/pnas.0802627105.
62. Li, R., Wu, F., Ruonala, R., Sapkota, D., Hu, Z., and Mu, X. (2014). Isl1 and Pou4f2 form a complex to regulate target genes in developing retinal ganglion cells. PLoS One *9*, e92105. 10.1371/journal.pone.0092105.
63. Pan, L., Deng, M., Xie, X., and Gan, L. (2008). ISL1 and BRN3B co-regulate the differentiation of murine retinal ganglion cells. Development *135*, 1981-1990. 10.1242/dev.010751.
64. Wu, F., Kaczynski, T.J., Sethuramanujam, S., Li, R., Jain, V., Slaughter, M., and Mu, X. (2015). Two transcription factors, Pou4f2 and Isl1, are sufficient to specify the retinal ganglion cell fate. Proc Natl Acad Sci U S A *112*, E1559-1568. 10.1073/pnas.1421535112.
65. de Melo, J., Zhou, Q.P., Zhang, Q., Zhang, S., Fonseca, M., Wigle, J.T., and Eisenstat, D.D. (2008). Dlx2 homeobox gene transcriptional regulation of Trkb neurotrophin receptor expression during mouse retinal development. Nucleic Acids Res *36*, 872-884. 10.1093/nar/gkm1099.
66. Jiang, Y., Ding, Q., Xie, X., Libby, R.T., Lefebvre, V., and Gan, L. (2013). Transcription factors SOX4 and SOX11 function redundantly to regulate the development of mouse retinal ganglion cells. J Biol Chem *288*, 18429-18438. 10.1074/jbc.M113.478503.
67. Nishida, A., Furukawa, A., Koike, C., Tano, Y., Aizawa, S., Matsuo, I., and Furukawa, T. (2003). Otx2 homeobox gene controls retinal photoreceptor cell fate and pineal gland development. Nat Neurosci *6*, 1255-1263. 10.1038/nn1155.
68. Koike, C., Nishida, A., Ueno, S., Saito, H., Sanuki, R., Sato, S., Furukawa, A., Aizawa, S., Matsuo, I., Suzuki, N., et al. (2007). Functional roles of Otx2 transcription factor in postnatal mouse retinal development. Mol Cell Biol *27*, 8318-8329. 10.1128/MCB.01209-07.
69. Beby, F., Housset, M., Fossat, N., Le Greneur, C., Flamant, F., Godement, P., and Lamonerie, T. (2010). Otx2 gene deletion in adult mouse retina induces rapid RPE dystrophy and slow photoreceptor degeneration. PLoS One *5*, e11673. 10.1371/journal.pone.0011673.
70. Chen, S., Wang, Q.L., Nie, Z., Sun, H., Lennon, G., Copeland, N.G., Gilbert, D.J., Jenkins, N.A., and Zack, D.J. (1997). Crx, a novel Otx-like paired-homeodomain protein, binds to

and transactivates photoreceptor cell-specific genes. Neuron *19*, 1017-1030. 10.1016/s0896-6273(00)80394-3.

71. Freund, C.L., Gregory-Evans, C.Y., Furukawa, T., Papaioannou, M., Looser, J., Ploder, L., Bellingham, J., Ng, D., Herbrick, J.A., Duncan, A., et al. (1997). Cone-rod dystrophy due to mutations in a novel photoreceptor-specific homeobox gene (CRX) essential for maintenance of the photoreceptor. Cell *91*, 543-553. 10.1016/s0092-8674(00)80440-7.
72. Furukawa, T., Morrow, E.M., and Cepko, C.L. (1997). Crx, a novel otx-like homeobox gene, shows photoreceptor-specific expression and regulates photoreceptor differentiation. Cell *91*, 531-541. 10.1016/s0092-8674(00)80439-0.
73. Samuel, A., Housset, M., Fant, B., and Lamonerie, T. (2014). Otx2 ChIP-seq reveals unique and redundant functions in the mature mouse retina. PLoS One *9*, e89110. 10.1371/journal.pone.0089110.
74. Fu, Y., Liu, H., Ng, L., Kim, J.W., Hao, H., Swaroop, A., and Forrest, D. (2014). Feedback induction of a photoreceptor-specific isoform of retinoid-related orphan nuclear receptor beta by the rod transcription factor NRL. J Biol Chem *289*, 32469-32480. 10.1074/jbc.M114.605774.
75. Jia, L., Oh, E.C., Ng, L., Srinivas, M., Brooks, M., Swaroop, A., and Forrest, D. (2009). Retinoid-related orphan nuclear receptor RORbeta is an early-acting factor in rod photoreceptor development. Proc Natl Acad Sci U S A *106*, 17534-17539. 10.1073/pnas.0902425106.
76. Oh, E.C., Khan, N., Novelli, E., Khanna, H., Strettoi, E., and Swaroop, A. (2007). Transformation of cone precursors to functional rod photoreceptors by bZIP transcription factor NRL. Proc Natl Acad Sci U S A *104*, 1679-1684. 10.1073/pnas.0605934104.
77. Montana, C.L., Kolesnikov, A.V., Shen, S.Q., Myers, C.A., Kefalov, V.J., and Corbo, J.C. (2013). Reprogramming of adult rod photoreceptors prevents retinal degeneration. Proc Natl Acad Sci U S A *110*, 1732-1737. 10.1073/pnas.1214387110.
78. Mears, A.J., Kondo, M., Swain, P.K., Takada, Y., Bush, R.A., Saunders, T.L., Sieving, P.A., and Swaroop, A. (2001). Nrl is required for rod photoreceptor development. Nat Genet *29*, 447-452. 10.1038/ng774.
79. Chen, J., Rattner, A., and Nathans, J. (2005). The rod photoreceptor-specific nuclear receptor Nr2e3 represses transcription of multiple cone-specific genes. J Neurosci *25*, 118-129. 10.1523/JNEUROSCI.3571-04.2005.
80. Cheng, H., Khan, N.W., Roger, J.E., and Swaroop, A. (2011). Excess cones in the retinal degeneration rd7 mouse, caused by the loss of function of orphan nuclear receptor Nr2e3, originate from early-born photoreceptor precursors. Hum Mol Genet *20*, 4102-4115. 10.1093/hmg/ddr334.
81. Cheng, H., Khanna, H., Oh, E.C., Hicks, D., Mitton, K.P., and Swaroop, A. (2004). Photoreceptor-specific nuclear receptor NR2E3 functions as a transcriptional activator in rod photoreceptors. Hum Mol Genet *13*, 1563-1575. 10.1093/hmg/ddh173.
82. Peng, G.H., Ahmad, O., Ahmad, F., Liu, J., and Chen, S. (2005). The photoreceptor-specific nuclear receptor Nr2e3 interacts with Crx and exerts opposing effects on the transcription of rod versus cone genes. Hum Mol Genet *14*, 747-764. 10.1093/hmg/ddi070.

83. Fujitani, Y., Fujitani, S., Luo, H., Qiu, F., Burlison, J., Long, Q., Kawaguchi, Y., Edlund, H., MacDonald, R.J., Furukawa, T., et al. (2006). Ptf1a determines horizontal and amacrine cell fates during mouse retinal development. Development *133*, 4439-4450. 10.1242/dev.02598.
84. Li, S., Mo, Z., Yang, X., Price, S.M., Shen, M.M., and Xiang, M. (2004). Foxn4 controls the genesis of amacrine and horizontal cells by retinal progenitors. Neuron *43*, 795-807. 10.1016/j.neuron.2004.08.041.
85. Nakhai, H., Sel, S., Favor, J., Mendoza-Torres, L., Paulsen, F., Duncker, G.I., and Schmid, R.M. (2007). Ptf1a is essential for the differentiation of GABAergic and glycinergic amacrine cells and horizontal cells in the mouse retina. Development *134*, 1151-1160. 10.1242/dev.02781.
86. Dyer, M.A., Livesey, F.J., Cepko, C.L., and Oliver, G. (2003). Prox1 function controls progenitor cell proliferation and horizontal cell genesis in the mammalian retina. Nat Genet *34*, 53-58. 10.1038/ng1144.
87. Wu, F., Sapkota, D., Li, R., and Mu, X. (2012). Onecut 1 and Onecut 2 are potential regulators of mouse retinal development. J Comp Neurol *520*, 952-969. 10.1002/cne.22741.
88. Cherry, T.J., Wang, S., Bormuth, I., Schwab, M., Olson, J., and Cepko, C.L. (2011). NeuroD factors regulate cell fate and neurite stratification in the developing retina. J Neurosci *31*, 7365-7379. 10.1523/JNEUROSCI.2555-10.2011.
89. Watanabe, T., and Raff, M.C. (1990). Rod photoreceptor development in vitro: intrinsic properties of proliferating neuroepithelial cells change as development proceeds in the rat retina. Neuron *4*, 461-467. 10.1016/0896-6273(90)90058-n.
90. Brzezinski, J.A.t., Kim, E.J., Johnson, J.E., and Reh, T.A. (2011). Ascl1 expression defines a subpopulation of lineage-restricted progenitors in the mammalian retina. Development *138*, 3519-3531. 10.1242/dev.064006.
91. Arendt, D. (2008). The evolution of cell types in animals: emerging principles from molecular studies. Nat Rev Genet *9*, 868-882. 10.1038/nrg2416.
92. Vitorino, M., Jusuf, P.R., Maurus, D., Kimura, Y., Higashijima, S., and Harris, W.A. (2009). Vsx2 in the zebrafish retina: restricted lineages through derepression. Neural Dev *4*, 14. 10.1186/1749-8104-4-14.
93. Chen, C.M., and Cepko, C.L. (2000). Expression of Chx10 and Chx10-1 in the developing chicken retina. Mech Dev *90*, 293-297. 10.1016/s0925-4773(99)00251-8.
94. Norrie, J.L., Lupo, M.S., Xu, B., Al Diri, I., Valentine, M., Putnam, D., Griffiths, L., Zhang, J., Johnson, D., Easton, J., et al. (2019). Nucleome Dynamics during Retinal Development. Neuron *104*, 512-528 e511. 10.1016/j.neuron.2019.08.002.
95. Brzezinski, J.A.t., Lamba, D.A., and Reh, T.A. (2010). Blimp1 controls photoreceptor versus bipolar cell fate choice during retinal development. Development *137*, 619-629. 10.1242/dev.043968.
96. Katoh, K., Omori, Y., Onishi, A., Sato, S., Kondo, M., and Furukawa, T. (2010). Blimp1 suppresses Chx10 expression in differentiating retinal photoreceptor precursors to ensure proper photoreceptor development. J Neurosci *30*, 6515-6526. 10.1523/JNEUROSCI.0771-10.2010.

97. Bian, F., Daghsni, M., Lu, F., Liu, S., Gross, J.M., and Aldiri, I. (2022). Functional analysis of the Vsx2 super-enhancer uncovers distinct cis-regulatory circuits controlling Vsx2 expression during retinogenesis. Development *149*. 10.1242/dev.200642.
98. Livne-Bar, I., Pacal, M., Cheung, M.C., Hankin, M., Trogadis, J., Chen, D., Dorval, K.M., and Bremner, R. (2006). Chx10 is required to block photoreceptor differentiation but is dispensable for progenitor proliferation in the postnatal retina. Proc Natl Acad Sci U S A *103*, 4988-4993. 10.1073/pnas.0600083103.
99. de Melo, J., Clark, B.S., and Blackshaw, S. (2016). Multiple intrinsic factors act in concert with Lhx2 to direct retinal gliogenesis. Sci Rep *6*, 32757. 10.1038/srep32757.
100. de Melo, J., Zibetti, C., Clark, B.S., Hwang, W., Miranda-Angulo, A.L., Qian, J., and Blackshaw, S. (2016). Lhx2 Is an Essential Factor for Retinal Gliogenesis and Notch Signaling. J Neurosci *36*, 2391-2405. 10.1523/JNEUROSCI.3145-15.2016.
101. Muto, A., Iida, A., Satoh, S., and Watanabe, S. (2009). The group E Sox genes Sox8 and Sox9 are regulated by Notch signaling and are required for Muller glial cell development in mouse retina. Exp Eye Res *89*, 549-558. 10.1016/j.exer.2009.05.006.
102. Furukawa, T., Mukherjee, S., Bao, Z.Z., Morrow, E.M., and Cepko, C.L. (2000). rax, Hes1, and notch1 promote the formation of Muller glia by postnatal retinal progenitor cells. Neuron *26*, 383-394. 10.1016/s0896-6273(00)81171-x.
103. Satow, T., Bae, S.K., Inoue, T., Inoue, C., Miyoshi, G., Tomita, K., Bessho, Y., Hashimoto, N., and Kageyama, R. (2001). The basic helix-loop-helix gene hesr2 promotes gliogenesis in mouse retina. J Neurosci *21*, 1265-1273. 10.1523/JNEUROSCI.21-04-01265.2001.
104. Hojo, M., Ohtsuka, T., Hashimoto, N., Gradwohl, G., Guillemot, F., and Kageyama, R. (2000). Glial cell fate specification modulated by the bHLH gene Hes5 in mouse retina. Development *127*, 2515-2522. 10.1242/dev.127.12.2515.
105. Tomita, K., Ishibashi, M., Nakahara, K., Ang, S.L., Nakanishi, S., Guillemot, F., and Kageyama, R. (1996). Mammalian hairy and Enhancer of split homolog 1 regulates differentiation of retinal neurons and is essential for eye morphogenesis. Neuron *16*, 723-734. 10.1016/s0896-6273(00)80093-8.
106. Baek, J.H., Hatakeyama, J., Sakamoto, S., Ohtsuka, T., and Kageyama, R. (2006). Persistent and high levels of Hes1 expression regulate boundary formation in the developing central nervous system. Development *133*, 2467-2476. 10.1242/dev.02403.
107. Bai, G., Sheng, N., Xie, Z., Bian, W., Yokota, Y., Benezra, R., Kageyama, R., Guillemot, F., and Jing, N. (2007). Id sustains Hes1 expression to inhibit precocious neurogenesis by releasing negative autoregulation of Hes1. Dev Cell *13*, 283-297. 10.1016/j.devcel.2007.05.014.
108. Imayoshi, I., Isomura, A., Harima, Y., Kawaguchi, K., Kori, H., Miyachi, H., Fujiwara, T., Ishidate, F., and Kageyama, R. (2013). Oscillatory control of factors determining multipotency and fate in mouse neural progenitors. Science *342*, 1203-1208. 10.1126/science.1242366.
109. Kageyama, R., Shimojo, H., and Imayoshi, I. (2015). Dynamic expression and roles of Hes factors in neural development. Cell Tissue Res *359*, 125-133. 10.1007/s00441-014-1888-7.

110. Kageyama, R., Ochi, S., Sueda, R., and Shimojo, H. (2020). The significance of gene expression dynamics in neural stem cell regulation. Proc Jpn Acad Ser B Phys Biol Sci *96*, 351-363. 10.2183/pjab.96.026.
111. Ohtsuka, T., Ishibashi, M., Gradwohl, G., Nakanishi, S., Guillemot, F., and Kageyama, R. (1999). Hes1 and Hes5 as notch effectors in mammalian neuronal differentiation. EMBO J *18*, 2196-2207. 10.1093/emboj/18.8.2196.
112. Nelson, B.R., Hartman, B.H., Georgi, S.A., Lan, M.S., and Reh, T.A. (2007). Transient inactivation of Notch signaling synchronizes differentiation of neural progenitor cells. Dev Biol *304*, 479-498. 10.1016/j.ydbio.2007.01.001.
113. Nelson, B.R., Ueki, Y., Reardon, S., Karl, M.O., Georgi, S., Hartman, B.H., Lamba, D.A., and Reh, T.A. (2011). Genome-wide analysis of Muller glial differentiation reveals a requirement for Notch signaling in postmitotic cells to maintain the glial fate. PLoS One *6*, e22817. 10.1371/journal.pone.0022817.
114. Deng, Y., Qiao, L., Du, M., Qu, C., Wan, L., Li, J., and Huang, L. (2022). Age-related macular degeneration: Epidemiology, genetics, pathophysiology, diagnosis, and targeted therapy. Genes Dis *9*, 62-79. 10.1016/j.gendis.2021.02.009.
115. Kovach, J.L., Schwartz, S.G., Flynn, H.W., Jr., and Scott, I.U. (2012). Anti-VEGF Treatment Strategies for Wet AMD. J Ophthalmol *2012*, 786870. 10.1155/2012/786870.
116. Verbakel, S.K., van Huet, R.A.C., Boon, C.J.F., den Hollander, A.I., Collin, R.W.J., Klaver, C.C.W., Hoyng, C.B., Roepman, R., and Klevering, B.J. (2018). Non-syndromic retinitis pigmentosa. Prog Retin Eye Res *66*, 157-186. 10.1016/j.preteyeres.2018.03.005.
117. da Cruz, L., Dorn, J.D., Humayun, M.S., Dagnelie, G., Handa, J., Barale, P.O., Sahel, J.A., Stanga, P.E., Hafezi, F., Safran, A.B., et al. (2016). Five-Year Safety and Performance Results from the Argus II Retinal Prosthesis System Clinical Trial. Ophthalmology *123*, 2248-2254. 10.1016/j.ophtha.2016.06.049.
118. Russell, S., Bennett, J., Wellman, J.A., Chung, D.C., Yu, Z.F., Tillman, A., Wittes, J., Pappas, J., Elci, O., McCague, S., et al. (2017). Efficacy and safety of voretigene neparvovec (AAV2-hRPE65v2) in patients with RPE65-mediated inherited retinal dystrophy: a randomised, controlled, open-label, phase 3 trial. Lancet *390*, 849-860. 10.1016/S0140-6736(17)31868-8.
119. NIH. ClinicalTrials.gov. https://clinicaltrials.gov/ct2/results?cond=%22Retinitis+Pigmentosa%22.
120. Teotia, P., Van Hook, M.J., Wichman, C.S., Allingham, R.R., Hauser, M.A., and Ahmad, I. (2017). Modeling Glaucoma: Retinal Ganglion Cells Generated from Induced Pluripotent Stem Cells of Patients with SIX6 Risk Allele Show Developmental Abnormalities. Stem Cells *35*, 2239-2252. 10.1002/stem.2675.
121. Wang, W., and Lo, A.C.Y. (2018). Diabetic Retinopathy: Pathophysiology and Treatments. Int J Mol Sci *19*. 10.3390/ijms19061816.
122. Mansour, S.E., Browning, D.J., Wong, K., Flynn, H.W., Jr., and Bhavsar, A.R. (2020). The Evolving Treatment of Diabetic Retinopathy. Clin Ophthalmol *14*, 653-678. 10.2147/OPTH.S236637.
123. Smith, L.E., Wesolowski, E., McLellan, A., Kostyk, S.K., D'Amato, R., Sullivan, R., and D'Amore, P.A. (1994). Oxygen-induced retinopathy in the mouse. Invest Ophthalmol Vis Sci *35*, 101-111.

124. Fan, B., Zhang, C., Chi, J., Liang, Y., Bao, X., Cong, Y., Yu, B., Li, X., and Li, G.Y. (2022). The Molecular Mechanism of Retina Light Injury Focusing on Damage from Short Wavelength Light. Oxid Med Cell Longev *2022*, 8482149. 10.1155/2022/8482149.
125. Wan, J., and Goldman, D. (2016). Retina regeneration in zebrafish. Curr Opin Genet Dev *40*, 41-47. 10.1016/j.gde.2016.05.009.
126. Sperry, R.W. (1948). Patterning of central synapses in regeneration of the optic nerve in teleosts. Physiol Zool *21*, 351-361. 10.1086/physzool.21.4.30152014.
127. Vihtelic, T.S., and Hyde, D.R. (2000). Light-induced rod and cone cell death and regeneration in the adult albino zebrafish (Danio rerio) retina. J Neurobiol *44*, 289-307. 10.1002/1097-4695(20000905)44:3<289::aid-neu1>3.0.co;2-h.
128. Maier, W., and Wolburg, H. (1979). Regeneration of the goldfish retina after exposure to different doses of ouabain. Cell Tissue Res *202*, 99-118. 10.1007/BF00239223.
129. Hitchcock, P.F., Lindsey Myhr, K.J., Easter, S.S., Jr., Mangione-Smith, R., and Jones, D.D. (1992). Local regeneration in the retina of the goldfish. J Neurobiol *23*, 187-203. 10.1002/neu.480230209.
130. Fischer, A.J., and Reh, T.A. (2001). Muller glia are a potential source of neural regeneration in the postnatal chicken retina. Nat Neurosci *4*, 247-252. 10.1038/85090.
131. Fausett, B.V., and Goldman, D. (2006). A role for alpha1 tubulin-expressing Muller glia in regeneration of the injured zebrafish retina. J Neurosci *26*, 6303-6313. 10.1523/jneurosci.0332-06.2006.
132. Bernardos, R.L., Barthel, L.K., Meyers, J.R., and Raymond, P.A. (2007). Late-stage neuronal progenitors in the retina are radial Muller glia that function as retinal stem cells. J Neurosci *27*, 7028-7040. 10.1523/jneurosci.1624-07.2007.
133. Kassen, S.C., Ramanan, V., Montgomery, J.E., C, T.B., Liu, C.G., Vihtelic, T.S., and Hyde, D.R. (2007). Time course analysis of gene expression during light-induced photoreceptor cell death and regeneration in albino zebrafish. Dev Neurobiol *67*, 1009-1031. 10.1002/dneu.20362.
134. Wilken, M.S., and Reh, T.A. (2016). Retinal regeneration in birds and mice. Curr Opin Genet Dev *40*, 57-64. 10.1016/j.gde.2016.05.028.
135. Goldman, D. (2014). Muller glial cell reprogramming and retina regeneration. Nat Rev Neurosci *15*, 431-442. 10.1038/nrn3723.
136. Powell, C., Cornblath, E., Elsaeidi, F., Wan, J., and Goldman, D. (2016). Zebrafish Muller glia-derived progenitors are multipotent, exhibit proliferative biases and regenerate excess neurons. Sci Rep *6*, 24851. 10.1038/srep24851.
137. Kubota, R., Hokoc, J.N., Moshiri, A., McGuire, C., and Reh, T.A. (2002). A comparative study of neurogenesis in the retinal ciliary marginal zone of homeothermic vertebrates. Brain Res Dev Brain Res *134*, 31-41. 10.1016/s0165-3806(01)00287-5.
138. Conner, C., Ackerman, K.M., Lahne, M., Hobgood, J.S., and Hyde, D.R. (2014). Repressing notch signaling and expressing TNFalpha are sufficient to mimic retinal regeneration by inducing Muller glial proliferation to generate committed progenitor cells. J Neurosci *34*, 14403-14419. 10.1523/JNEUROSCI.0498-14.2014.
139. Wan, J., Ramachandran, R., and Goldman, D. (2012). HB-EGF is necessary and sufficient for Muller glia dedifferentiation and retina regeneration. Dev Cell *22*, 334-347. 10.1016/j.devcel.2011.11.020.

140. Wan, J., and Goldman, D. (2017). Opposing Actions of Fgf8a on Notch Signaling Distinguish Two Muller Glial Cell Populations that Contribute to Retina Growth and Regeneration. Cell Rep *19*, 849-862. 10.1016/j.celrep.2017.04.009.
141. Fausett, B.V., Gumerson, J.D., and Goldman, D. (2008). The proneural basic helix-loop-helix gene ascl1a is required for retina regeneration. J Neurosci *28*, 1109-1117. 10.1523/JNEUROSCI.4853-07.2008.
142. Nelson, C.M., Ackerman, K.M., O'Hayer, P., Bailey, T.J., Gorsuch, R.A., and Hyde, D.R. (2013). Tumor necrosis factor-alpha is produced by dying retinal neurons and is required for Muller glia proliferation during zebrafish retinal regeneration. J Neurosci *33*, 6524-6539. 10.1523/JNEUROSCI.3838-12.2013.
143. Cimadamore, F., Amador-Arjona, A., Chen, C., Huang, C.T., and Terskikh, A.V. (2013). SOX2-LIN28/let-7 pathway regulates proliferation and neurogenesis in neural precursors. Proc Natl Acad Sci U S A *110*, E3017-3026. 10.1073/pnas.1220176110.
144. Ramachandran, R., Fausett, B.V., and Goldman, D. (2010). Ascl1a regulates Muller glia dedifferentiation and retinal regeneration through a Lin-28-dependent, let-7 microRNA signalling pathway. Nat Cell Biol *12*, 1101-1107. 10.1038/ncb2115.
145. Newman, M.A., Thomson, J.M., and Hammond, S.M. (2008). Lin-28 interaction with the Let-7 precursor loop mediates regulated microRNA processing. RNA *14*, 1539-1549. 10.1261/rna.1155108.
146. Elsaeidi, F., Macpherson, P., Mills, E.A., Jui, J., Flannery, J.G., and Goldman, D. (2018). Notch Suppression Collaborates with Ascl1 and Lin28 to Unleash a Regenerative Response in Fish Retina, But Not in Mice. J Neurosci *38*, 2246-2261. 10.1523/jneurosci.2126-17.2018.
147. Pollak, J., Wilken, M.S., Ueki, Y., Cox, K.E., Sullivan, J.M., Taylor, R.J., Levine, E.M., and Reh, T.A. (2013). ASCL1 reprograms mouse Muller glia into neurogenic retinal progenitors. Development *140*, 2619-2631. 10.1242/dev.091355.
148. Ueki, Y., Wilken, M.S., Cox, K.E., Chipman, L., Jorstad, N., Sternhagen, K., Simic, M., Ullom, K., Nakafuku, M., and Reh, T.A. (2015). Transgenic expression of the proneural transcription factor Ascl1 in Muller glia stimulates retinal regeneration in young mice. Proc Natl Acad Sci U S A *112*, 13717-13722. 10.1073/pnas.1510595112.
149. Jorstad, N.L., Wilken, M.S., Grimes, W.N., Wohl, S.G., VandenBosch, L.S., Yoshimatsu, T., Wong, R.O., Rieke, F., and Reh, T.A. (2017). Stimulation of functional neuronal regeneration from Muller glia in adult mice. Nature *548*, 103-107. 10.1038/nature23283.
150. Jorstad, N.L., Wilken, M.S., Todd, L., Finkbeiner, C., Nakamura, P., Radulovich, N., Hooper, M.J., Chitsazan, A., Wilkerson, B.A., Rieke, F., and Reh, T.A. (2020). STAT Signaling Modifies Ascl1 Chromatin Binding and Limits Neural Regeneration from Muller Glia in Adult Mouse Retina. Cell Rep *30*, 2195-2208 e2195. 10.1016/j.celrep.2020.01.075.
151. Todd, L., Squires, N., Suarez, L., and Fischer, A.J. (2016). Jak/Stat signaling regulates the proliferation and neurogenic potential of Muller glia-derived progenitor cells in the avian retina. Sci Rep *6*, 35703. 10.1038/srep35703.
152. Nelson, C.M., Gorsuch, R.A., Bailey, T.J., Ackerman, K.M., Kassen, S.C., and Hyde, D.R. (2012). Stat3 defines three populations of Muller glia and is required for initiating

maximal muller glia proliferation in the regenerating zebrafish retina. J Comp Neurol *520*, 4294-4311. 10.1002/cne.23213.

153. Todd, L., Finkbeiner, C., Wong, C.K., Hooper, M.J., and Reh, T.A. (2020). Microglia Suppress Ascl1-Induced Retinal Regeneration in Mice. Cell Rep *33*, 108507. 10.1016/j.celrep.2020.108507.
154. Fischer, A.J., Zelinka, C., Gallina, D., Scott, M.A., and Todd, L. (2014). Reactive microglia and macrophage facilitate the formation of Muller glia-derived retinal progenitors. Glia *62*, 1608-1628. 10.1002/glia.22703.
155. White, D.T., Sengupta, S., Saxena, M.T., Xu, Q., Hanes, J., Ding, D., Ji, H., and Mumm, J.S. (2017). Immunomodulation-accelerated neuronal regeneration following selective rod photoreceptor cell ablation in the zebrafish retina. Proc Natl Acad Sci U S A *114*, E3719-E3728. 10.1073/pnas.1617721114.
156. Todd, L., Hooper, M.J., Haugan, A.K., Finkbeiner, C., Jorstad, N., Radulovich, N., Wong, C.K., Donaldson, P.C., Jenkins, W., Chen, Q., et al. (2021). Efficient stimulation of retinal regeneration from Muller glia in adult mice using combinations of proneural bHLH transcription factors. Cell Rep *37*, 109857. 10.1016/j.celrep.2021.109857.
157. Ng, A.H.M., Khoshakhlagh, P., Rojo Arias, J.E., Pasquini, G., Wang, K., Swiersy, A., Shipman, S.L., Appleton, E., Kiaee, K., Kohman, R.E., et al. (2021). A comprehensive library of human transcription factors for cell fate engineering. Nat Biotechnol *39*, 510-519. 10.1038/s41587-020-0742-6.
158. Yao, K., Qiu, S., Wang, Y.V., Park, S.J.H., Mohns, E.J., Mehta, B., Liu, X., Chang, B., Zenisek, D., Crair, M.C., et al. (2018). Restoration of vision after de novo genesis of rod photoreceptors in mammalian retinas. Nature *560*, 484-488. 10.1038/s41586-018-0425-3.
159. Xiao, D., Jin, K., Qiu, S., Lei, Q., Huang, W., Chen, H., Su, J., Xu, Q., Xu, Z., Gou, B., et al. (2021). In vivo Regeneration of Ganglion Cells for Vision Restoration in Mammalian Retinas. Front Cell Dev Biol *9*, 755544. 10.3389/fcell.2021.755544.
160. Zhou, H., Su, J., Hu, X., Zhou, C., Li, H., Chen, Z., Xiao, Q., Wang, B., Wu, W., Sun, Y., et al. (2020). Glia-to-Neuron Conversion by CRISPR-CasRx Alleviates Symptoms of Neurological Disease in Mice. Cell *181*, 590-603 e516. 10.1016/j.cell.2020.03.024.
161. Wang, L.L., Serrano, C., Zhong, X., Ma, S., Zou, Y., and Zhang, C.L. (2021). Revisiting astrocyte to neuron conversion with lineage tracing in vivo. Cell *184*, 5465-5481 e5416. 10.1016/j.cell.2021.09.005.
162. Xie, Y., Zhou, J., and Chen, B. (2022). Critical examination of Ptbp1-mediated glia-to-neuron conversion in the mouse retina. Cell Rep *39*, 110960. 10.1016/j.celrep.2022.110960.
163. Rueda, E.M., Hall, B.M., Hill, M.C., Swinton, P.G., Tong, X., Martin, J.F., and Poche, R.A. (2019). The Hippo Pathway Blocks Mammalian Retinal Muller Glial Cell Reprogramming. Cell Rep *27*, 1637-1649 e1636. 10.1016/j.celrep.2019.04.047.
164. Hoang, T., Wang, J., Boyd, P., Wang, F., Santiago, C., Jiang, L., Yoo, S., Lahne, M., Todd, L.J., Jia, M., et al. (2020). Gene regulatory networks controlling vertebrate retinal regeneration. Science *370*. 10.1126/science.abb8598.

165. Elshatory, Y., Deng, M., Xie, X., and Gan, L. (2007). Expression of the LIM-homeodomain protein Isl1 in the developing and mature mouse retina. J Comp Neurol *503*, 182-197. 10.1002/cne.21390.
166. Usui, A., Mochizuki, Y., Iida, A., Miyauchi, E., Satoh, S., Sock, E., Nakauchi, H., Aburatani, H., Murakami, A., Wegner, M., and Watanabe, S. (2013). The early retinal progenitor-expressed gene Sox11 regulates the timing of the differentiation of retinal cells. Development *140*, 740-750. 10.1242/dev.090274.
167. Stuart, T., Butler, A., Hoffman, P., Hafemeister, C., Papalexi, E., Mauck, W.M., 3rd, Hao, Y., Stoeckius, M., Smibert, P., and Satija, R. (2019). Comprehensive Integration of Single-Cell Data. Cell *177*, 1888-1902 e1821. 10.1016/j.cell.2019.05.031.
168. Chang, K.C., Hertz, J., Zhang, X., Jin, X.L., Shaw, P., Derosa, B.A., Li, J.Y., Venugopalan, P., Valenzuela, D.A., Patel, R.D., et al. (2017). Novel Regulatory Mechanisms for the SoxC Transcriptional Network Required for Visual Pathway Development. J Neurosci *37*, 4967-4981. 10.1523/jneurosci.3430-13.2017.
169. Reh, T.A., Tetzlaff, W., Ertlmaier, A., and Zwiers, H. (1993). Developmental study of the expression of B50/GAP-43 in rat retina. J Neurobiol *24*, 949-958. 10.1002/neu.480240708.
170. Peng, Y.R., Tran, N.M., Krishnaswamy, A., Kostadinov, D., Martersteck, E.M., and Sanes, J.R. (2017). Satb1 Regulates Contactin 5 to Pattern Dendrites of a Mammalian Retinal Ganglion Cell. Neuron *95*, 869-883 e866. 10.1016/j.neuron.2017.07.019.
171. Finkbeiner, C., Ortuno-Lizaran, I., Sridhar, A., Hooper, M., Petter, S., and Reh, T.A. (2022). Single-cell ATAC-seq of fetal human retina and stem-cell-derived retinal organoids shows changing chromatin landscapes during cell fate acquisition. Cell Rep *38*, 110294. 10.1016/j.celrep.2021.110294.
172. Lyu, P., Hoang, T., Santiago, C.P., Thomas, E.D., Timms, A.E., Appel, H., Gimmen, M., Le, N., Jiang, L., Kim, D.W., et al. (2021). Gene regulatory networks controlling temporal patterning, neurogenesis, and cell-fate specification in mammalian retina. Cell Rep *37*, 109994. 10.1016/j.celrep.2021.109994.
173. Kakebeen, A.D., Chitsazan, A.D., Williams, M.C., Saunders, L.M., and Wills, A.E. (2020). Chromatin accessibility dynamics and single cell RNA-Seq reveal new regulators of regeneration in neural progenitors. Elife *9*. 10.7554/eLife.52648.
174. Lindsey, B.W., Hall, Z.J., Heuze, A., Joly, J.S., Tropepe, V., and Kaslin, J. (2018). The role of neuro-epithelial-like and radial-glial stem and progenitor cells in development, plasticity, and repair. Prog Neurobiol *170*, 99-114. 10.1016/j.pneurobio.2018.06.004.
175. Bocchi, R., Masserdotti, G., and Gotz, M. (2021). Direct neuronal reprogramming: Fast forward from new concepts toward therapeutic approaches. Neuron. 10.1016/j.neuron.2021.11.023.
176. Blackshaw, S., and Sanes, J.R. (2021). Turning lead into gold: reprogramming retinal cells to cure blindness. J Clin Invest *131*. 10.1172/jci146134.
177. Lentini, C., d'Orange, M., Marichal, N., Trottmann, M.M., Vignoles, R., Foucault, L., Verrier, C., Massera, C., Raineteau, O., Conzelmann, K.K., et al. (2021). Reprogramming reactive glia into interneurons reduces chronic seizure activity in a mouse model of mesial temporal lobe epilepsy. Cell Stem Cell. 10.1016/j.stem.2021.09.002.

178. Torper, O., Pfisterer, U., Wolf, D.A., Pereira, M., Lau, S., Jakobsson, J., Bjorklund, A., Grealish, S., and Parmar, M. (2013). Generation of induced neurons via direct conversion in vivo. Proc Natl Acad Sci U S A *110*, 7038-7043. 10.1073/pnas.1303829110.
179. Heinrich, C., Bergami, M., Gascon, S., Lepier, A., Vigano, F., Dimou, L., Sutor, B., Berninger, B., and Gotz, M. (2014). Sox2-mediated conversion of NG2 glia into induced neurons in the injured adult cerebral cortex. Stem Cell Reports *3*, 1000-1014. 10.1016/j.stemcr.2014.10.007.
180. Mattugini, N., Bocchi, R., Scheuss, V., Russo, G.L., Torper, O., Lao, C.L., and Gotz, M. (2019). Inducing Different Neuronal Subtypes from Astrocytes in the Injured Mouse Cerebral Cortex. Neuron *103*, 1086-1095 e1085. 10.1016/j.neuron.2019.08.009.
181. Sholl, D.A. (1953). Dendritic organization in the neurons of the visual and motor cortices of the cat. J Anat *87*, 387-406.
182. Horton, R.E. (1945). Erosional development of streams and their drainage basins : hydrophysical approach to quantitative morphology (Geological Society of America).
183. Strahler, A.N. (1952). Hypsometric (Area-Altitude) analysis of erosional topography. Geological Society of America Bulletin, 1117–1142.
184. Shelton, D.P. (1985). Membrane resistivity estimated for the Purkinje neuron by means of a passive computer model. Neuroscience *14*, 111-131. 10.1016/0306-4522(85)90168-x.
185. Rothnie, P., Kabaso, D., Hof, P.R., Henry, B.I., and Wearne, S.L. (2006). Functionally relevant measures of spatial complexity in neuronal dendritic arbors. J Theor Biol *238*, 505-526. 10.1016/j.jtbi.2005.06.001.
186. Kolb, H. (1995). Morphology and Circuitry of Ganglion Cells. In Webvision: The Organization of the Retina and Visual System, H. Kolb, E. Fernandez, and R. Nelson, eds.
187. Kolsch, Y., Hahn, J., Sappington, A., Stemmer, M., Fernandes, A.M., Helmbrecht, T.O., Lele, S., Butrus, S., Laurell, E., Arnold-Ammer, I., et al. (2021). Molecular classification of zebrafish retinal ganglion cells links genes to cell types to behavior. Neuron *109*, 645-662 e649. 10.1016/j.neuron.2020.12.003.
188. Hayano, Y., Sasaki, K., Ohmura, N., Takemoto, M., Maeda, Y., Yamashita, T., Hata, Y., Kitada, K., and Yamamoto, N. (2014). Netrin-4 regulates thalamocortical axon branching in an activity-dependent fashion. Proc Natl Acad Sci U S A *111*, 15226-15231. 10.1073/pnas.1402095111.
189. Deiner, M.S., Kennedy, T.E., Fazeli, A., Serafini, T., Tessier-Lavigne, M., and Sretavan, D.W. (1997). Netrin-1 and DCC mediate axon guidance locally at the optic disc: loss of function leads to optic nerve hypoplasia. Neuron *19*, 575-589. 10.1016/s0896-6273(00)80373-6.
190. Walch-Solimena, C., Takei, K., Marek, K.L., Midyett, K., Sudhof, T.C., De Camilli, P., and Jahn, R. (1993). Synaptotagmin: a membrane constituent of neuropeptide-containing large dense-core vesicles. J Neurosci *13*, 3895-3903. 10.1523/JNEUROSCI.13-09-03895.1993.
191. Swanson, D.A., Steel, J.M., and Valle, D. (1998). Identification and characterization of the human ortholog of rat STXBP1, a protein implicated in vesicle trafficking and neurotransmitter release. Genomics *48*, 373-376. 10.1006/geno.1997.5202.

192. Walker, C.K., Greathouse, K.M., Tuscher, J.J., Dammer, E.B., Weber, A.J., Liu, E., Curtis, K.A., Boros, B.D., Freeman, C.D., Seo, J.V., et al. (2023). Cross-Platform Synaptic Network Analysis of Human Entorhinal Cortex Identifies TWF2 as a Modulator of Dendritic Spine Length. J Neurosci *43*, 3764-3785. 10.1523/JNEUROSCI.2102-22.2023.
193. Cheng, C.W., Chow, R.L., Lebel, M., Sakuma, R., Cheung, H.O., Thanabalasingham, V., Zhang, X., Bruneau, B.G., Birch, D.G., Hui, C.C., et al. (2005). The Iroquois homeobox gene, Irx5, is required for retinal cone bipolar cell development. Dev Biol *287*, 48-60. 10.1016/j.ydbio.2005.08.029.
194. Mummenhoff, J., Houweling, A.C., Peters, T., Christoffels, V.M., and Ruther, U. (2001). Expression of Irx6 during mouse morphogenesis. Mech Dev *103*, 193-195. 10.1016/s0925-4773(01)00353-7.
195. Star, E.N., Zhu, M., Shi, Z., Liu, H., Pashmforoush, M., Sauve, Y., Bruneau, B.G., and Chow, R.L. (2012). Regulation of retinal interneuron subtype identity by the Iroquois homeobox gene Irx6. Development *139*, 4644-4655. 10.1242/dev.081729.
196. Erkman, L., Yates, P.A., McLaughlin, T., McEvilly, R.J., Whisenhunt, T., O'Connell, S.M., Krones, A.I., Kirby, M.A., Rapaport, D.H., Bermingham, J.R., et al. (2000). A POU domain transcription factor-dependent program regulates axon pathfinding in the vertebrate visual system. Neuron *28*, 779-792. 10.1016/s0896-6273(00)00153-7.
197. Barber, A.C., Hippert, C., Duran, Y., West, E.L., Bainbridge, J.W., Warre-Cornish, K., Luhmann, U.F., Lakowski, J., Sowden, J.C., Ali, R.R., and Pearson, R.A. (2013). Repair of the degenerate retina by photoreceptor transplantation. Proc Natl Acad Sci U S A *110*, 354-359. 10.1073/pnas.1212677110.
198. Gonzalez-Cordero, A., West, E.L., Pearson, R.A., Duran, Y., Carvalho, L.S., Chu, C.J., Naeem, A., Blackford, S.J.I., Georgiadis, A., Lakowski, J., et al. (2013). Photoreceptor precursors derived from three-dimensional embryonic stem cell cultures integrate and mature within adult degenerate retina. Nat Biotechnol *31*, 741-747. 10.1038/nbt.2643.
199. MacLaren, R.E., Pearson, R.A., MacNeil, A., Douglas, R.H., Salt, T.E., Akimoto, M., Swaroop, A., Sowden, J.C., and Ali, R.R. (2006). Retinal repair by transplantation of photoreceptor precursors. Nature *444*, 203-207. 10.1038/nature05161.
200. Pearson, R.A., Barber, A.C., Rizzi, M., Hippert, C., Xue, T., West, E.L., Duran, Y., Smith, A.J., Chuang, J.Z., Azam, S.A., et al. (2012). Restoration of vision after transplantation of photoreceptors. Nature *485*, 99-103. 10.1038/nature10997.
201. Suen, H.C., Qian, Y., Liao, J., Luk, C.S., Lee, W.T., Ng, J.K.W., Chan, T.T.H., Hou, H.W., Li, I., Li, K., et al. (2019). Transplantation of Retinal Ganglion Cells Derived from Male Germline Stem Cell as a Potential Treatment to Glaucoma. Stem Cells Dev *28*, 1365-1375. 10.1089/scd.2019.0060.
202. Venugopalan, P., Wang, Y., Nguyen, T., Huang, A., Muller, K.J., and Goldberg, J.L. (2016). Transplanted neurons integrate into adult retinas and respond to light. Nat Commun *7*, 10472. 10.1038/ncomms10472.
203. Vrathasha, V., Nikonov, S., Bell, B.A., He, J., Bungatavula, Y., Uyhazi, K.E., and Murthy Chavali, V.R. (2022). Transplanted human induced pluripotent stem cells- derived retinal ganglion cells embed within mouse retinas and are electrophysiologically functional. iScience *25*, 105308. 10.1016/j.isci.2022.105308.

204. Wu, Y.R., Hashiguchi, T., Sho, J., Chiou, S.H., Takahashi, M., and Mandai, M. (2021). Transplanted Mouse Embryonic Stem Cell-Derived Retinal Ganglion Cells Integrate and Form Synapses in a Retinal Ganglion Cell-Depleted Mouse Model. Invest Ophthalmol Vis Sci *62*, 26. 10.1167/iovs.62.13.26.
205. Nickerson, P.E.B., Ortin-Martinez, A., and Wallace, V.A. (2018). Material Exchange in Photoreceptor Transplantation: Updating Our Understanding of Donor/Host Communication and the Future of Cell Engraftment Science. Front Neural Circuits *12*, 17. 10.3389/fncir.2018.00017.
206. Ortin-Martinez, A., Tsai, E.L., Nickerson, P.E., Bergeret, M., Lu, Y., Smiley, S., Comanita, L., and Wallace, V.A. (2017). A Reinterpretation of Cell Transplantation: GFP Transfer From Donor to Host Photoreceptors. Stem Cells *35*, 932-939. 10.1002/stem.2552.
207. Pearson, R.A., Gonzalez-Cordero, A., West, E.L., Ribeiro, J.R., Aghaizu, N., Goh, D., Sampson, R.D., Georgiadis, A., Waldron, P.V., Duran, Y., et al. (2016). Donor and host photoreceptors engage in material transfer following transplantation of post-mitotic photoreceptor precursors. Nat Commun *7*, 13029. 10.1038/ncomms13029.
208. Santos-Ferreira, T., Llonch, S., Borsch, O., Postel, K., Haas, J., and Ader, M. (2016). Retinal transplantation of photoreceptors results in donor-host cytoplasmic exchange. Nat Commun *7*, 13028. 10.1038/ncomms13028.
209. Singh, M.S., Balmer, J., Barnard, A.R., Aslam, S.A., Moralli, D., Green, C.M., Barnea-Cramer, A., Duncan, I., and MacLaren, R.E. (2016). Transplanted photoreceptor precursors transfer proteins to host photoreceptors by a mechanism of cytoplasmic fusion. Nat Commun *7*, 13537. 10.1038/ncomms13537.
210. Waldron, P.V., Di Marco, F., Kruczek, K., Ribeiro, J., Graca, A.B., Hippert, C., Aghaizu, N.D., Kalargyrou, A.A., Barber, A.C., Grimaldi, G., et al. (2018). Transplanted Donor- or Stem Cell-Derived Cone Photoreceptors Can Both Integrate and Undergo Material Transfer in an Environment-Dependent Manner. Stem Cell Reports *10*, 406-421. 10.1016/j.stemcr.2017.12.008.
211. Rocha-Martins, M., de Toledo, B.C., Santos-Franca, P.L., Oliveira-Valenca, V.M., Vieira-Vieira, C.H., Matos-Rodrigues, G.E., Linden, R., Norden, C., Martins, R.A.P., and Silveira, M.S. (2019). De novo genesis of retinal ganglion cells by targeted expression of Klf4 in vivo. Development *146*. 10.1242/dev.176586.
212. Xu, D., Zhong, L.T., Cheng, H.Y., Wang, Z.Q., Chen, X.M., Feng, A.Y., Chen, W.Y., Chen, G., and Xu, Y. (2023). Overexpressing NeuroD1 reprograms Muller cells into various types of retinal neurons. Neural Regen Res *18*, 1124-1131. 10.4103/1673-5374.355818.
213. Le, N., Appel, H., Pannullo, N., Hoang, T., and Blackshaw, S. (2022). Ectopic insert-dependent neuronal expression of GFAP promoter-driven AAV constructs in adult mouse retina. Front Cell Dev Biol *10*, 914386. 10.3389/fcell.2022.914386.
214. Butler, A., Hoffman, P., Smibert, P., Papalexi, E., and Satija, R. (2018). Integrating single-cell transcriptomic data across different conditions, technologies, and species. Nat Biotechnol *36*, 411-420. 10.1038/nbt.4096.
215. Satpathy, A.T., Granja, J.M., Yost, K.E., Qi, Y., Meschi, F., McDermott, G.P., Olsen, B.N., Mumbach, M.R., Pierce, S.E., Corces, M.R., et al. (2019). Massively parallel single-cell chromatin landscapes of human immune cell development and intratumoral T cell exhaustion. Nat Biotechnol *37*, 925-936. 10.1038/s41587-019-0206-z.

216. Stuart, T., Srivastava, A., Madad, S., Lareau, C.A., and Satija, R. (2021). Single-cell chromatin state analysis with Signac. Nat Methods *18*, 1333-1341. 10.1038/s41592-021-01282-5.
217. Zhang, Y., Liu, T., Meyer, C.A., Eeckhoute, J., Johnson, D.S., Bernstein, B.E., Nusbaum, C., Myers, R.M., Brown, M., Li, W., and Liu, X.S. (2008). Model-based analysis of ChIP-Seq (MACS). Genome Biol *9*, R137. 10.1186/gb-2008-9-9-r137.
218. Neph, S., Kuehn, M.S., Reynolds, A.P., Haugen, E., Thurman, R.E., Johnson, A.K., Rynes, E., Maurano, M.T., Vierstra, J., Thomas, S., et al. (2012). BEDOPS: high-performance genomic feature operations. Bioinformatics *28*, 1919-1920. 10.1093/bioinformatics/bts277.
219. Cao, J., Spielmann, M., Qiu, X., Huang, X., Ibrahim, D.M., Hill, A.J., Zhang, F., Mundlos, S., Christiansen, L., Steemers, F.J., et al. (2019). The single-cell transcriptional landscape of mammalian organogenesis. Nature *566*, 496-502. 10.1038/s41586-019-0969-x.
220. McLean, C.Y., Bristor, D., Hiller, M., Clarke, S.L., Schaar, B.T., Lowe, C.B., Wenger, A.M., and Bejerano, G. (2010). GREAT improves functional interpretation of cis-regulatory regions. Nat Biotechnol *28*, 495-501. 10.1038/nbt.1630.